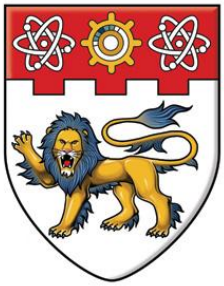

NANYANG TECHNOLOGICAL UNIVERSITY

SYSTEM IDENTIFICATION USING WAVELET TRANSFORM

SRIRAM SWAMINATHAN

SCHOOL OF ELECTRICAL AND ELECTRONIC ENGINEERING

2010

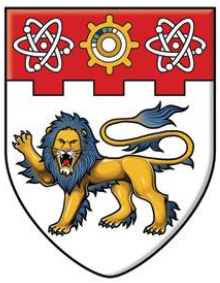

NANYANG TECHNOLOGICAL UNIVERSITY

SYSTEM IDENTIFICATION USING WAVELET TRANSFORM

SRIRAM SWAMINATHAN

A DISSERTATION SUBMITTED IN PARTIAL FULFILMENT OF

THE REQUIREMENTS FOR THE DEGREE OF

MASTER OF SCIENCE IN COMPUTER CONTROL AND AUTOMATION

2010

ACKNOWLEDGEMENTS

Taking this opportunity, I would like to express my deepest appreciation and sincere gratitude to my project supervisor, Associate professor, Koh Tong San for his invaluable support and motivation which made me to widen my research horizon and thus to a successful completion of the project. It was indeed a great opportunity to work under him as he extracted a good work from me without the feel of any pressure.

In addition, I would like to thank my parents, who have given me a very great opportunity to explore such opportunities at Nanyang Technological University. Their support, love and encouragement have made me to grow from all obstacles.

Last but not least, I thank my friends, who gave me constant motivation and support in the bad times.

SUMMARY

System identification is the estimation of the type of desired ideal system. The practical system with noisy input, noisy output or being a non-ideal system is identified and corrected with the deconvolution coupled denoising algorithm to achieve the desired output signal. This leads to the estimation of the desired system.

The noisy output signal is first made to pass through Fourier transformation and the deconvolution of the non-ideal system characteristics is done to extract the signal with some distortions. The output of the Fourier deconvolution is passed through wavelet denoising algorithm to reduce the distortion in the signal. This tends to approach the desired signal by appropriate thresholding by checking for the minimum percentage root mean square difference. The desired system is then determined by passing the corrected signal and the noisy original signal to the System Identification toolbox of MATLAB.

TABLE OF CONTENTS

LIST OF FIGURES

LIST OF TABLES

CHAPTER 1

1. INTRODUCTION

System identification is defined as the process of determining the model of the dynamic system. The input and output data combine together to define a system. There are many measuring instruments which are used to measure various parameters for the purpose of analysis. Often, these measurements come along with the noise. The noise is added to the information signal either at the input side or the output side of the measuring system. Apart from the additive noise, the signal is further distorted due to the convolution of the signal with the system transfer function. Traditionally, the deconvolution of the system transfer function is done using Fourier transformation, but it generates a noisy signal or the noise is not reduced to a great amount **[16, 28 and 34].** The reason being that the window used in the Fourier transformation is the exponential signal, which covers the entire signal at a stretch and does not localize any part of the signal for efficient tracking. The FFT analysis is done only for the stationary period signals. The disadvantage of FFT in giving only time-and amplitude resolution is overcome by using STFT (Short-Time Fourier transform), which uses a rectangular window (of very small length compared to signal) to move it along the signal in periodic steps to analyze the non-stationary signals. This gives both time-frequency and amplitude resolution, but it is not that efficient enough to trace for noise on the signal as it uses a constant window size **[30-32].** As an improvement, wavelet analysis is done to analyze the localized variations of power of the noisy signal using a window whose size varies according to the fluctuation of the signal in the time-domain **[1, 8].** Wavelet analysis based approach is a popular tool used extensively in biological applications with ECG signals and MRI **[2, 19]**. The

wavelets based application is a very good technique as it decides to de-noise the signal by the removal of unwanted signal leading to the compression of the signal. These compression techniques are widely used for image-based applications **[11].**

1.1 MOTIVATION

Every application needs a faithful output but get distorted due to noise. The noise can either be externally or already present in the system. The perfect recovery of the original signal is the motive of any de-noising algorithm. There is always a demand for the correct estimate of the signal for various applications and is widely used in biomedical areas. Hence, a wavelet combined Fourier analysis can be effective for non-stationary signals.

The strength of the wavelets is that it analyzes the signal by decomposing into low-frequency components and high-frequency components. The undesired noise is then reduced using wavelet decomposition of the signal which depends on the concept of thresholding. Apart from the added noise, the measuring system gets convoluted with the signal. Hence, while applying devoncolution, there should be a choice for the ratio of the noise to the signal distortion and which is application dependent.

1.2 OBJECTIVE

To identify the system that can generate the desired signal with minimal noise, minimal distortion and maximum compression ratio from a noisy, distorted input signal, using Fourier coupled wavelet de-noising algorithm.

1.3 MAJOR CONTRIBUTION OF THE THESIS

The thesis majorly contributes to the retrieval of the desired signal with the identification of the approximately ideal system. The different objectives for this contribution and the organization of the thesis are as follows:

1) The concept of Fourier transformation is generally used only for the stationary signal, but the thesis experiments with the non-stationary signal convoluted with the system function. The deconvolution is extensively analyzed to determine the optimal ratio of the noise to the distorted signal and this is done with the help of a regularization parameter. These are done in CHAPTER 2.
2) The wavelet domain is chosen to approach the desired signal by focussing only the amplitude of the coefficients above the threshold level. Haar wavelet and Daubechies4 are chosen for the analysis of the noise and their efficiencies are compared; which are done in CHAPTER 3. In CHAPTER 4, the optimal threshold determines the accuracy of the de-noising technique. The various methods to determine the threshold are researched and the best threshold for each application is chosen using appropriate error analysis. In CHAPTER 6, the error is analyzed by determining the minimum percentage root mean square error and the performance is analyzed using many methods.
3) In CHAPTER 5, a proper algorithm is designed to combine both the Fourier deconvolution and the wavelet de-noising techniques and the necessary functions are defined. The retrieved signal and the original signal are then used to identify the system in System Identification Toolbox of MATLAB 2007b.

The best fit of the measured system is researched by continuously experimenting with various models to define the simulated system.

4) CHAPTER 7 finally, concludes that the desired signal is retrieved efficiently.
5) Other types of wavelets are analyzed and their various shapes are noted for future scope of the project, which are added in the APPENDIX.

CHAPTER 2

2 DECONVOLUTION USING INVERSE FOURIER TRANSFORMATION

2.1 SYSTEM IDENTIFICATION

Identification of linear systems is the estimation of the characteristics function of the system. The parametric identification consists of two steps. Firstly, an appropriate model is setup for the structure of the system, and secondly, the parameters of the system are estimated. The non-parametric identification method on the other hand, uses time or other domain waveform of the system characteristic function and this is used when the structure of the system is without any explicit information.

Fig 2.1: Schematic diagram of a processes being measured.

The output signal of a measuring system is the convolution of the impulse response of the system and the input signal to the system. The non-parametric identification of a system is achieved through the problem of deconvolution.

$$y(t) = x(t) * h(t) \qquad eqn\ (2.1)$$

Where, '*' represents the convolution operator, and

y(t)- the output signal

x(t)-the excitation input signal

h(t)-impulse transfer function of the system

Converting, ***equation (2.1)*** from time-domain to frequency domain using Fourier transformation, we can transfer the convolution operator into multiplication operator. Hence, the excitation input signal is retrieved by,

$$X(jw) = \frac{Y(jw)}{H(jw)} \qquad eqn(2.2)$$

in the frequency domain. Thus, the distorted output signal is corrected by deconvoluting the impulse transfer function from the system output. But, the deconvolution process amplifies the noise already present in the signal. If the ***equation (2.2)*** is inverse Fourier transformed, and if the inverse system satisfies at or near the poles, then the magnitude of the system transfer function increases leading to the amplification of the noise. Again, when H(jw) is transformed to h(t), the noise-errors at the poles or zeros are spread throughout the signal, swamping the original signal. Hence, the suppression of the noise is needed but it also leads to the bias of the useful signal.

Each situation needs to satisfy certain conditions, where, one needs to no noise at all but doesn't care about the final distorted output, and the other needs an optimal parameter such that the output doesn't get distorted and quite a big amount of noise is removed. **[16, 18, 28, 34, 26]**

2.2 FOURIER TRANFORMATION

A continuous time domain signal is considered and a Fourier transformation is applied.

Then,

$$F(\omega) = \int_{-\infty}^{\infty} e^{-j\omega t} f(t).dt \qquad eqn(2.3)$$

The time domain signal is transformed into a frequency domain signal by a complex exponential window. This complex exponential window analyses each and every part of the signal and extracts the frequency content of that part.

A Fourier transform is transforming a signal into its Fourier series, which is nothing but the expansion of a signal into sum of sine and cosine signals with infinite duration. This makes Fourier transformation less optimal to compress or analyze a signal's transients.

Further, Fourier transformation gives knowledge about frequency-amplitude relationship but not frequency-time relationship. As a result, we know about the frequency components of a signal but cannot localize the component to analyze transients of the time-domain signal.

$$F(\omega) = |F(\omega)|e^{\theta(\omega)}, \qquad eqn(2.4)$$

where, $|F(\omega)|$ is the Fourier spectrum and $\theta(\omega)$ is the phase angle of the $f(t)$. **[11]**

2.2.1 DISCRETE FOURIER TRANSFORM

The discrete Fourier transform of a complex vector y with n elements is another complex vector Y with n elements

$$Y_k = \sum_{j=0}^{n-1} \omega^{jk} y_j, \quad k = 0, \dots, n-1 \qquad eqn(2.5)$$

where, ω is a complex nth root of unity:

$$\omega = e^{-2\pi i/n}. \qquad eqn(2.6)$$

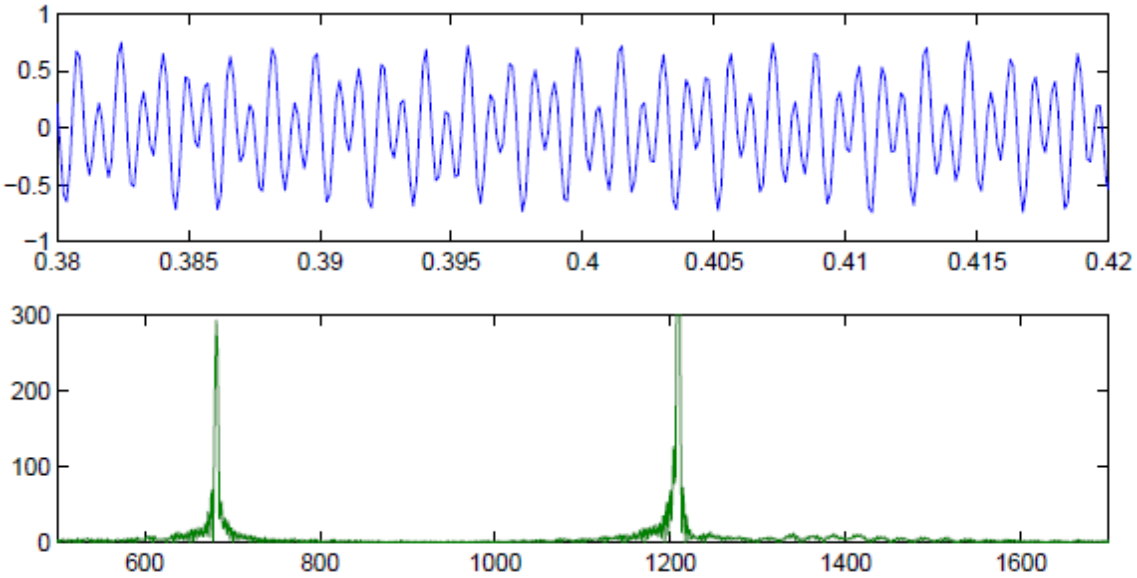

Fig 2.2: The display of a sampled signal and the DFT of the same signal

where, $i = \sqrt{-1}$ is the complex unit and *j* and *k* are indices that from 0 to n-1.

The Fourier transform can be expresses with matrix-vector notation:

$$Y = F.y\,, \qquad eqn(2.7)$$

where the Fourier matrix F has elements

$$f_{k,j} = \omega^{jk}. \qquad eqn(2.8)$$

Mathematically, *F* is nearly its own inverse, with F^T, the complex conjugate transpose of *F*, satisfying:

$$F^T F = nI\,, \qquad eqn(2.9)$$

And

$$F^{-1} = \frac{1}{n}F^T. \qquad eqn(2.10)$$

Hence, the inverse Fourier transform is

$$y = \frac{1}{n}F^T Y. \qquad eqn(2.11)$$

Thus,

$$y_j = \frac{1}{n}\sum_{k=0}^{n-1} Y_k \varpi^{jk} \qquad eqn(2.12)$$

where ϖ is the complex conjugate of ω: **[11]**

$$\varpi = e^{2\pi i/n}. \qquad eqn(2.13)$$

2.2.2 FAST FINITE FOURIER TRANSFORM

One-dimensional FFTs with million points are very common in signal processing. Hence, a rapid and efficient computational algorithm is needed, which is satisfied by FFT.

$$Y_k = \sum_{j=0}^{n-1} \omega^{jk} y_j, \quad k = 0, \dots, n-1 \qquad eqn(2.14)$$

requires *n* multiplications and *n* additions for each of the *n* components of *Y* for a total of $2n^2$ floating-point operations. This does not include the generation of the powers of ω. Hence, the computational complexity is $O(n\log_2 n)$ instead of $O(n^2)$.

The FFT algorithm is fast because of the fact that the square of the 2nth root of unity is the nth root of unity. Using complex notation,

$$\omega = \omega_n = e^{-2\pi i/n}, \qquad eqn(2.15)$$

we have

$$\omega_{2n}^2 = \omega_n . \qquad eqn(2.16)$$

The derivation of the fast algorithm starts with the definition of the discrete Fourier transform:

$$Y_k = \sum_{j=0}^{n-1} \omega^{jk} y_j, \quad k = 0, \dots, n-1 \qquad eqn(2.17)$$

Assuming that *n* is even and that $k \leq n/2 - 1$. The sum is divided into even subscript terms and odd subscript terms like,

$$Y_k = \sum_{even\ j} \omega^{jk} y_j + \sum_{odd\ j} \omega^{jk} y_j \qquad eqn(2.18)$$

$$= \sum_{j=0}^{n/2-1} \omega^{2jk}\, y_{2j} + \omega^k \sum_{j=0}^{n/2-1} \omega^{2jk}\, y_{2j+1}. \qquad eqn(2.19)$$

Here, the two FFTs of length n/2 are calculated and then concatenated to get the FFT for the entire length of the signal of length n. **[11, 30-32]**

2.2.3 FOURIER TRANSFORM AND SERIES

$$Y_k = \sum_{j=0}^{n-1} y_j\, e^{-2ijk\pi/n}, \quad k = 0, \dots, n-1 \qquad eqn(2.20)$$

The inverse Fourier transform is:

$$Y_k = \frac{1}{n} \sum_{j=0}^{n-1} y_j\, e^{2ijk\pi/n}, \quad k = 0, \dots, n-1 \qquad eqn(2.21)$$

The Fourier integral transform converts one complex function into another. And the transform is defined by:

$$F(\mu) = \int_{-\infty}^{\infty} f(t) e^{-2\pi i \mu t} dt\,. \qquad eqn(2.22)$$

And its inverse Fourier transform is defined as,

$$f(t) = \int_{-\infty}^{\infty} F(\mu) e^{2\pi i \mu t} d\mu\,. \qquad eqn(2.23)$$

where, both $f(t)$ *and* $F(\mu)$ are complex valued numbers and the variables *t* and μ run over the entire real line, and *t* represents the time in seconds and μ represents the frequency in radians per second.

A Fourier series converts a periodic function into an infinite sequence of Fourier coefficients. Let *f(t)* be the periodic function and let *L* be the period of the signal, hence,

$$f(t+L) = f(t) \qquad for\ all\ t. \qquad eqn(2.24)$$

The Fourier coefficients are given by integrals over the period

$$c_j = \frac{1}{L}\int_{L/2}^{-L/2} f(t)e^{-2\pi ijt}dt, \qquad j = \cdots, -1,0,1, \ldots. \qquad eqn(2.25)$$

With these coefficients, the complex form of the Fourier series is

$$f(t) = \sum_{j=-\infty}^{\infty} c_j e^{2\pi ijt/L}. \qquad eqn(2.26)$$

A discrete time Fourier transform is used to convert an infinite sequence of data values into a period function. Let x_k be the sequence, and the index *k* taking all positive and negative values.

Hence, the discrete time Fourier transform will be a complex-valued period function as,

$$X\left(e^{j\omega}\right) = \sum_{k=-\infty}^{\infty} x_k e^{ik\omega}. \qquad eqn(2.27)$$

The sequence can then be represented as, **[11, 30-32]**

$$x_k = \frac{1}{2\pi}\int_{-\pi}^{\pi} X\left(e^{i\omega}\right)e^{-ik\omega}d\omega, \quad k = \ldots, -1,0,1, \ldots\ldots \qquad eqn(2.28)$$

2.2.4 IMPORTANT THEOREMS

PARSEVAL'S THEOREM:

The total power of the signal is represented as, **[12]**

$$\int_{-\infty}^{\infty} |f(t)|^2 dt = \int_{-\infty}^{\infty} |F(\mu)|^2 d\mu \qquad eqn(2.29)$$

SAMPLING THEOREM:

A band limited signal is a signal, *f(t)*, which has no spectral components beyond a frequency '*w*' Hz., i.e., F(s)=0 for |s|>2πw. The sampling theorem states that the signal can be reconstructed without error if the rate of sampling is greater than twice the maximum frequency of the signal and this frequency is called Nyquist frequency. **[12]**

2.3 FOURIER ANALYSIS

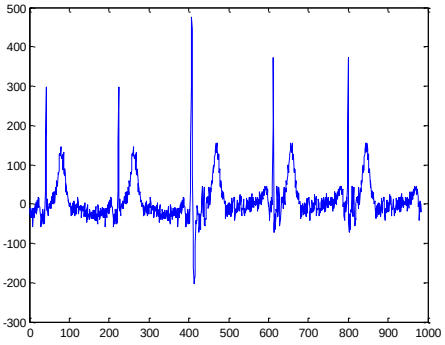

Fig 2.3: ECG input signal

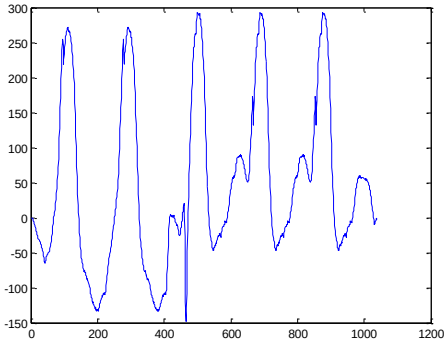

Fig 2.4: Convoluted output of the ECG signal and the system transfer function 1/((s+1)(s+9)).

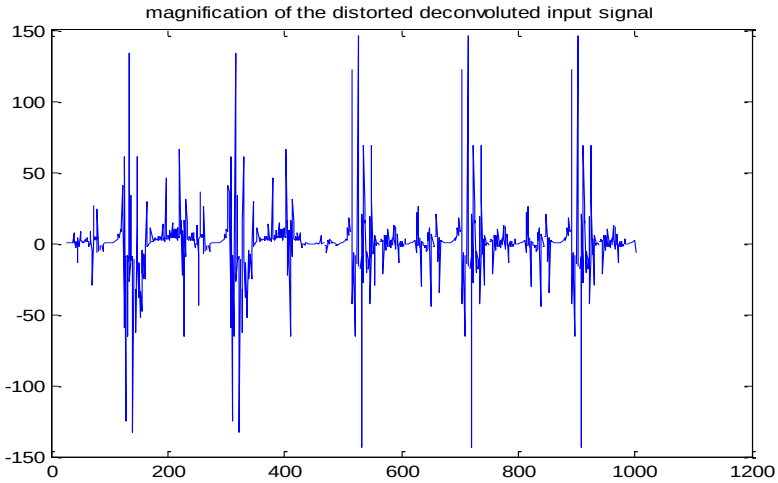

Fig 2.5: Magnified version of the deconvoluted output after Inverse Fourier transformation.

This proves that Fourier deconvolution doesn't work properly for non-stationary signal. ECG signal is a non-stationary signal and with Fourier deconvolution of the system, a highly distorted output is generated.

Fourier is generally used for stationary signals. To support non-stationary signals, we need the analysis of frequency component of the frequency-domain signal at that particular time of the time-domain signal. This idea introduces to Short-Time Fourier transformation, which analyzes the transients of a non-stationary signal using a constant-sized window. **[19, 24, 27, 30, 31, 32]**

2.4 SHORT TIME FOURIER TRANSFORM

The Short Time Fourier Transform gives the time-frequency analysis. It is also known as the Windowed Fourier Transform. A window of constant size is chosen and made to traverse along the time axis. Each time the window covers a part of the non-stationary signal, it becomes stationary and easy to be analysable with Fourier transformation.

$$STFT(t,w) = \int_{-\infty}^{\infty} e^{-jws}.f(s).g(s-t)ds \qquad eqn(2.30)$$

The Fourier transform of this windowed signal is computed by the above sequence, by convoluting a part of the signal covered by the window and the window signal, then shifting the window equally along the time axis to do the same convolution operation until the window covers the entire non-stationary signal.

With this, we get a fixed time-frequency resolution. The window length gives the time translation content of the signal and DTFT gives the frequency components of the signal.

Commonly, the chosen window function is Gaussian, where it will be termed as Gabor Transform. In general, the STFT can be applied with any type of window function. **[13, 19, 24, 27]**

2.5 STFT ANALYSIS

The same ECG signal and the convoluted output of the system characteristics 1/(s+1)(s+9) is analyzed and is shown as the figure (2.6) below:

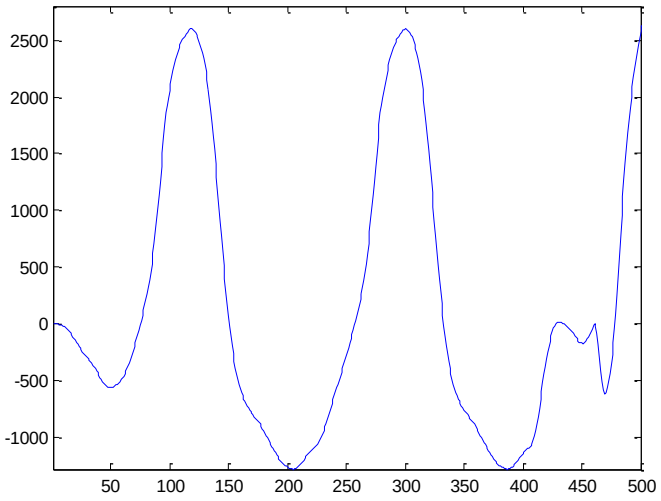

Fig 2.6: The deconvoluted output after STFT.

It is understood that, the ECG signal is very non-stationary, but the STFT uses a constant window to analyze, although it gives time and frequency resolution.

The constant window used here is exp(-x) for x=[1/16,1] with increments of 1/16. This pre-decided window makes difficult to analyze the dynamically varying signal.

Hence, a dynamically varying window is needed to analyze such highly non-stationary signal. Thus, the wavelet transformation should be the apt one to decipher such signals which are complex.

2.6 REGULARIZATION PARAMETER

Considering, the importance of the trade-off between system characteristics and the desired signal characteristics, it is necessary to include a regularized inverse with the optimal regularization parameter α.

$$\hat{X}_\alpha(f) = G_\alpha(f)Y(f) \qquad eqn(2.31)$$

With

$$G_\alpha(f) = \left(\frac{1}{|H(f)|}\right)\left(\frac{|H(f)|^2 P_x(f)}{|H(f)|^2 P_x(f) + \alpha\sigma^2}\right) \qquad eqn(2.32)$$

where, σ is the standard deviation of the noisy signal.

The regularization parameter α, controls the inverse function for deconvoluting the system characteristics from the desired signal which is also added with noise. Keeping α=0, means that, the output generated is the unbiased noisy estimate and keeping α=∞, means the regularized inverse generates a signal, which completely suppresses the noise along with the signal distortion. Thus the optimal α will account for the non-stationarities in the desired signal. **[34]**

2.7 REGULARIZED INVERSE ANALYSIS

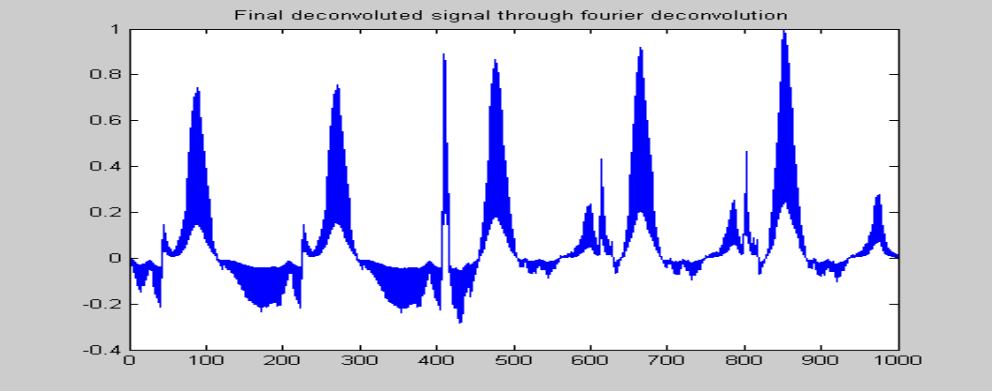

Fig 2.7: Normalized ECG signal after regularized Fourier deconvolution with α=0.6

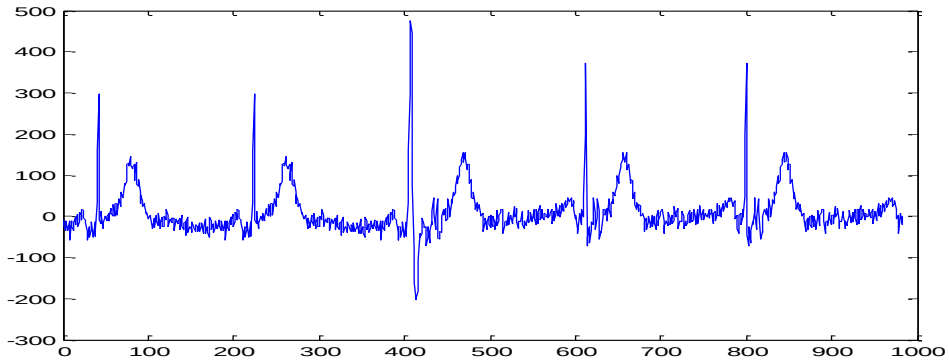

Fig 2.8: Original ECG signal

The output ECG signal observed is noisy but the shape of the signal is reproduced. This result is achieved by proper tuning of the regularization parameter until minimum square error is achieved compared with the original signal.

The noisy output shall be denoised by passing on this output to the wavelet domain. The proper thresholding of the signal will lead to the retrieval of the desired signal. **[34]**

CHAPTER 3

3. WAVELET TRANSFORMATION FOR A PREFFERED RESOLUTION

3.1 WAVELET ANALYSIS

The wavelet transformation (WT) decomposes a one-dimensional signal by a basis function obtained from a wavelet, possessing important characteristics of translation and dilation. Each of the basis function has a specific spatial frequency and its localization in time domain. Unlike, Fourier transformation, Wavelet transformation gives multi-resolution analysis in both frequency and time. This property of it is particularly useful for analysing signals which are aperiodic, non-stationary, noisy and transient signals. **[13, 20, 23,27]**

3.2 CONTINUOUS WAVELET TRANSFORM

WT analysis uses wavelets to convolve them with the signal under investigation. The WT of a continuous signal with respect to the wavelet basis function is defined as, **[2, 5, 8, 13, 21, 25]**

$$W(a,b) = \int_{-\infty}^{\infty} s(t)\psi_{a,b}^{*}(t)dt, \qquad eqn(3.1)$$

Where s(t), is the continuous time signal, $\psi_{a,b}(t)$ is the mother wavelet scaled by the parameter 'a' and dilated by the parameter 'b' , $\psi_{a,b}^{*}(t)$ is the complex conjugate of the mother wavelet.

$$\psi_{a,b}(t) = \frac{1}{\sqrt{a}}\psi\left(\frac{t-b}{a}\right) \qquad eqn(3.2)$$

Substituting, **equation (3.2)** in **(3.1)**, we get the definition of continuous wavelet transform as,

$$W_{a,b}(t) = \frac{1}{\sqrt{a}} \int_{-\infty}^{\infty} s(t)\psi^*\left(\frac{t-b}{a}\right) dt \qquad eqn(3.3)$$

For a special case, if there is no translation of the basis function along the inspected signal, then b=0;

$$W_a(t) = \frac{1}{\sqrt{a}} \int_{-\infty}^{\infty} s(t)\psi^*\left(\frac{t}{a}\right) dt \qquad eqn(3.4)$$

Using inverse continuous wavelet transform, we can recover the original signal, by

$$x(t) = \frac{1}{C_g} \int_{-\infty}^{\infty} \int_{0}^{\infty} W(a,b)\psi_{a,b}(t) \frac{dadb}{a^2}, \qquad eqn(3.5)$$

Where,C_g is an admissibility constant, and its value depends on the chosen wavelet.

3.3 DISCRETE WAVELET TRANSFORM AND MULTIRESOLUTION REPRESENTATION

DWT is computed by selecting the parameters ‘a’ and ‘b’ as discrete values. When there is a dyadic grid arrangement, a power-of-two logarithmic scaling of both the dilation and translation steps is adopted as,

$$\psi_{j,k}(t) = 2^{-j/2}\psi\left(2^{-j}t - k\right), \qquad eqn(3.6)$$

where, m and n are integers which control the wavelet dilation and translation, respectively. Discrete dyadic grid wavelets are chosen to be orthonormal to each other and have unit energy when they are normalized. DWT is then defined as, **[2, 5, 11, 21, 26, 27]**

$$T_{j,k} = \int_{-\infty}^{\infty} x(t)\psi_{j,k}(t)dt, \qquad eqn(3.7)$$

And with inverse DWT,

$$x(t) = \sum_{j=-\infty}^{\infty}\sum_{k=-\infty}^{\infty} T_{j.k}\psi_{j,k}(t). \qquad eqn(3.8)$$

Orthonormal dyadic discrete wavelets are associated with scaling function and their dilation equations. The scaling function smoothes the signal and is given by,

$$\varphi_{j,k}(t) = 2^{-j/2}\varphi\left(2^{-j}t - k\right). \qquad eqn(3.9)$$

The scaling function is orthogonal to translations of itself and not with dilations. The convolution of the scaling function with the signal produces approximation coefficients, that is

$$S_{j,k} = \int_{-\infty}^{\infty} x(t)\phi_{j,k}(t)dt \qquad eqn(3.10)$$

that are simply weighted averages of the continuous signal factored by $2^{j/2}$.

The signal x(t) can be represented using a combined series expansion of approximation coefficients and the detail coefficients by the following form:

$$x(t) = \sum_{k=-\infty}^{\infty} S_{j_0 k}\varphi_{j_0 k}(t) + \sum_{j=-\infty}^{\infty}\sum_{k=-\infty}^{\infty} T_{j,k}\psi_{j,k}(t), \qquad eqn(3.11)$$

revealing that the original are expressed as a combination of an approximation of itself, at arbitrary scale index j_0, and summation of signal details from scales j_0 down to negative infinity.

We can denote the signal detail at scale j as

$$d_j(t) = \sum_{k=-\infty}^{\infty} T_{j,k}\psi_{j,k}(t) \qquad eqn(3.12)$$

$$x(t) = x_{j_0}(t) + \sum_{j=-\infty}^{\infty} d_j(t). \qquad eqn(3.13)$$

Hence,

$$x_{j-1}(t) = x_j(t) + d_j(t). \qquad eqn(3.14)$$

The above equation represents multi-resolution analysis, when the detail signal with the scale 'j' is added with the approximation signal of the same scale, the resulting signal is of higher resolution and a lower scale 'j-1'.

Multi-resolution approximation is the decomposition of investigated signal into approximation and detail signal, which are realized by a pair of finite impulse response filters, which are high pass and low pass filters, defining a multi-resolution decomposition and reconstruction scheme. **[1, 3, 10]**

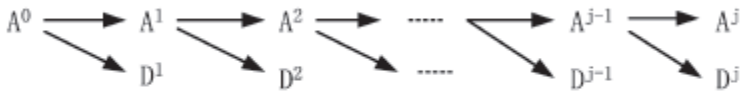

Fig 3.1: Decomposition scheme

Fig 3.2: Reconstruction scheme

3.4 PERFECT RECONSTRUCTION FILTER BANK

A perfect reconstruction (PR) filter bank consists of filters that divide the input signal into two sub-bands; the synthesis part of the filter bank reconstructs the original signal by recombining the sub-bands. The structure of one-dimensional signal

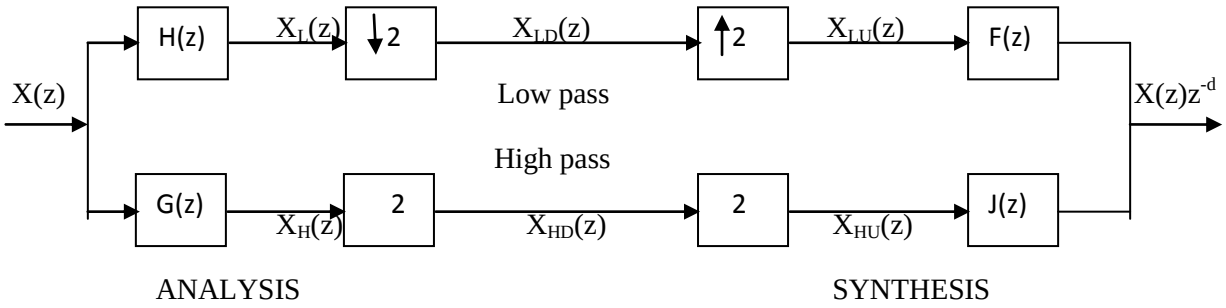

Fig 3.3: 1-D, 1 level PR filter bank

The analysis filters H(z) and G(z) split the input signal X(z) into two subbands, lowpass $(X_L(z))$ and $(X_H(z))$, which are then downsampled to produce $(X_{LD}(z))$ and $(X_{HD}(z))$. These signals are then upsampled and passed through a set of synthesis filters F(z) and J(z) to reconstruct the original signal but with some group delay 'd'.

The analysis filters preserves the original sampling rate but causes aliasing along with phase and amplitude distortion. This decides the choice of synthesis filters, which can correct for the errors and generate the desired signal. The relation between analysis and synthesis filters is given by following conditions:

$$F(z)H(z) + J(z)G(z) = 2z^{-d} \qquad eqn(3.14)$$

$$F(z)H(-z) + J(z)G(-z) = 0 \qquad eqn(3.15)$$

The ***equations (3.14)*** and ***(3.15)*** are called 'no distortion' condition and 'anti-aliasing' condition respectively.

The relations between analysis and synthesis filters vary for orthogonal and biorthogonal PR filter banks. In the case of orthogonal PR filter bank, the synthesis filters are time reversed versions of analysis filters: $F(z) = H(z^{-1})$ and $J(z) = G(z^{-1})$. Moreover, the highpass filter is the alternating flip of the lowpass filter, $G(z) = -z^{N}H(-z^{-1})$, where N is the length of the filter. Thus the entire filter bank is derived by analysis filter. On the other hand, the biorthogonal PR filter bank is defined by two filters H(z) and F(z),having certain conditions as $G(z) = F(-z)$ and $J(z) = -H(-z)$. The biorthogonal filters give linear phase response unlike orthogonal filters. **[3]**

3.5 HAAR WAVELET TRANSFORM

A Haar wavelet us the simplest type of wavelet. In discrete form, Haar wavelets are related to a mathematical operation called the Haar transform. The discrete time signal is defined as: f=(f1,f2...fN), where N is the length of f.

The Haar transform decomposes a discrete signal into two subbands of half its length. One subband is a running average or trend' the other subsignal is a running difference or fluctuation. **[1, 8, 9]**

3.5.1 APPROXIMATION SIGNAL

The first trend, $a^1=(a_1,a_2,..,a_{N/2})$, for the signal f is computed by taking a running average and multiplying by $\sqrt{2}$ to conserve the energy of the signal. Hence, the approximation coefficients or the trend is defined as: **[1, 8, 9]**

$$a_m = \frac{f_{2m-1} + f_{2m}}{\sqrt{2}} \qquad eqn(3.15)$$

where m=1, 2, 3,.., N/2

3.5.2 DETAIL SIGNAL

The first fluctuation of the signal f, which is denoted by $d^1 = (d_1, d_2, .., d_{N/2})$ is computed by taking a running difference and multiplying by $\sqrt{2}$ to conserve the energy of the signal. Hence, the detailed coefficients are defined as: **[1, 8, 9]**

$$d_m = \frac{f_{2m-1} - f_{3m}}{\sqrt{2}}, \qquad eqn(3.16)$$

for m=1, 2, 3,.., N/2.

3.5.3 HAAR TRANSFORM, 1-level

The Haar transform is performed in several stages, or levels. The first level is the mapping H_1 defined by:

$$f \xrightarrow{H_1} (a^1 | d^1) \qquad eqn(3.17)$$

from a discrete signal *f* to its first trend a^1 and first fluctuation d^1. Its inverse maps the transform signal $(a^1|d^1)$ back to the signal *f* by:

$$f = \left(\frac{a_1 + d_1}{\sqrt{2}}, \frac{a_1 - d_1}{\sqrt{2}}, \dots, \frac{a_{N/2} + d_{N/2}}{\sqrt{2}}, \frac{a_{N/2} - d_{N/2}}{\sqrt{2}}\right) \qquad eqn(3.18)$$

Fluctuations Feature: The magnitudes of the fluctuation values are often significantly smaller than the magnitudes of the values of the original signal. **[1, 8, 9]**

3.5.4 HAAR TRANSFORM, MULTIPLE LEVELS

The approximation signal after first level of decomposition using Haar transform is then transformed using Haar wavelets to further decompose into its approximation signal and the detailed signal. The detail signal after first level decomposition is then passed through the second level to be added with the detailed signal of the second

level of decomposition. Thus, the full signal is the sum of the approximation signal of the second level of decomposition and the sum of the detail signals of both the levels of decomposition. This, procedure is continued until the desired level of decomposition is desired .Thus, the m-level Haar transform of *f* is the signal, **[1, 8, 9]**

$$\langle a^m | d^m | d^{m-1} \dots | d^1 \rangle$$

where (m=1,2,3..log $_2$N) and N is the length of the signal.

3.5.5 HAAR WAVELETS

Haar wavelets are defined as,

$$w_1^1 = \left(\frac{1}{\sqrt{2}}, -\frac{1}{\sqrt{2}}, 0,0,..,0\right)$$

$$w_2^1 = \left(0,0, \frac{1}{\sqrt{2}}, -\frac{1}{\sqrt{2}}, 0,0,..,0\right)$$

$$w_3^1 = \left(0,0,0,0, \frac{1}{\sqrt{2}}, -\frac{1}{\sqrt{2}}, 0,0,..,0\right)$$

$$w_{N/2}^1 = \left(0,0,\dots,0, \frac{1}{\sqrt{2}}, -\frac{1}{\sqrt{2}}\right)$$

Their properties are as follows:

1) Each wavelet has energy of 1.
2) Each wavelet consist of a rapid fluctuation between $\pm\sqrt{2}$, with an average value of 0.
3) All the wavelets are similar to each other, except of a translation by 2 units from the previous wavelet.

Hence, the fluctuation value can be generalized as,

$$d_m = \frac{f_1 - f_2}{\sqrt{2}} = f.W_m^L \qquad eqn(3.19)$$

where, d_m gives the mth detail signal and L stands for the Lth level of decomposition.

m= 1,2,...N/2 and N is the length of the signal passed through wavelet transformation. The fluctuation value, will be zero if the signal *f* is constant over the support of the L-level Haar transform. **[1, 8. 9]**

3.5.6 HAAR SCALING COEFFICIENTS

$$v_1^1 = \left(\frac{1}{\sqrt{2}}, \frac{1}{\sqrt{2}}, 0,0,..,0\right)$$

$$v_2^1 = \left(0,0, \frac{1}{\sqrt{2}}, \frac{1}{\sqrt{2}}, 0,0,..,0\right)$$

$$v_3^1 = \left(0,0,0,0, \frac{1}{\sqrt{2}}, \frac{1}{\sqrt{2}}, 0,0,..,0\right)$$

$$v_{N/2}^1 = \left(0,0,\dots,0, \frac{1}{\sqrt{2}}, \frac{1}{\sqrt{2}}\right)$$

The approximation coefficients are then defined as,

$$a_m = \frac{f_1 + f_2}{\sqrt{2}} = f.V_m^L \qquad eqn(3.20)$$

where, d_m gives the mth detail signal and L stands for the Lth level of decomposition.

m= 1,2,...N/2 and N is the length of the signal passed through wavelet transformation.

Their properties are as follows:

1) Each wavelet has energy of 1.
2) Each wavelet consist of a rapid fluctuation between $\pm\sqrt{2}$, with an average value not equal to 0.
3) All the wavelets are similar to each other, except of a translation by 2 units from the previous wavelet. **[1, 8, 9]**

3.5.7 WAVELETS AND SCALING COEFFICIENTS FOR MULTIPLE LEVELS

The Haar scaling and the wavelet coefficients differ when they are defined for the levels above 1. Their generalized formula for the both the coefficients for various levels is as follows, **[1, 8, 9]**

$$v_1^L = \left(\frac{1}{(\sqrt{2})^L}, \frac{1}{(\sqrt{2})^L}, 0,0,..,0\right)$$

$$v_2^L = \left(0,0, \frac{1}{(\sqrt{2})^L}, \frac{1}{(\sqrt{2})^L}, 0,0,..,0\right)$$

$$v_3^L = \left(0,0,0,0, \frac{1}{(\sqrt{2})^L}, \frac{1}{(\sqrt{2})^L}, 0,0,..,0\right)$$

:

$$v_{N/2}^L = \left(0,0,\dots,0, \frac{1}{(\sqrt{2})^L}, \frac{1}{(\sqrt{2})^L}\right)$$

$$W_1^L = \left(\frac{1}{(\sqrt{2})^L}, -\frac{1}{(\sqrt{2})^L}, 0,0,..,0\right)$$

$$W_2^L = \left(0,0,\frac{1}{\left(\sqrt{2}\right)^L},-\frac{1}{\left(\sqrt{2}\right)^L},0,0,..,0\right)$$

$$W_3^L = \left(0,0,0,0,\frac{1}{\left(\sqrt{2}\right)^L},-\frac{1}{\left(\sqrt{2}\right)^L},0,0,..,0\right)$$

:

$$W_{N/2}^L = \left(0,0,\ldots,0,\frac{1}{\left(\sqrt{2}\right)^L},-\frac{1}{\left(\sqrt{2}\right)^L}\right)$$

where,

N defines the length of the signal to undergo the wavelet transform, and L =1,2,3,...,log $_2$(N).

3.5.8 INVERSE HAAR WAVELET TRANSFORMATION

The downsampled approximation and detailed signal are then upsampled before they can get reconstructed by the synthesis filters, which are described by the same scaling and wavelet coefficients. Hence, the first level Haar MRA of a signal f is defined as,

$$f = \left(\frac{a_1}{\sqrt{2}},\frac{a_1}{\sqrt{2}},\frac{a_2}{\sqrt{2}},\frac{a_2}{\sqrt{2}},\ldots,\frac{a_{N/2}}{\sqrt{2}},\frac{a_{N/2}}{\sqrt{2}}\right) + \left(\frac{d_1}{\sqrt{2}},\frac{d_1}{\sqrt{2}},\frac{d_2}{\sqrt{2}},\frac{d_2}{\sqrt{2}},\ldots,\frac{d_{N/2}}{\sqrt{2}},\frac{d_{N/2}}{\sqrt{2}}\right) \qquad eqn(3.21)$$

The signal *f* is expressed as the sum of two signals, which are approximation and detail signals.

Where, the Lth level approximation signal is defined as,

$$A^L = \left(\frac{a_1}{\sqrt{2}},\frac{a_1}{\sqrt{2}},\frac{a_2}{\sqrt{2}},\frac{a_2}{\sqrt{2}},\ldots,\frac{a_{N/2}}{\sqrt{2}},\frac{a_{N/2}}{\sqrt{2}}\right)$$

And the Lth level detail signal is defined as,

$$D^L = \left(\frac{d_1}{\sqrt{2}}, \frac{d_1}{\sqrt{2}}, \frac{d_2}{\sqrt{2}}, \frac{d_2}{\sqrt{2}}, \dots, \frac{d_{N/2}}{\sqrt{2}}, \frac{d_{N/2}}{\sqrt{2}}\right)$$

Hence, the algebraic expression of the approximation signal and detail signal are expressed as follows:

$$A^L = (f.V_1^L)V_1^L + (f.V_2^L)V_2^L + \cdots + \left(f.V_{N/2}^L\right)V_{N/2}^L \qquad eqn(3.22)$$

$$D^L = (f.W_1^L)W_1^L + (f.W_2^L)W_2^L + \cdots + \left(f.W_{N/2}^L\right)W_{N/2}^L \qquad eqn(3.23)$$

where, 'N' is the length of the signal f for the first level of decomposition or it is the length of the approximation signal which is passed to the subsequent level of decomposition and 'L' defines the number of the level of wavelet reconstruction. **[1, 8, 9]**

3.6 THE DAUB4 WAVELETS

The Daub4 wavelet transform is defined in essentially the same way as the Haar wavelet transform. The differences lie in the scaling signals and the wavelets. The scaling signals and the wavelets for the Daub4 transform is defined by four coefficients. **[1, 8, 9]**

Let the scaling numbers be $\alpha_1, \alpha_2, \alpha_3, \alpha_4$ and are defined as,

$$\alpha_1 = \frac{1+\sqrt{3}}{4\sqrt{2}}, \alpha_2 = \frac{3+\sqrt{3}}{4\sqrt{2}},$$

$$\alpha_3 = \frac{3-\sqrt{3}}{4\sqrt{2}}, \alpha_4 = \frac{1-\sqrt{3}}{4\sqrt{2}}.$$

3.6.1 APPROXIMATION SIGNALS

$$V_1^1 = (\alpha_1, \alpha_2, \alpha_3, \alpha_4, 0,0, \dots 0)$$

$$V_2^1 = (0,0, \alpha_1, \alpha_2, \alpha_3, \alpha_4, 0,0, \dots 0)$$

$$V_3^1 = (0,0,0,0, \alpha_1, \alpha_2, \alpha_3, \alpha_4, 0,0, \dots 0)$$

$$\vdots$$

$$V_{N/2-1}^1 = (0,0, \dots, 0, \alpha_1, \alpha_2, \alpha_3, \alpha_4)$$

$$V_{N/2}^1 = (\alpha_3, \alpha_4, 0,0, \dots 0, \alpha_1, \alpha_2)$$

The scaling signals are similar to each other except that in the sequence, the next scaling signal is translated by two time units compared to the previous scaling signal. The Daub4 approximation or scaling signal differs from the Haar approximation signal in the last approximation signal. The last approximation signal, which is, the N/2th scaling signal is computed by translating V_1^1 by N-2 time units. This process is called as *wrap-around*.

The natural basis of signals, $V_1^0, V_2^0, \dots, V_N^0$ are used to generate the first level approximation scaling as,

$V_m^1 = \alpha_1 V_{2m-1}^0 + \alpha_2 V_{2m}^0 + \alpha_3 V_{2m+1}^0 + \alpha_4 V_{2m+2}^0$, and the wrap-around is defined by $V_{n+N}^0 = V_N^0$.

The second level Daub4 approximation signals are defined as,

$V_m^2 = \alpha_1 V_{2m-1}^1 + \alpha_2 V_{2m}^1 + \alpha_3 V_{2m+1}^1 + \alpha_4 V_{2m+2}^1$ and the wrap-around is defined by $V_{n+N}^1 = V_N^1$.

And the generalized the next level Daub4 approximation signal is defined as, **[1, 8, 9]**

$$V_m^L = \alpha_1 V_{2m-1}^{L-1} + \alpha_2 V_{2m}^{L-1} + \alpha_3 V_{2m+1}^{L-1} + \alpha_4 V_{2m+2}^{L-1} \qquad eqn(3.24)$$

with the wrap-around defined as,

$$V_{n+N}^{L-1} = V_N^{L-1} \qquad eqn(3.25)$$

3.6.2 IMPORTANT PROPERTIES OF SCALING NUMBERS

$$\alpha_1^2 + \alpha_2^2 + \alpha_3^2 + \alpha_4^2 = 1 \qquad eqn(3.26)$$

This implies that each one-level approximation energy is 1. **[1, 8, 9]**

$$\alpha_1 + \alpha_2 + \alpha_3 + \alpha_4 = \sqrt{2} \qquad eqn(3.27)$$

3.6.3 WAVELET NUMBERS

$$\beta_1 = \frac{1-\sqrt{3}}{4\sqrt{2}}, \beta_2 = \frac{\sqrt{3}-3}{4\sqrt{2}},$$

$$\beta_3 = \frac{3+\sqrt{3}}{4\sqrt{2}}, \beta_4 = \frac{-1-\sqrt{3}}{4\sqrt{2}}.$$

The relations between wavelet numbers and the scaling numbers are:

$$\beta_1 = \alpha_4, \beta_2 = -\alpha_3, \beta_3 = \alpha_2 \; and \; \beta_4 = -\alpha_1, \qquad eqn(3.28)$$

The 1-level Daub4 wavelets $W_1^1, \dots, W_{N/2}^1$ are defined by,

$$W_1^1 = (\beta_1, \beta_2, \beta_3, \beta_4, 0, 0, \dots, 0)$$

$$W_2^1 = (0, 0, \beta_1, \beta_2, \beta_3, \beta_4, 0, 0, \dots, 0)$$

$$W_3^1 = (0,0,0,0,\beta_1,\beta_2,\beta_3,\beta_4,0,0,\dots,0)$$

:

$$W_{N/2-1}^1 = (0,0,\dots,0,\beta_1,\beta_2,\beta_3,\beta_4)$$

$$W_{N/2}^1 = (\beta_3,\beta_4,0,0,\dots,0,\beta_1,\beta_2)$$

All the above wavelets translate by two units compared to the previous wavelet of the same level and with the wrap-around for the last wavelet. The L-level Daub4 wavelets satisfy, **[1, 8, 9]**

$$W_m^L = \beta_1 V_{2m-1}^{L-1} + \beta_2 V_{2m}^{L-1} + \beta_3 V_{2m+1}^{L-1} + \beta_4 V_{2m+2}^{L-1} \qquad eqn(3.29)$$

3.6.4 IMPORTANT PROPERTIES OF WAVELET NUMBERS

1) All the Daub4 wavelets have energy 1.

$$\beta_1^2 + \beta_2^2 + \beta_3^2 + \beta_4^2 = 1 \qquad eqn(3.30)$$

2) Each fluctuation value $d_m = f.W_m^L$ is viewed as a differencing operation on the values of *f*, as,

$$\beta_1 + \beta_2 + \beta_3 + \beta_4 = 0 \qquad eqn(3.31)$$

3) $0.\beta_1 + 1.\beta_2 + 2.\beta_3 + 3.\beta_4 = 0 \qquad eqn(3.32)$

4) If a signal f is approximately linear over the support of a L-level Daub4 wavelet W_m^L, then the L-level fluctuation value is approximately zero. **[1, 8, 9]**

3.6.5 INVERSE WAVELET TRANSFORM

The approximation signal and detail signal after Daub4 inverse wavelet transform are expressed as follows:

$$A^L = (f.V_1^L)V_1^L + (f.V_2^L)V_2^L + \cdots + \left(f.V_{N/2}^L\right)V_{N/2}^L \qquad eqn(3.33)$$

$$D^L = (f.W_1^L)W_1^L + (f.W_2^L)W_2^L + \cdots + \left(f.W_{N/2}^L\right)W_{N/2}^L \qquad eqn(3.34)$$

where, 'N' is the length of the signal f for the first level of decomposition or it is the length of the approximation signal which is passed to the subsequent level of decomposition and 'L' defines the number of the level of wavelet reconstruction. **[1, 8, 9]**

3.6.6 MULTIRESOLUTION ANALYSIS

Multiresolution analysis is the synthesis of a low resolution discrete signal by successively adding on details to create a signal with the finest resolution.

Hence, according to the multiresolution analysis, the reconstructed signal is defined as,

$$f^L = A^L + D^L + D^{L-1} + .. + D^1 \qquad eqn(3.35)$$

where, 'L' defines the decomposed level from which the signal is getting reconstructed by MRA.

and L= L, L-1, L-2,..., 1. **[1, 8, 9]**

3.6.7 CONSERVATION AND COMPACTION OF ENERGY

3.6.7.1 CONSERVATION OF ENERGY

An important property of Haar wavelet transform is that it conserves the energies of signals. The energy of the signal is defined as the sum of the squares of its values. Thus, the energy ε_f of a signal *f* is defined by **[9]**

$$\varepsilon_f = f_1^2 + f_2^2 + \cdots + f_N^2 \qquad eqn(3.36)$$

After m-level of decomposition, energy of trend or approximation signal is defined as,

$$\varepsilon_a^L = a_1^2 + a_2^2 + \cdots + a_L^2 \qquad eqn(3.37)$$

$$\varepsilon_{d^m}^L = d_1^2 + d_2^2 + \cdots + d_L^2, \qquad at\ m^{th}\ level\ of\ decomposition \qquad eqn(3.38)$$

Thus, the detail signal is the summation of all the levels of decomposed detail signals.

$$\varepsilon_d^L = \varepsilon_{d^m}^L + \varepsilon_{d^{m-1}}^L + \cdots + \varepsilon_{d^1}^L \qquad eqn(3.39)$$

where, $L = \frac{2^{level}}{2}$, and level=$\log_2$N,$\log_2$(N/2),....,1

Thus, the cumulative energy profile is defined as,

$$\varepsilon_f = \varepsilon_{a^m} + \varepsilon_{d^m} + \varepsilon_{d^{m-1}} + \cdots + \varepsilon_{d^1} \qquad eqn(3.40)$$

3.6.7.2 COMPACTION OF ENERGY

The energy of the trend subsignal accounts for a large percentage of the energy of the transformed signal. This will occur whenever the magnitudes of the detail signal are significantly smaller than the approximation signal. **[9]**

3.6.8 CUMULATIVE ENERGY PROFILE

By Heisenberg's Uncertainty Principle, it is impossible to localize a fixed amount of energy into an arbitrarily small time interval. This is the reason why the energy drops when the number of level decomposition increases. The cumulative energy profile of a signal *f* is defined by:

$$\left(\frac{f_1^2}{\varepsilon_f}, \frac{f_1^2 + f_2^2}{\varepsilon_f}, \frac{f_1^2 + f_2^2 + f_3^2}{\varepsilon_f}, \ldots, 1\right). \qquad eqn(3.41)$$

The cumulative energy profile of *f* provides the details of the accumulation of energy in the signal as time proceeds. **[9]**

3.7 SIGNAL COMPRESSION

There are two basic categories of compression techniques.

1) Lossless compression and
2) Lossy compression

Lossless compression achieves completely error free decompression of the original signal and the lossy compression produces inaccuracies in the decompressed signal. These inaccuracies are so small to be imperceptible. The lossy compression has an advantage of higher compression rate compared to lossless compression. **[8, 11]**

3.7.1 METHOD OF WAVELET TRANSFORM COMPRESSION

Step 1: Wavelet transform of the signal is performed.

Step 2: The values of the wavelet transform which lie below the threshold value should set equal to 0.

Step 3: Transmit only the significant values of the transform.

Step 4: The inverse wavelet transform of the data at the receiving end is performed. The insignificant values which are not transmitted are assigned zeros. This decompression step produces an approximation of the original signal. **[11]**

3.8 TYPE OF NOISE

Random Noise: This noise signal is highly oscillatory, its values switches rapidly between values above and below the mean value.

Pop Noise: This noise is perceived as randomly occurring, isolated ‘pops’. This noise model is made by adding few non-zero values to the original signal at isolated locations.

Localized Random Noise: This noise is a short-lived disturbance in the environment during transmission of the signal. **[13]**

3.9 THRESHOLD METHOD OF WAVELET DENOISING

Contaminated signal=transmitted signal + noise signal

1) A high percentage of energy of the transmitted signal is captured using appropriate thresholding, and the transformed signals which are above the threshold are captured.
2) The noise signal's transform values have their magnitudes below the threshold value. These values are then made zero.
3) Both the modified transformed values are then passed for inverse wavelet transformation.

The effectiveness of the denoising is that the transform compresses the energy of the original signal into few high-energy values and the added noise transforms into low-energy values. **[7, 8, 11]**

CHAPTER 4

4 THRESHOLDING CONCEPTS FOR DENOISING SIGNALS

4.1 WAVELET DENOISING

Considering a system with input additive noise as given below:

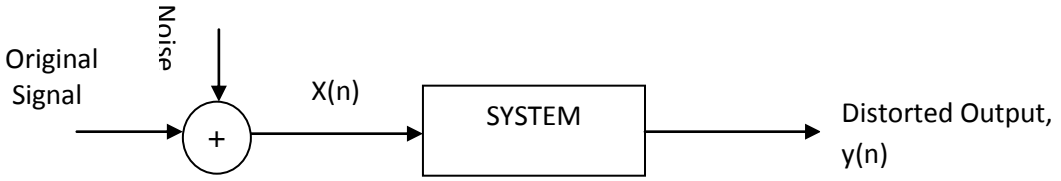

Fig 4.1: Schematic representation of a system with noisy input and output

$$X(n) = s(n) + w(n) \quad for\ n = 0,1, \dots, N-1 \qquad eqn(4.1)$$

where s(n) is the noise free signal,and w(n) is the added noise at the input which gives the distorted signal x(n).

When this signal is measured from a measuring instrument, the noisy signal gets convoluted with the system transfer function to generate even more distorted signal at the output.

To eliminate the noise in the signal and for the removal of the distortion caused due to system transfer function, we use varied transformation techniques like Fourier transformation, Wavelet transformation, etc. Fourier transformation removes the noise efficiently by using a linear time-invariant filter, only if it is out of the band of the

useful signal. The deconvolution technique doesn't work properly if the noise band overlaps with the signal spectrum. **[16, 18, 28, 29. 34, 36]**

However, with Wavelet transformation, the denoising approach is done by examining the amplitude of the wavelet coefficients. The assumption is that, the amplitude of the noisy wavelet coefficients are generally smaller than the amplitude of the main signal coefficients. This localising property of the wavelet aids thresholding and shrinking of the wavelet coefficients to separate the noise and the desired signal. Due to the introduction of the thresholding function in the wavelet denoising, this technique is a non-linear filtering unlike traditional linear filtering approaches. **[2, 7, 8, 33]**

4.2 WAVELET ANALYSIS

Three basic steps which are required for denoising the signals are: decomposition, thresholding and reconstruction.

The main function which differentiates the extent of denoising is the kind of thresholding done for the wavelet coefficients. The thresholding step is divided into two steps; the first step defines the threshold and the second step defines the way to use the threshold on the wavelet coefficients to get the modified coefficients for the estimating the noiseless signal. **[8, 23]**

4.3 CHOICE OF THRESHOLDING

The denoising algorithms are divided into linear and non-linear methods. The linear method is independent of the amplitude of the wavelet coefficients and hence, the coefficient size is not taken into account. It assumes that the noise is only found in the finer scaled coefficients and not in coarse scaled coefficients. Hence, for such type of a signal, hard thresholding is done.

The non-linear method is based on the idea that the white noise is found in every coefficient of all scales. This method uses either hard- or soft-thresholding depending on the amount of reduction of the noise factor from the investigated signal.

Sometimes, the type of thresholding entirely depends upon the application and the kind of resolution expected from the result. The author uses the linear method of denoising algorithm and soft thresholding. As, some amount of fluctuations are necessary in the final signal, such a kind of option is chosen. **[7, 10, 20, 21, 22]**

4.4 THRESHOLD CALCULATION

UNIVERSAL THRESHOLD:
It is a fixed form threshold, which is defined as,

$$\lambda = \sigma\sqrt{2\log(n)} \qquad eqn(4.2)$$

where, n denotes the length of the signal and σ is the standard deviation of the additive noise and is defined as

$$\sigma = \frac{Median(|w_{j,k}|)}{0.6745} \qquad eqn(4.3)$$

The statistical parameter σ, is entirely signal and application dependent. This can also be chosen as, median, mean average deviation, median average deviation and variance. The type of statistical parameter chosen, changes the threshold and hence, the result of the modified signal. **[21, 22]**

4.5 THRESHOLDING FUNCTIONS

Hard-thresholding: The standard hard threshold function gives a sudden change at the point of threshold. The wavelet coefficients just below the threshold are made 0 and the coefficients above the threshold are remained the same. This leads to the sharp

transition in the image or a signal removing smoothness in the continuous signal or the image **[21, 22]**.

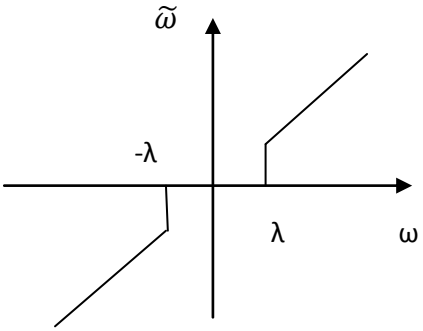

$$\widetilde{w}_{j,k} = \begin{cases} w_{j,k}, |w_{j,k}| \geq \lambda \\ 0, |w_{j,k}| < \lambda \end{cases}$$

Fig 4.2: Hard-thresholding

Soft-thresholding:

$$\widetilde{w}_{j,k} = \begin{cases} sgn(w_{j,k}).(|w_{j,k}| - \lambda), & |w_{j,k}| \geq \lambda \\ 0, & |w_{j,k}| < \lambda \end{cases} \qquad eqn(4.4)$$

where sgn(*) is used as the sign function.

$$sgn(n) = \begin{cases} 1, n > 0 \\ -1, n < 0 \end{cases} \qquad eqn(4.5)$$

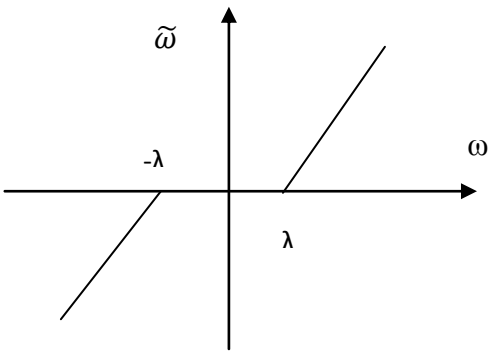

Fig 4.3: Soft-Thresholding

To avoid such sharp transitions in the signal, the soft thresholding is done, resulting in smoother transitions. Here, the coefficients above the threshold limit are reduced by

the same thresholding constant. This gives a view of reducing the full set of coefficients by the threshold value. **[6, 21, 22]**

Hyperbolic thresholding: **[21, 22]**

It is also called as "almost hard thresholding".

$$y_{hyper}(n) = \begin{cases} sgn(y(n))\sqrt{y^2(n) - \delta^2} & if\ |y(n)| > \delta \\ 0 & if\ |y(n)| \leq \delta \end{cases} \qquad eqn(4.6)$$

4.6 ANALYSIS

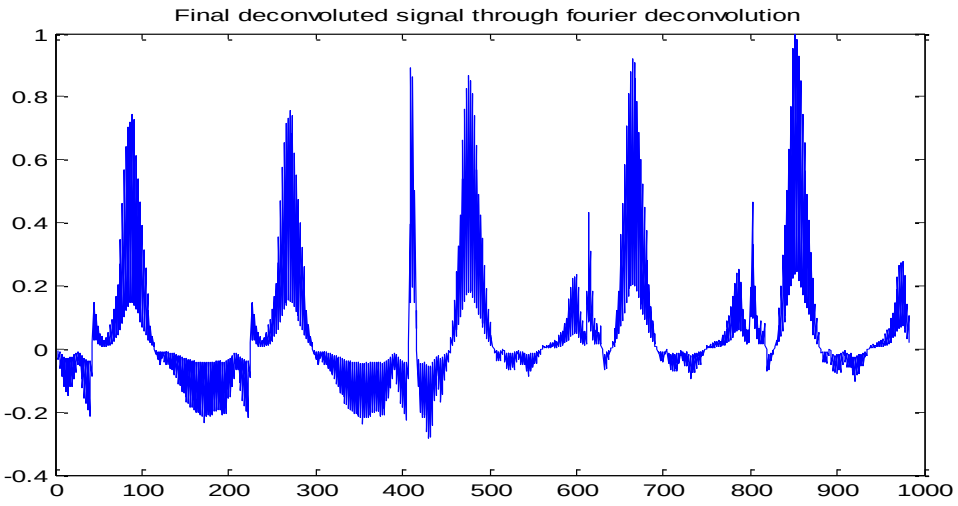

Fig 4.4: Noisy ECG signal after Fourier regularized deconvolution

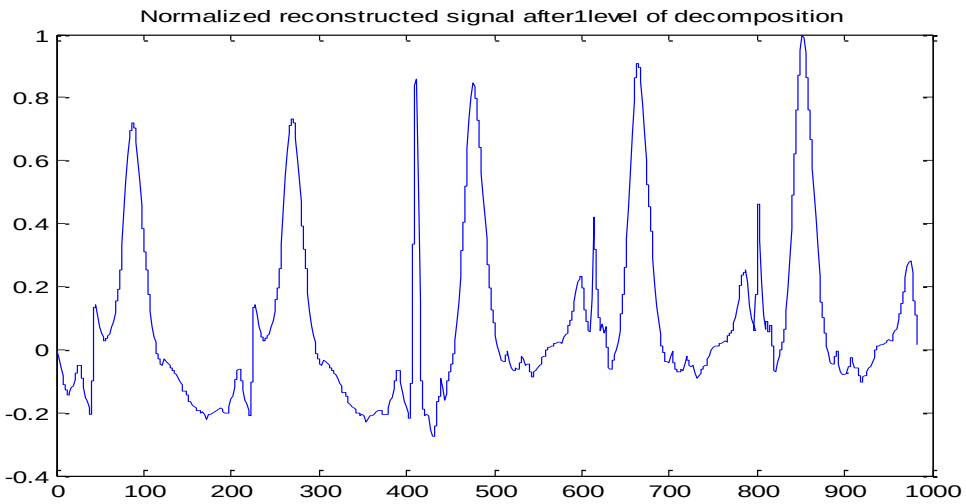

Fig 4.5: The denoised signal after wavelet transformation using soft thresholding

Thus, the desired signal is totally dependent upon the threshold level and the type of thresholding.

CHAPTER 5

5 ALGORITHM & SYSTEM IDENTIFICATION

5.1 ALGORITHM TO IDENTIFY THE TYPE OF SYSTEM AND INPUT

1) The clean signal s(n) of length N gets corrupted with the noise w(n) of standard normal distribution N(0,σ^2), producing a noisy excitation signal for the measuring system.
2) The noisy excitation signal and the system characteristic function gets convoluted to generate a distorted output signal.
3) This distorted output signal is passed through the regularized Fourier deconvolution with a properly tuned regularization parameter 'α' according to the application.
4) The output of the regularized Fourier deconvolution produces a signal which would have deconvoluted the system characteristics and produce an approachable signal towards the desired SNR.
5) Hence, in the process of improving SNR, the noisy signal is passed through the wavelet denoising algorithm.
6) The noisy signal x(n) is transformed to the wavelet domain and the wavelet coefficients $w_{j,k}$ are obtained, with scales j =1…J and time indices k=1…N;
7) The soft- or hard-thresholding is applied to $w_{j,k}$ using universal thresholding function $\lambda = \sigma\sqrt{2 * \log_{10}(N)}$ and the processed wavelet coefficients $\widetilde{w}_{j,k}$ are obtained.

8) The inverse wavelet transformation is performed on the newly processed wavelet coefficients, $\widetilde{w}_{j,k}$ to obtain the denoised signal, $\tilde{x}(n)$.
9) The trade-off between the compression and the distortion is then chosen for the application dependent retrieval of the signal.

Two wavelets are used by the author to denoise the noisy output signal by the regularized Fourier deconvolution and they are Haar wavelets and the Daubechies4 wavelets.

The Haar basis use two coefficients to represent the wavelet and the Daub4 basis use four coefficients to represent its wavelet. As the number of coefficients increases, the basis represents the original signal very well. Hence, the Daub4 wavelets represent the desired signal very well compared to the Haar wavelets. **[8]**

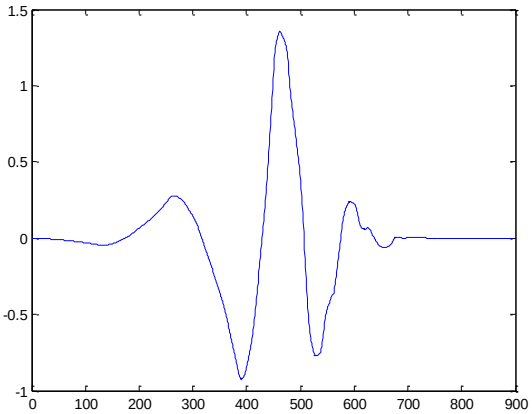

Fig 5.1: Daubechies 4 wavelet with continuous contact support.

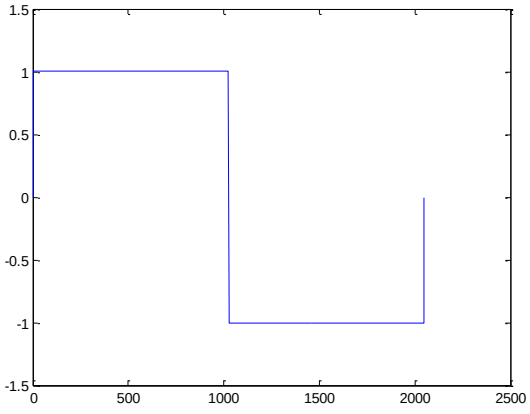

Fig 5.2: Haar wavelet with non-smooth contact support.

5.2 Desirable features of Wavelets:

i. Generate orthogonal and biorthogonal basis functions in space L^2 through dilation and translation.

ii. Local in both time and frequency domains.

iii. Vanishing moments:

$$\int_{-\infty}^{\infty} t^k \psi(t) dt = 0 \qquad for\ k = 0,1,..,k-1 \qquad eqn(5.1)$$

5.3 BASIC BLOCK DIAGRAM

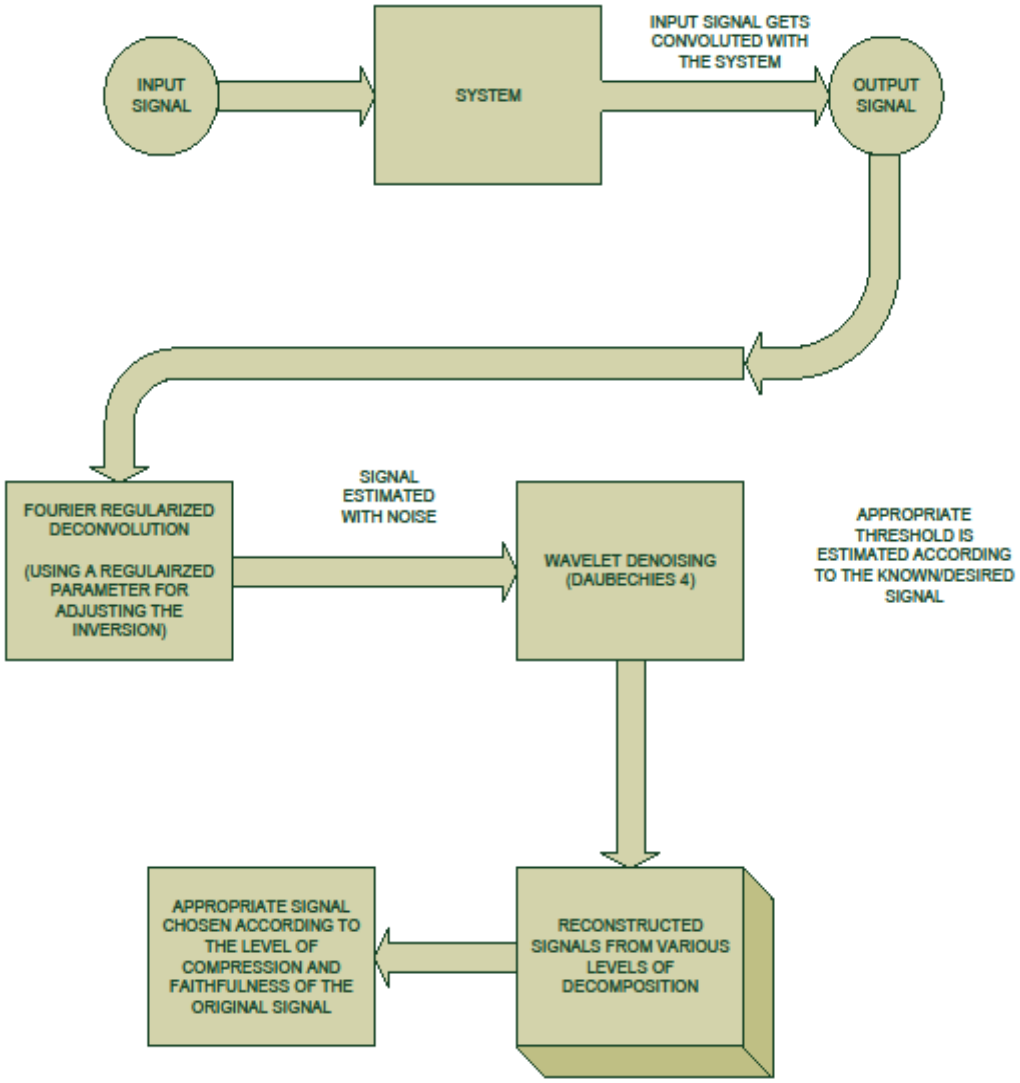

Fig 5.3: Block diagram of the implemented algorithm

5.4 FLOWCHART

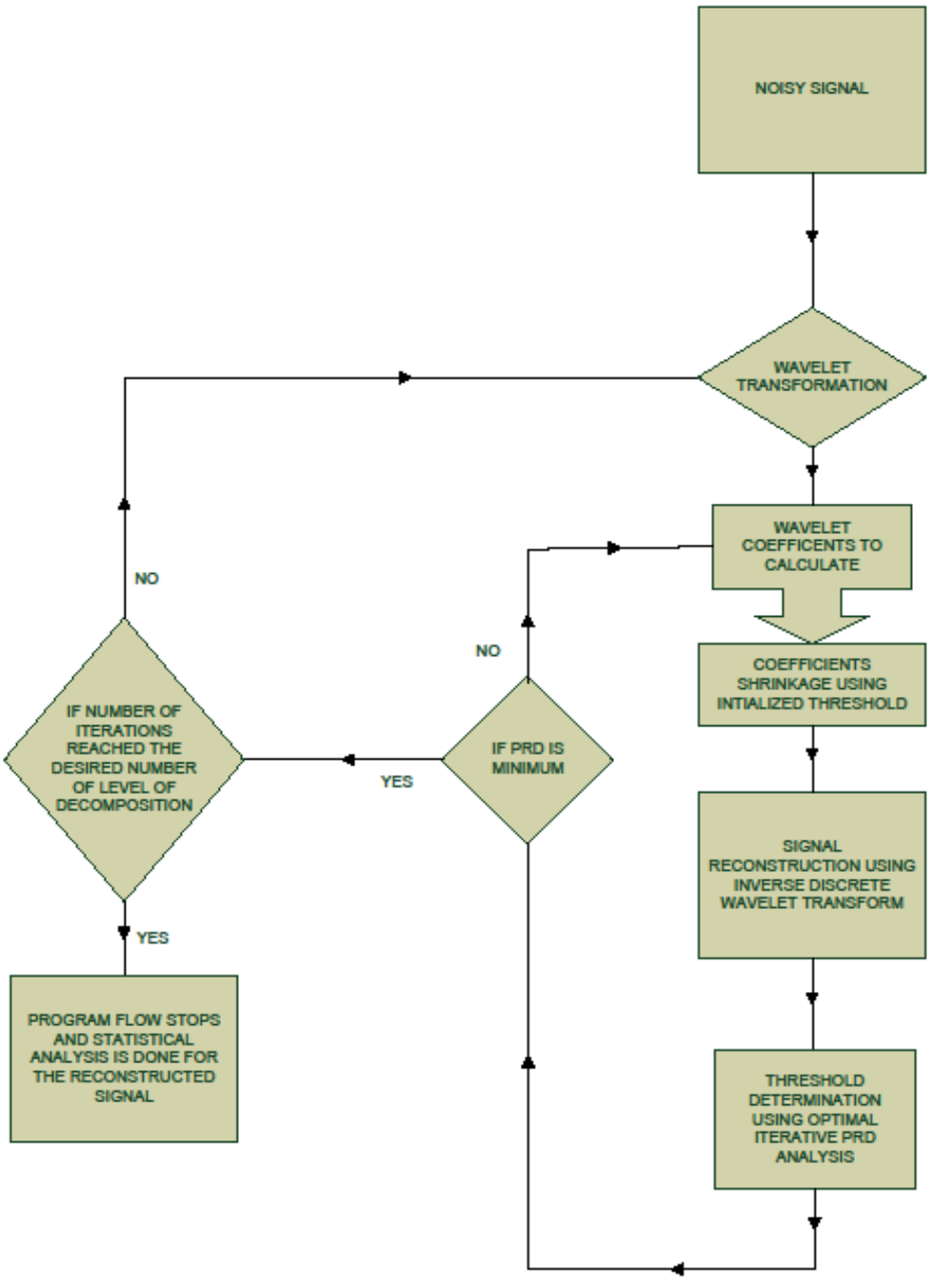

Fig 5.4: Flow chart of the algorithm

5.5 HAAR ANALYSIS

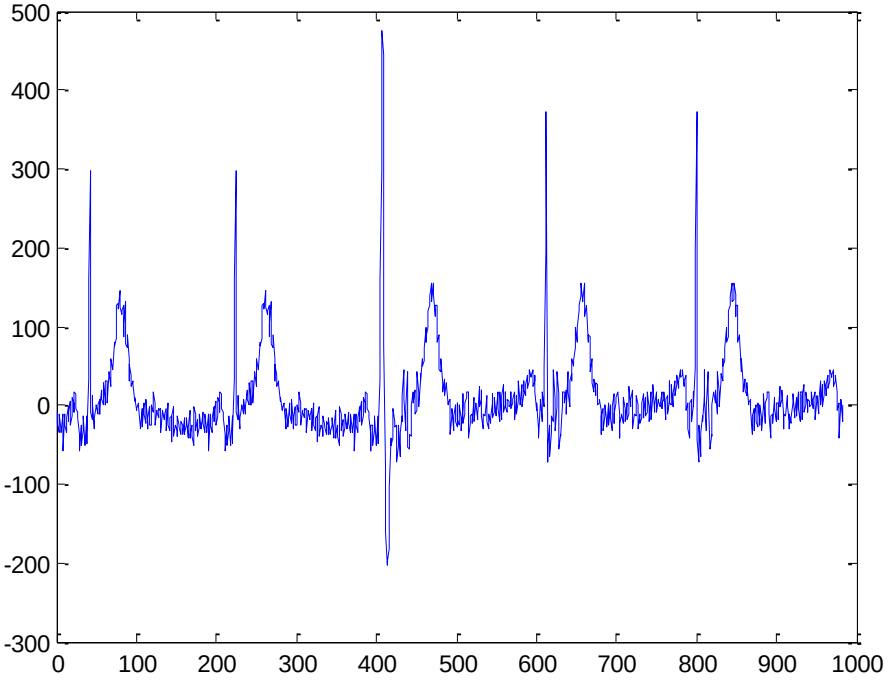

Fig 5.5: Original ECG signal

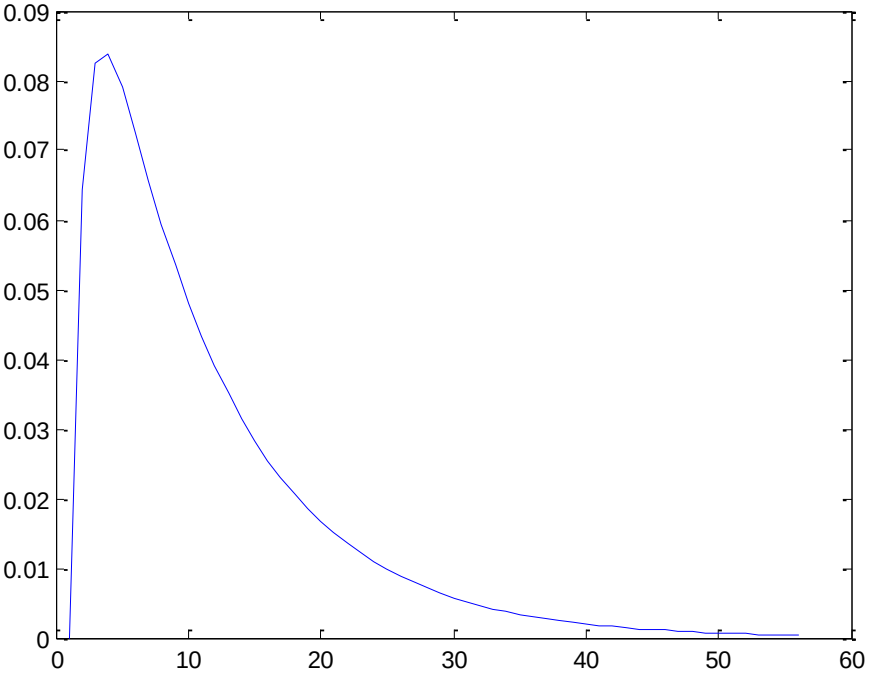

Fig 5.6: Impulse transfer function of the system

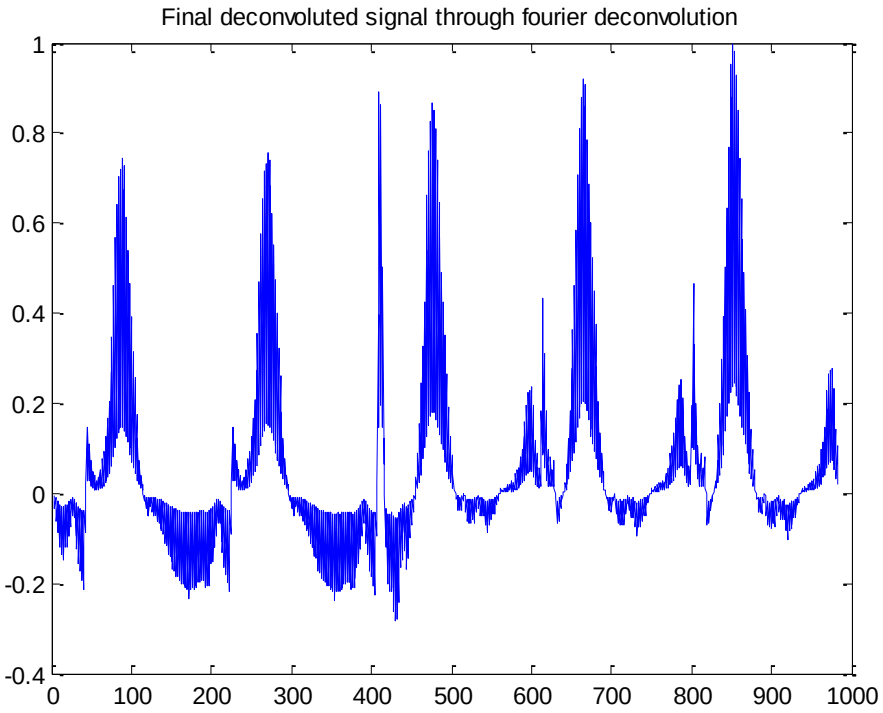

Fig 5.7: Fourier deconvoluted noisy signal output

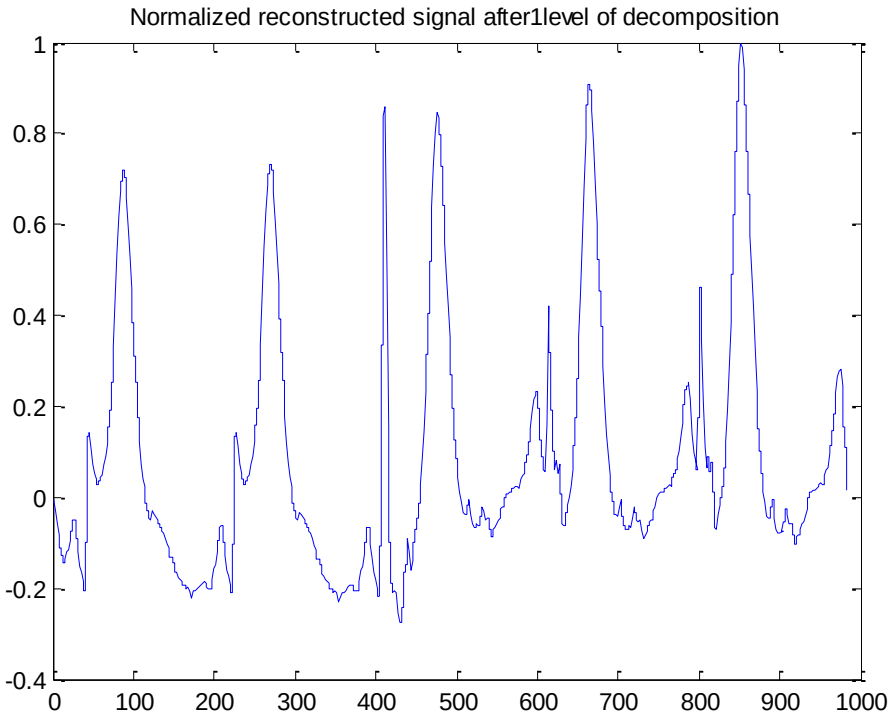

Fig 5.8: Normalized reconstructed signal by 1 level Haar wavelet transformation.

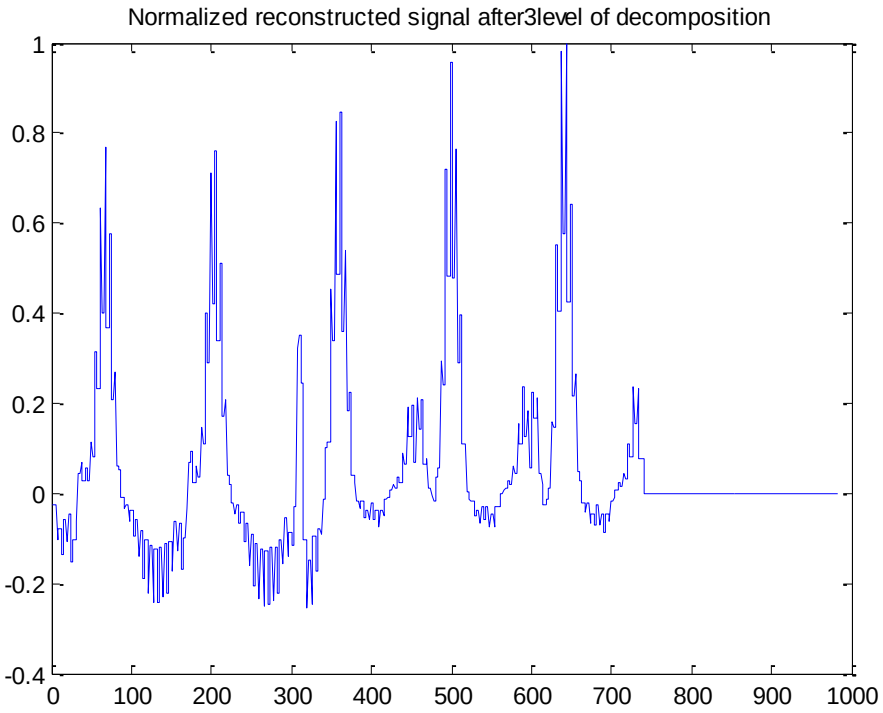

Fig 5.9: Normalized reconstructed signal after 3 levels of Haar wavelet transformation.

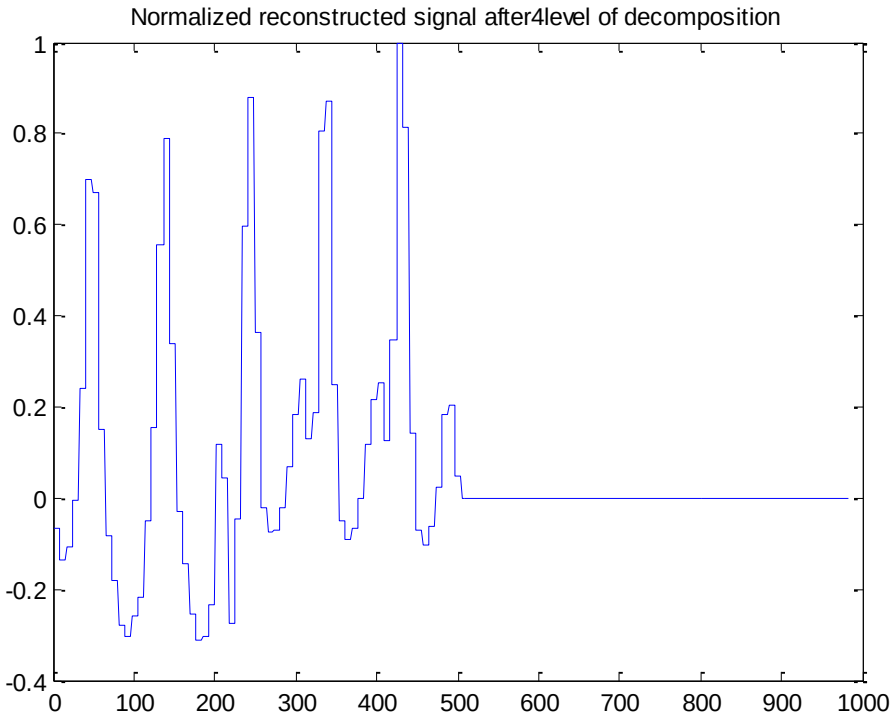

Fig 5.10: Normalized reconstructed signal after 4 levels of Haar wavelet transformation.

5.6 DAUBECHIES 4 ANALYSIS

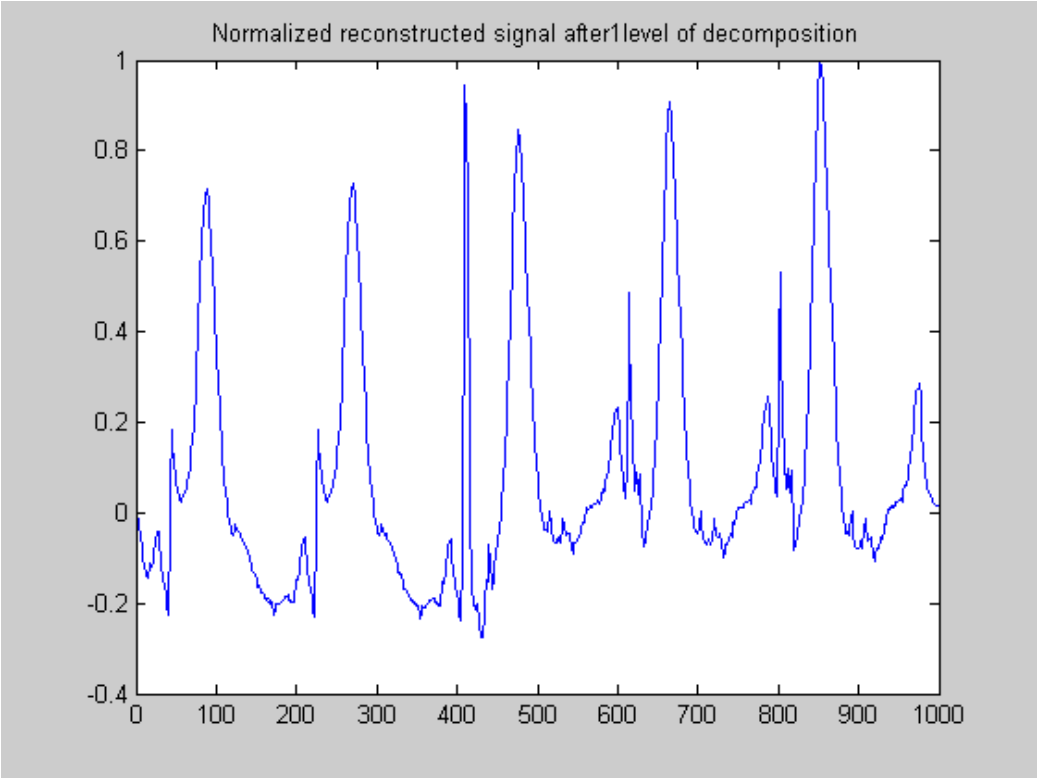

Fig 5.11: Normalized reconstructed signal after 1 level of Daub4 wavelet transformation

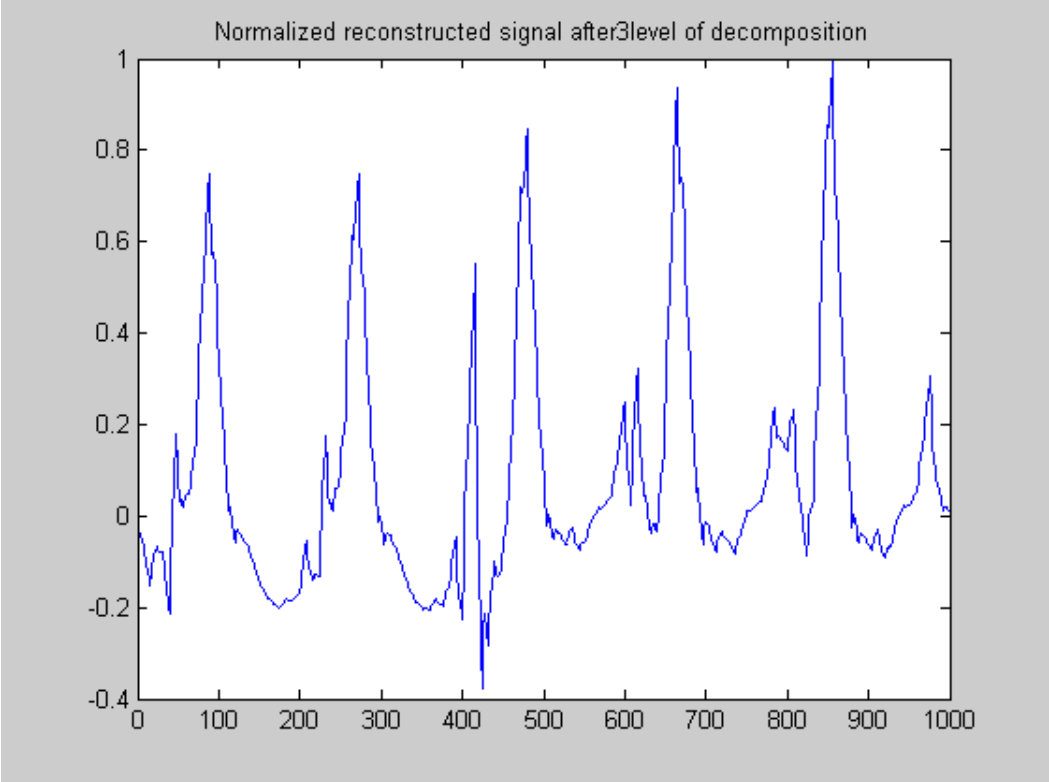

Fig 5.12: Normalized reconstructed signal after 3 levels of Daub4 wavelet transformation

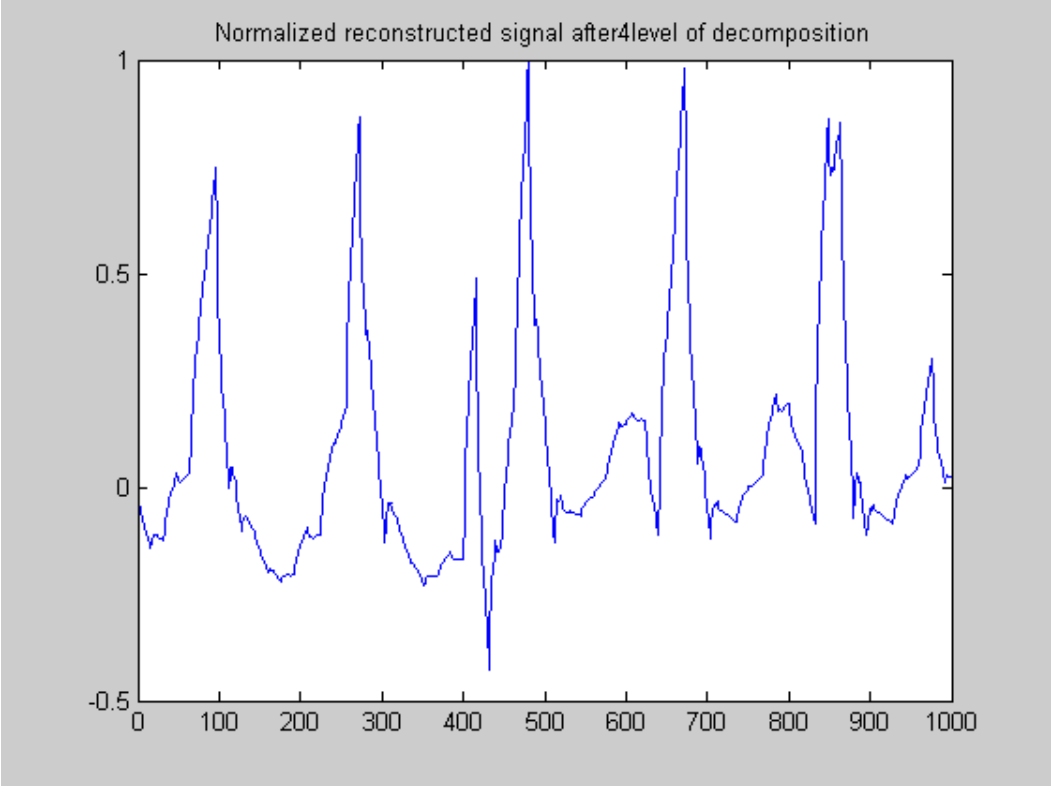

Fig 5.13: Normalized reconstructed signal after 4 levels of Daub4 wavelet transformation

5.7 CONCLUSIONS

The Fourier and wavelet coupled system identification algorithm is executed in MATLAB 2007b. The algorithm identifies the type of the system which can produce the desired signal.

After Fourier deconvolution produces a noisy output, the wavelet transform denoise this noisy signal by subtracting the amplitude of the wavelet coefficients with the calculated threshold. At each level, there is some reduction in the amplitude of the wavelet coefficients, which leads to the compression of the signal. Thus, the desired denoised signal with the optimal compression ratio is the objective of the wavelet denoising algorithm.

Apart from the generalized decision to choose a proper trade-off between the compression ratio and the SNR, the choice of the wavelet transform also approaches to the desired signal.

This choice of the type of wavelet transform is application dependent. The reconstructed signals using Haar transform are shown in the ***figures (5.8, 5.9 and 5.10).*** It is observed that the Haar wavelets which are represented by only two numbers very roughly trace the desired signal. As the number of levels of decomposition increases, the investigated signal is compressed at each level which is observed as distortions and improper trace of the signal. The compression is because of the reduction in the length of the signal by a power of two. The reconstructed signals using Daub4 transform are shown in the ***figures (5.11, 5.12 and 5.13).*** As it is observed, the Daub4 wavelets are represented four coefficients; hence, the signal is well traced compared to the Haar transform. The investigated signal, even after several stages of compression by Daub4 transform, represents the desired signal quite well compared to the Haar transform.

5.8 SYSTEM IDENTIFICATION

The system to get the desired signal by the combined effect of Fourier deconvolution and wavelet denoising is determined using System Identification Toolbox of MATLAB 2008b.

Thus, the system identified is:

$$G(s) = -0.0048911 \times \left(\frac{1 + 1.0543s}{(1 + 0.0955s + 0.1311s^2)(1 + 0.57768s)}\right), \quad eqn(5.2)$$

And its best fit is 89.14%.

5.9 SYSTEM CHARACTERISTICS

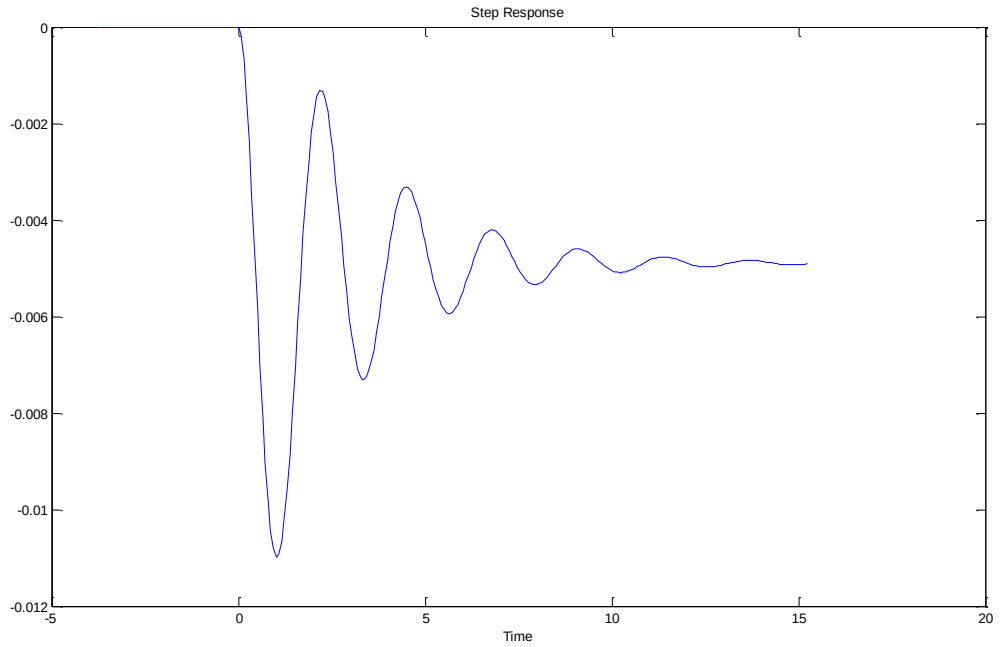

Fig 5.14: Damping oscillatory step response of the system

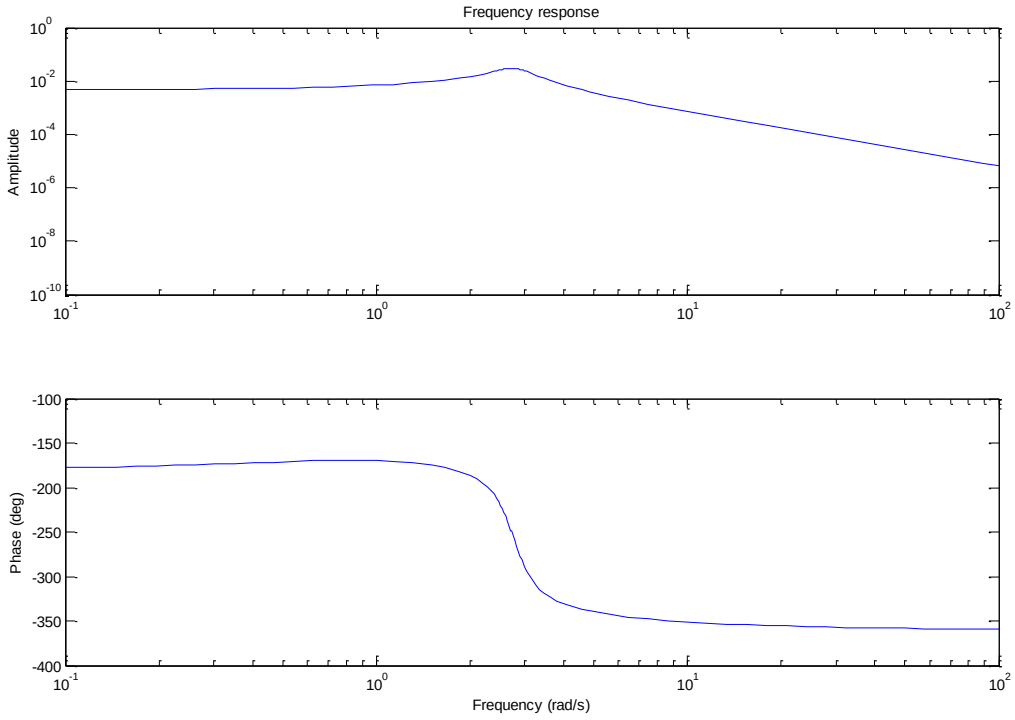

Fig 5.15: Bode plot of the system

There are three cut-off frequencies which determines the characteristics of the system and it is a type 0 and order 3 system.

The phase of the system starts from -180^0, which starts with a phase shift because of the involvement of the Fourier deconvolution in the first part of the algorithm and rolls off to end at -360^0 as it is a third order system.

The magnitude of the system experiences an overshoot at the cross-over frequency of the second order system, which is 2.77 rad/sec. The damping factor is calculated to be 0.13 and this small value gives the magnitude response an overshoot at 2.77 rad/sec and a sharp turn in the phase plot to approach -360^0.

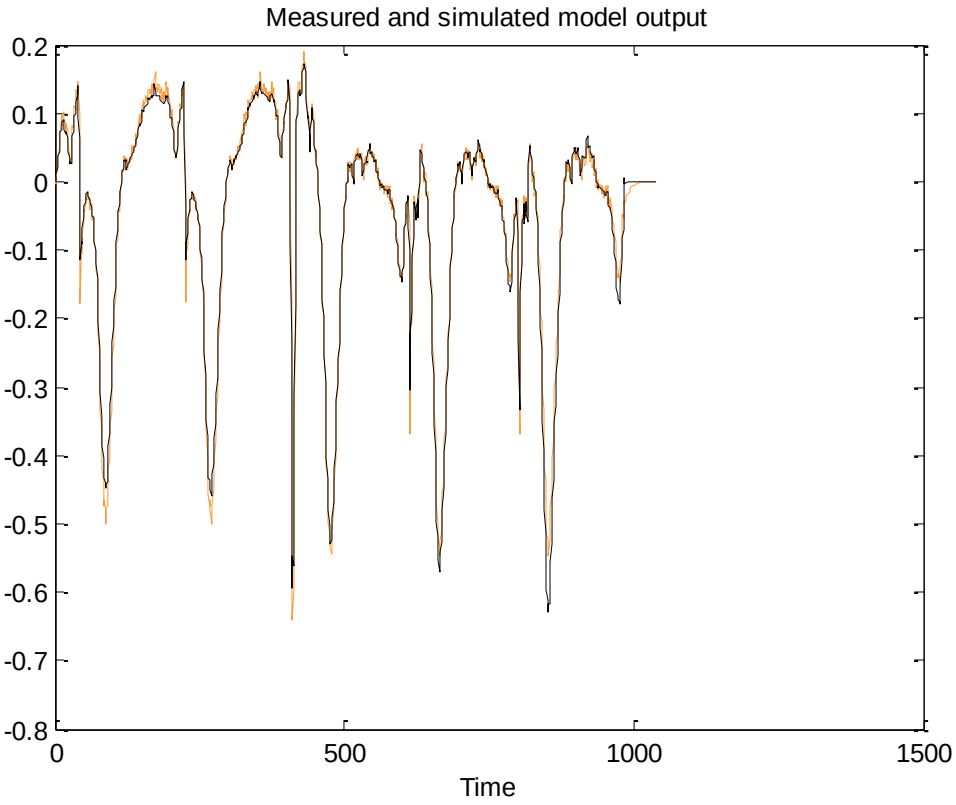

Fig 5.16: Model output from the System Identification Toolbox

Thus, the above figure justifies that the simulated model output almost matches the measured model giving 89.14% fit.

CHAPTER 6

6. PERFORMANCE ANALYSIS

6.1 APPROXIMATION COEFFICIENTS USING DAUB4 TRANSFORMATION

The signal is transformed into approximation coefficients and detail coefficients after passing it through the wavelet transformation.

Approximation coefficients, give the trend of the signal. The number of coefficients reduces by the power of two with each increase in the level of decomposition. The magnitude of these coefficients is for the analysis and modifications only when non-linear thresholding is done.

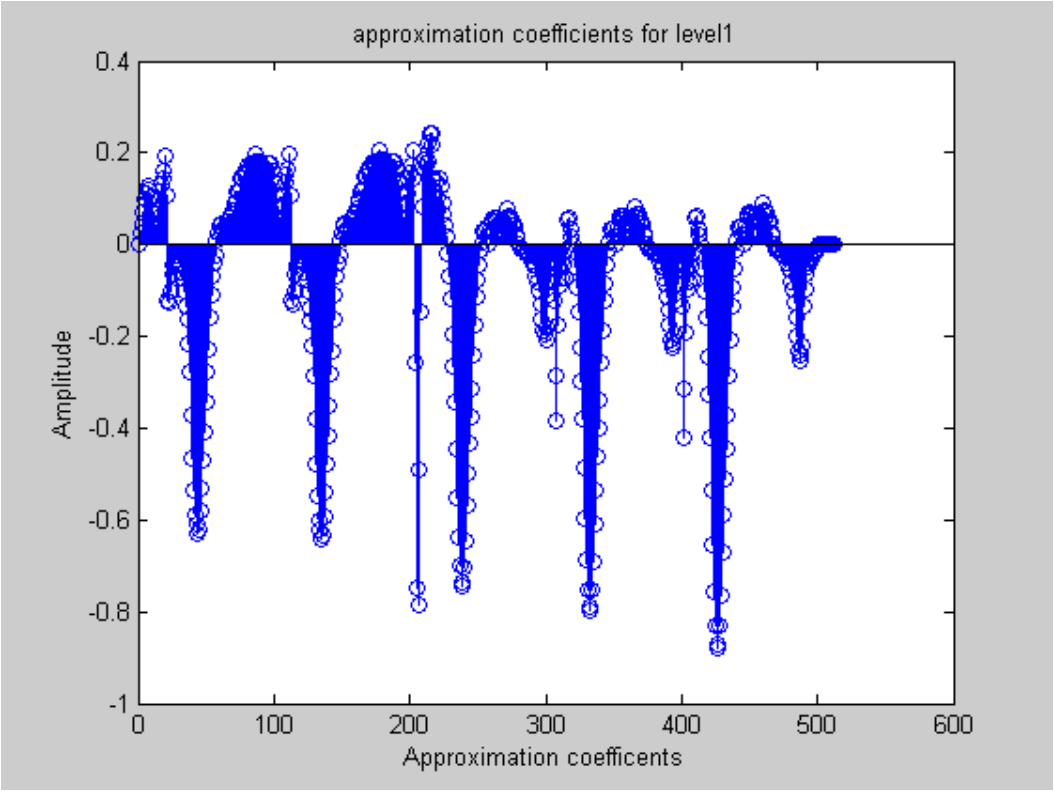

Fig 6.1: Approximation coefficients after 1 level of Daub4 decomposition.

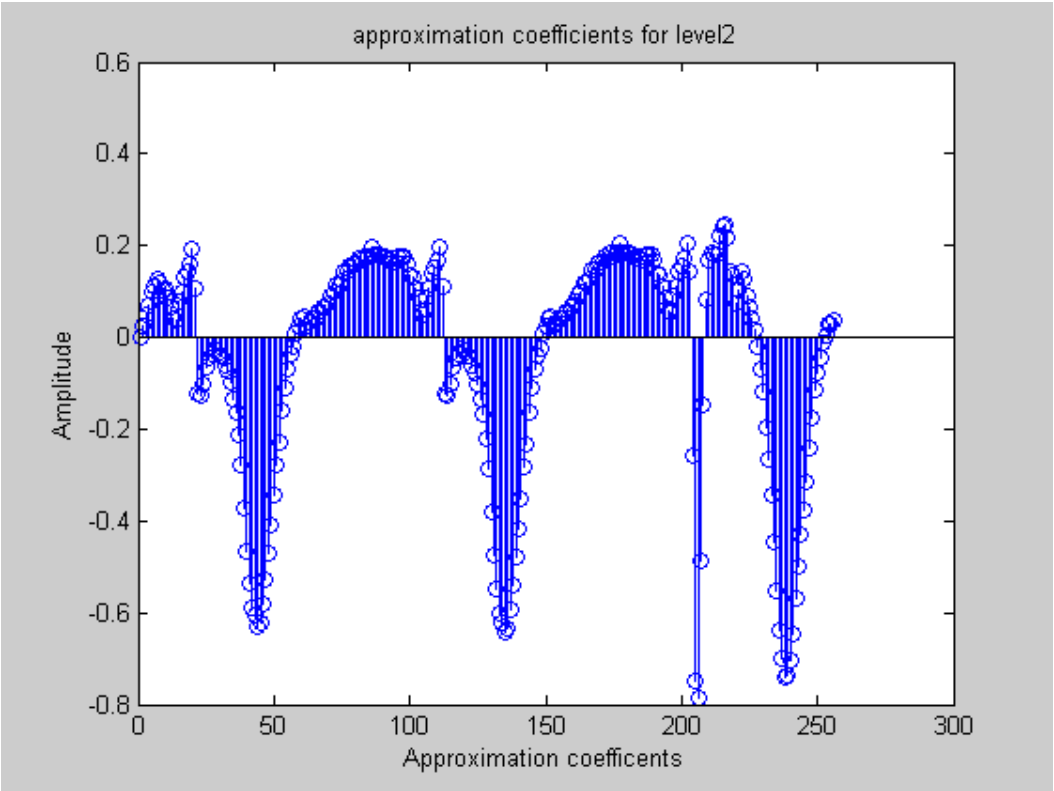

Fig 6.2: Approximation coefficients after 2 levels of Daub4 decomposition.

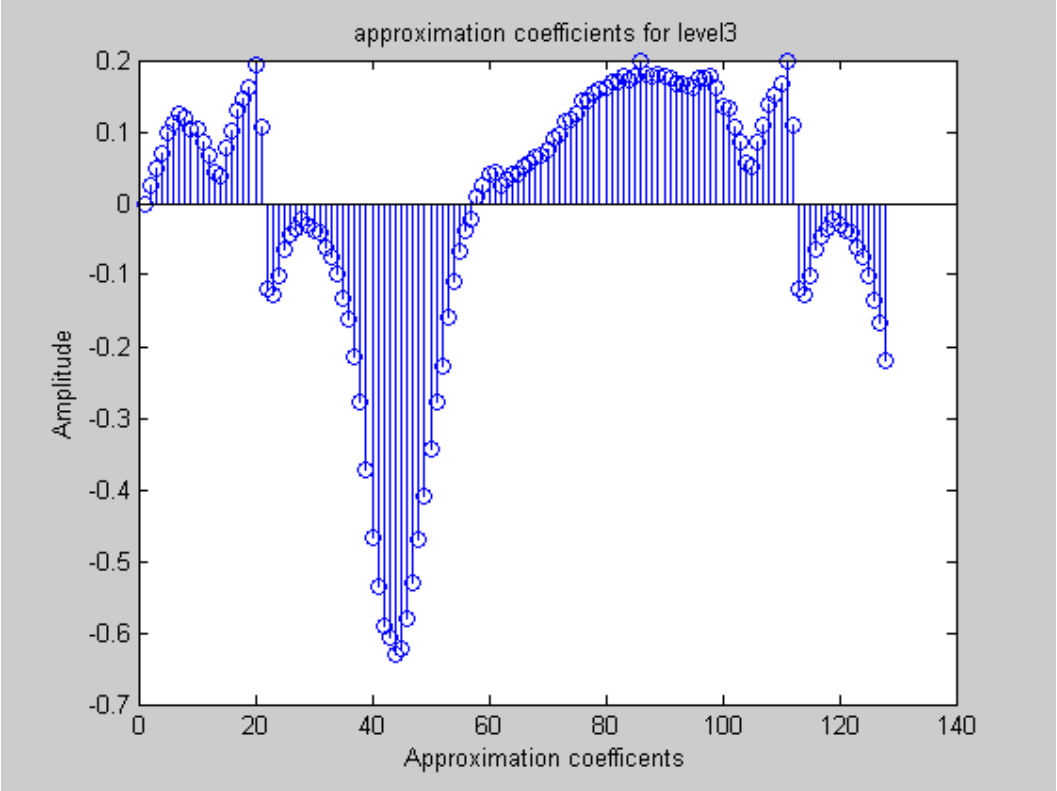

Fig 6.3: Approximation coefficients after 3 levels of Daub4 decomposition.

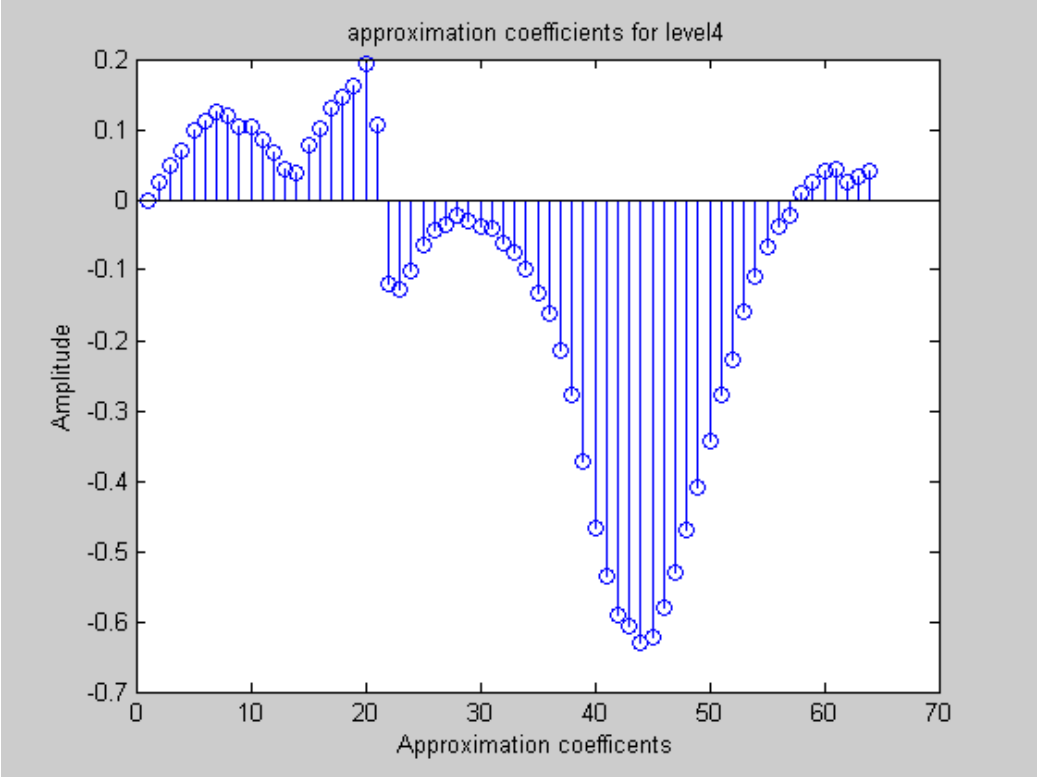

Fig 6.4: Approximation coefficients after 4 levels of Daub4 decomposition.

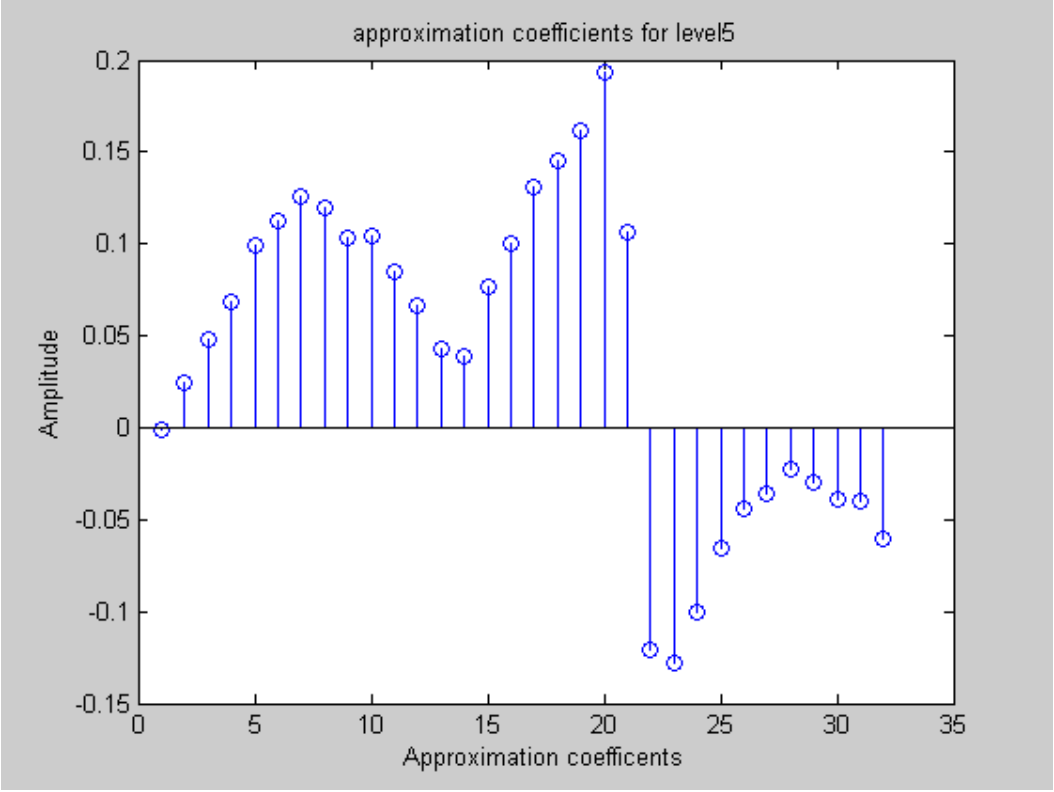

Fig 6.5: Approximation coefficients after 5 levels of Daub4 decomposition.

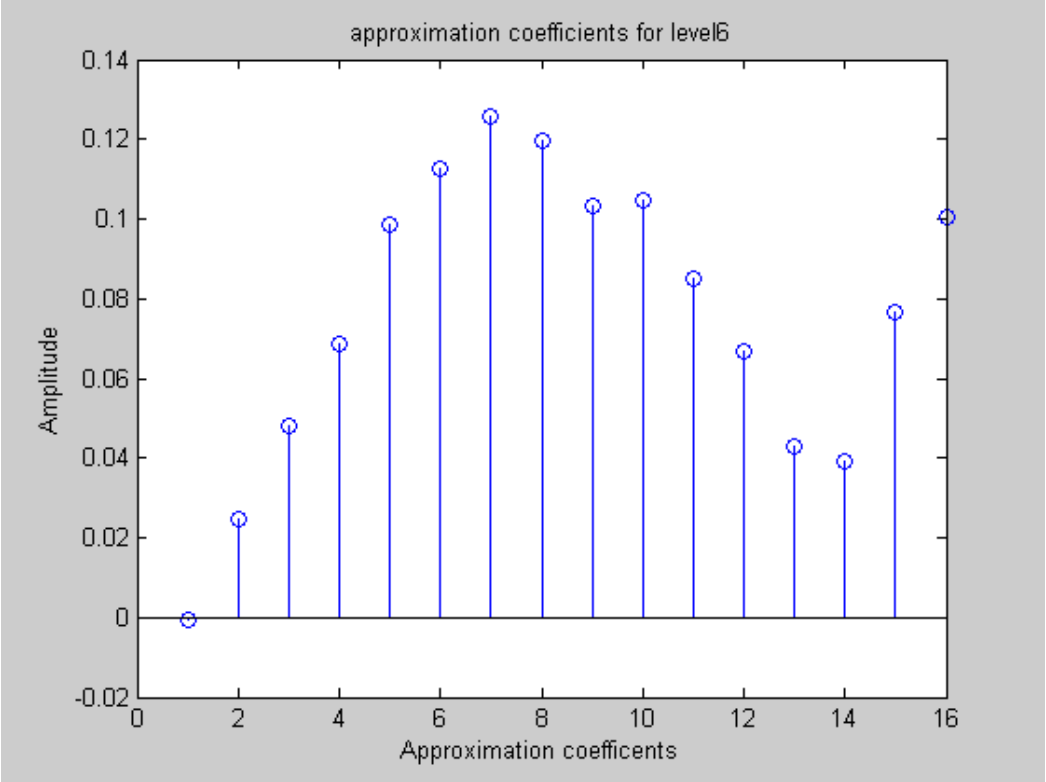

Fig 6.6: Approximation coefficients after 6 levels of Daub4 decomposition.

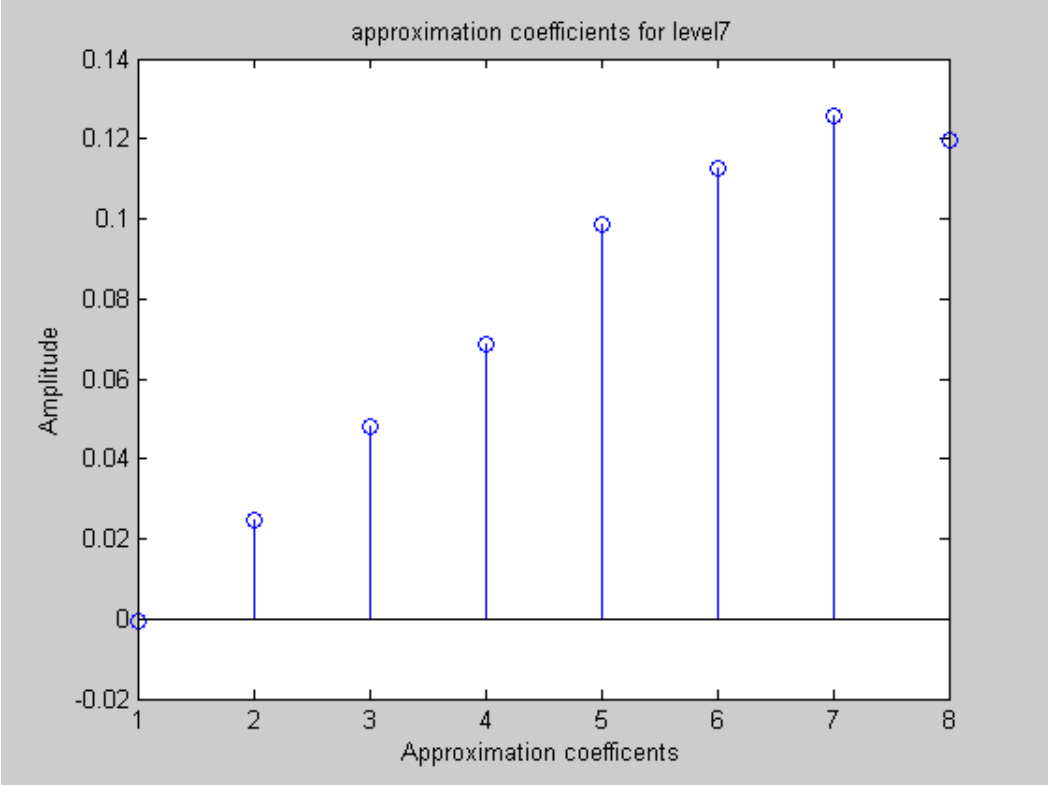

Fig 6.7: Approximation coefficients after 7 levels of Daub4 decomposition.

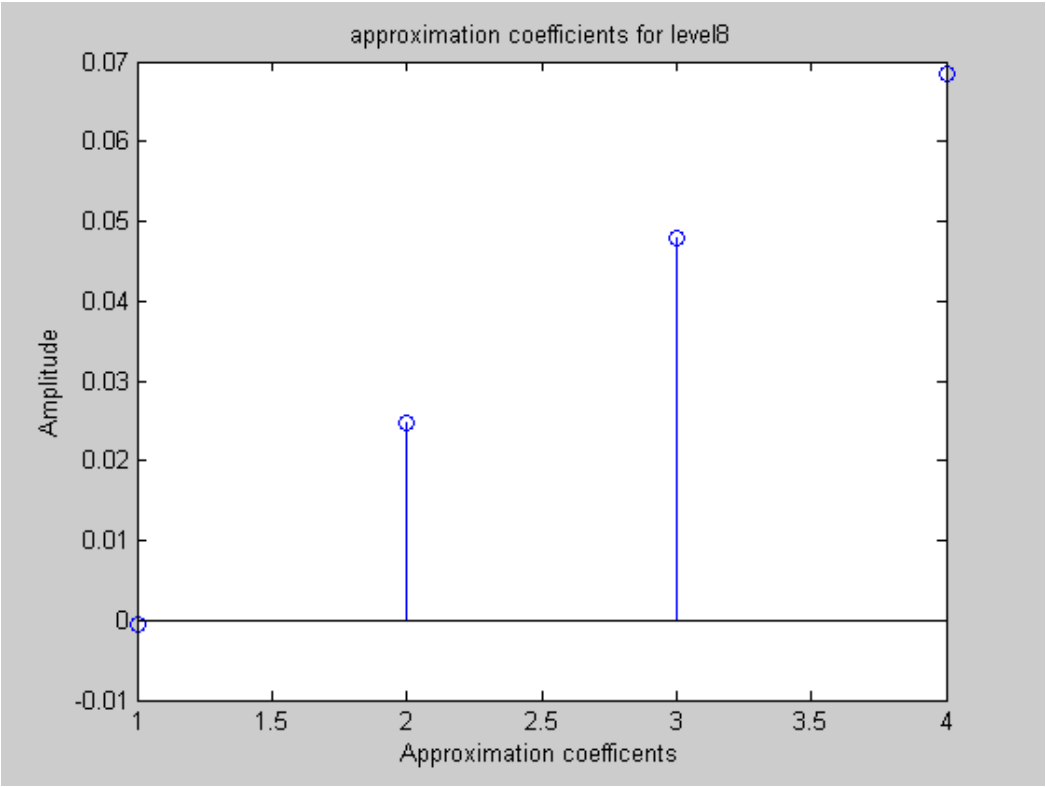

Fig 6.8: Approximation coefficients after 8 levels of Daub4 decomposition.

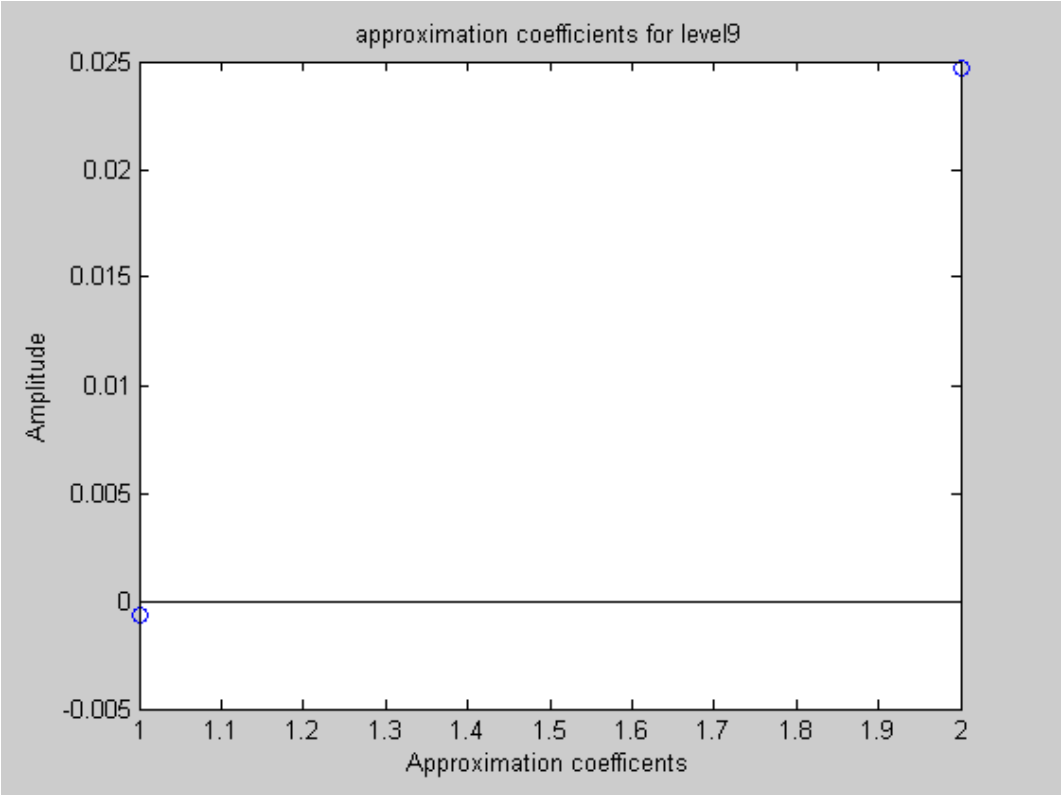

Fig 6.9: Approximation coefficients after 9 levels of Daub4 decomposition.

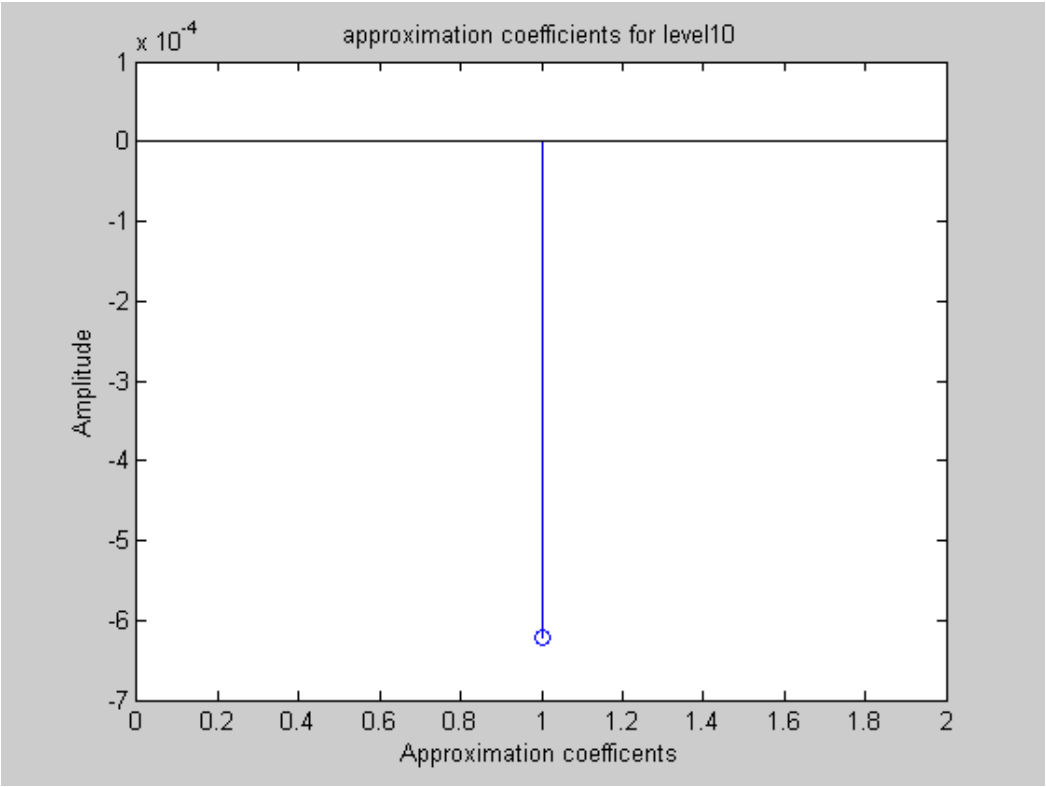

Fig 6.10: Approximation coefficients after 10 levels of Daub4 decomposition.

6.2 DETAIL COEFFICIENTS AFTER DAUB4 TRANSFORM

The detail coefficients give the finer details of the signal in the wavelet domain. This generally represents the fluctuation of the signal and hence, the proper calculation of the threshold is used to remove the noise in the signal to be retrieved.

The number of detail coefficients increases with each level by the same number of the coefficients by which it is reduced for the approximation coefficients at each level. This will bring the sum of the number of detail and approximation coefficients to be equal to the length of the signal.

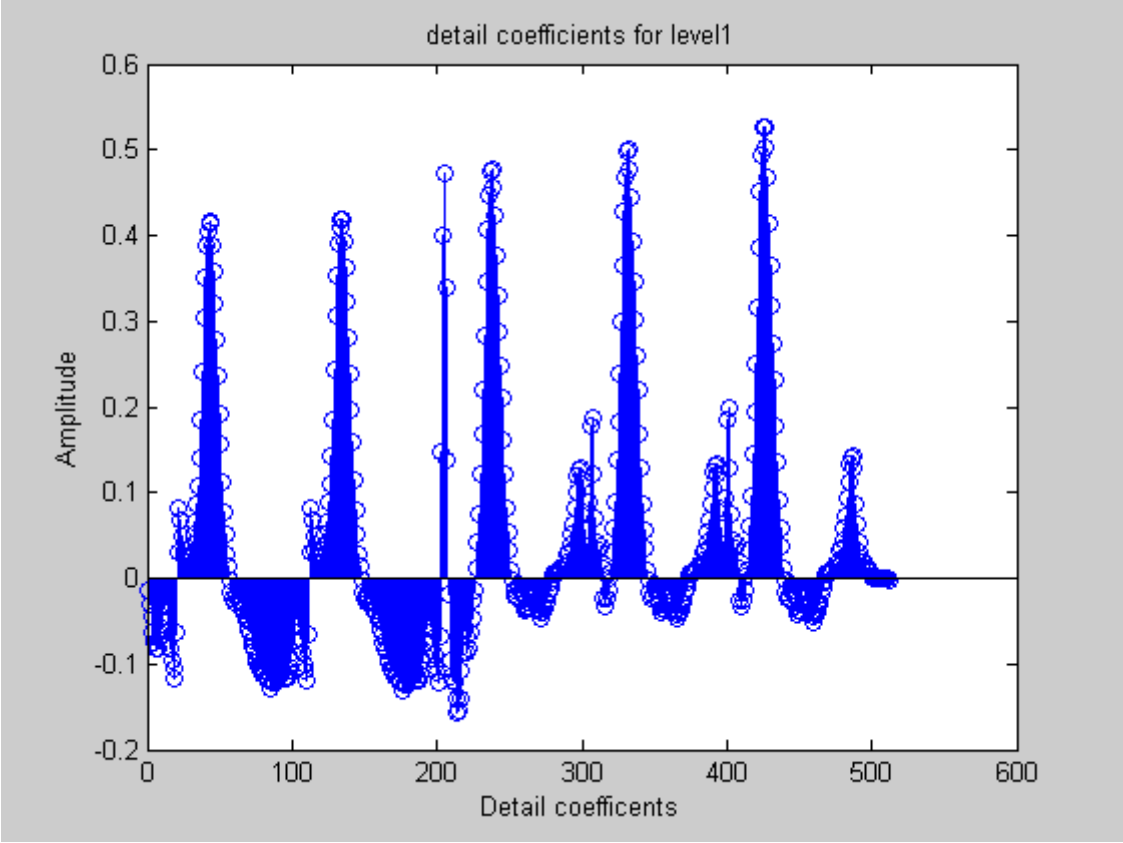

Fig 6.11: Detail coefficients after 1 level of Daub4 decomposition.

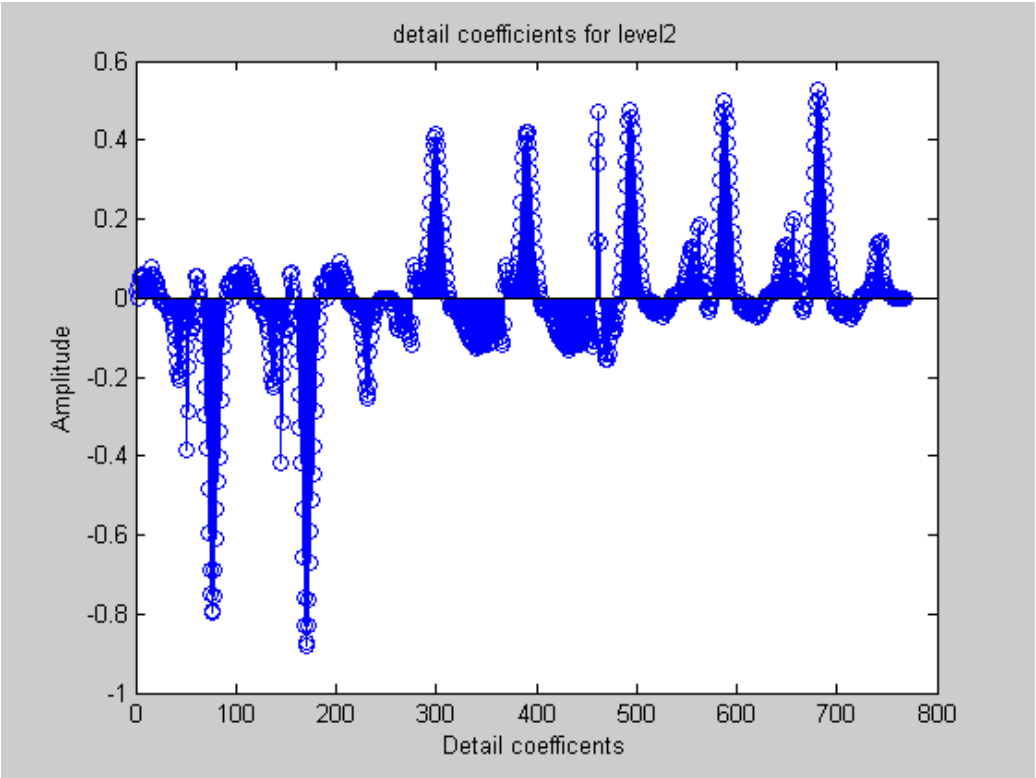

Fig 6.12: Detail coefficients after 2 levels of Daub4 decomposition.

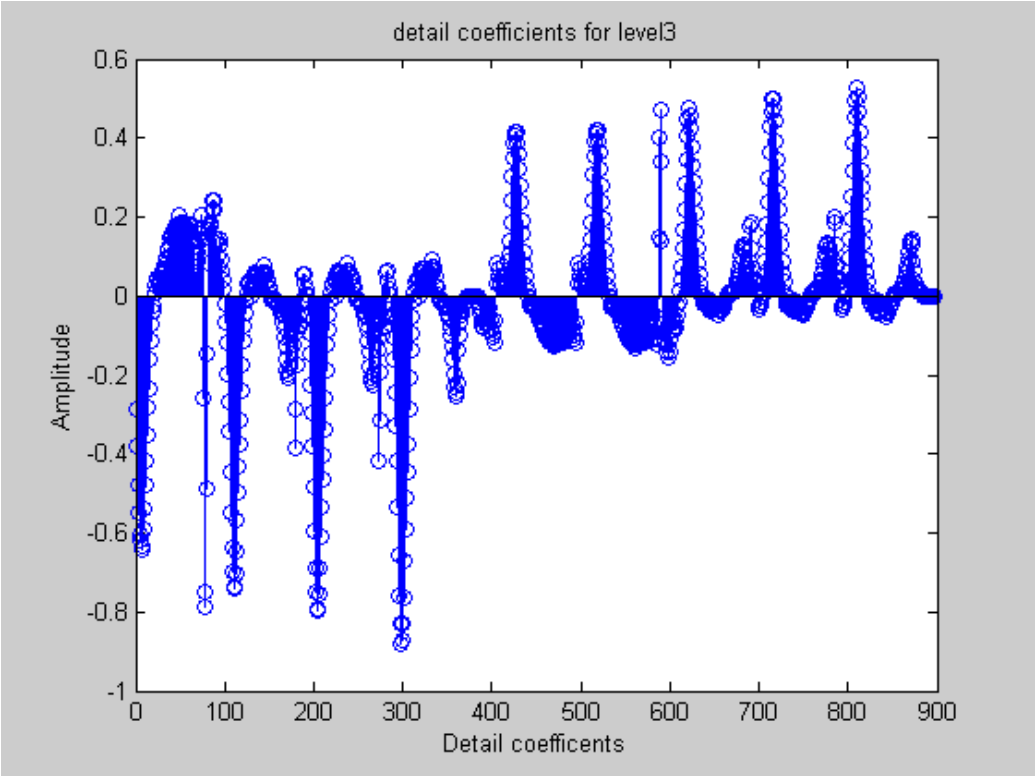

Fig 6.13: Detail coefficients after 3 levels of Daub4 decomposition.

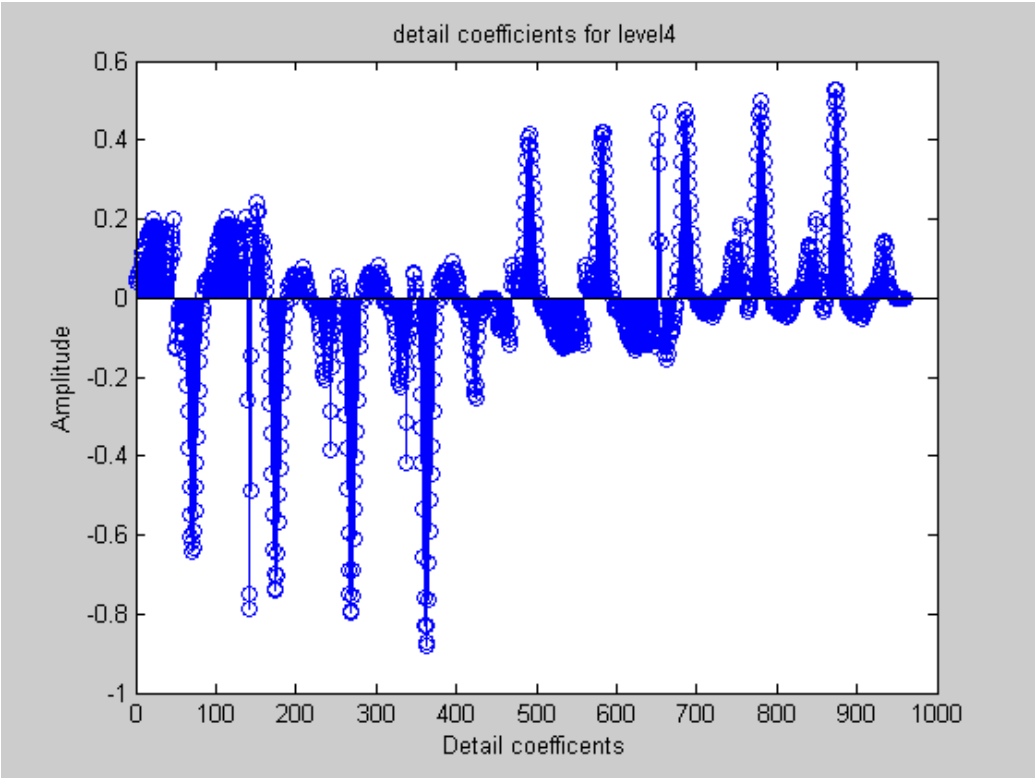

Fig 6.14: Detail coefficients after 4 levels of Daub4 decomposition.

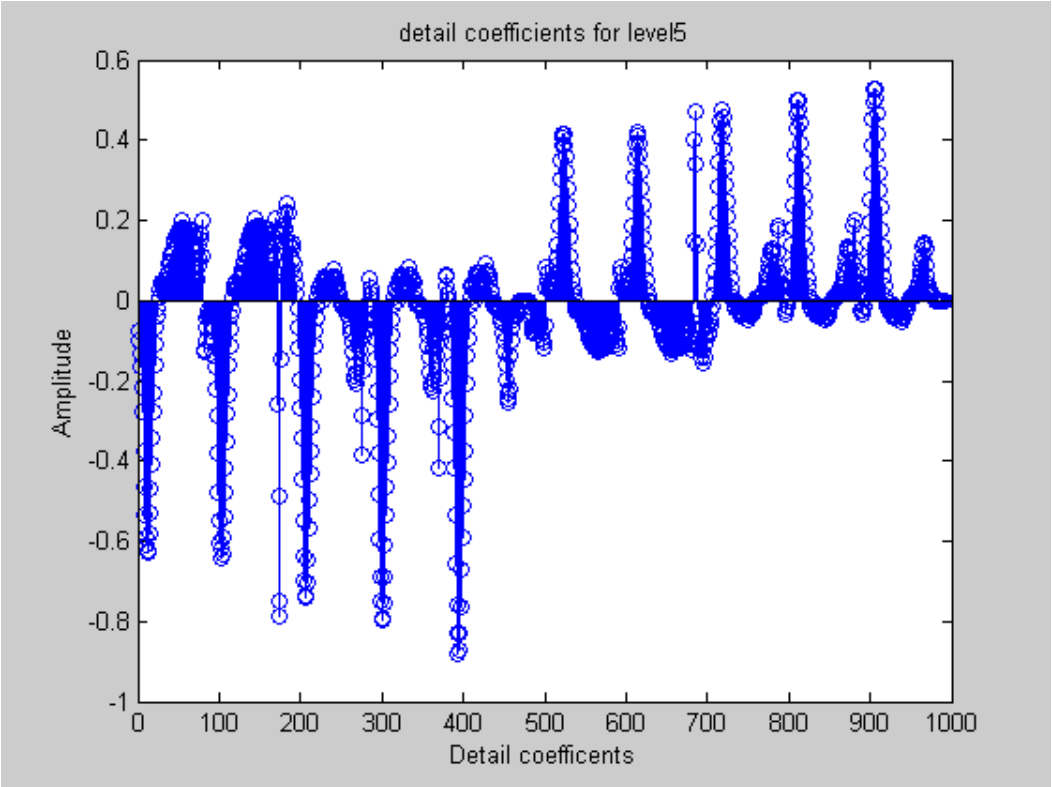

Fig 6.15: Detail coefficients after 5 levels of Daub4 decomposition.

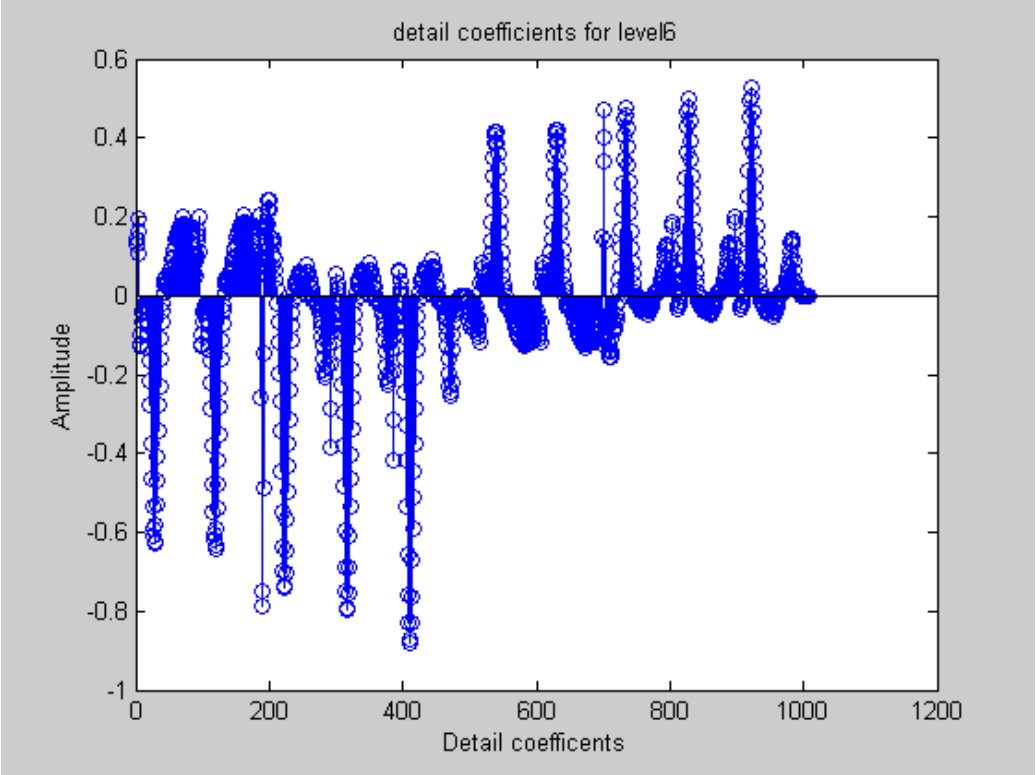

Fig 6.16: Detail coefficients after 6 levels of Daub4 decomposition.

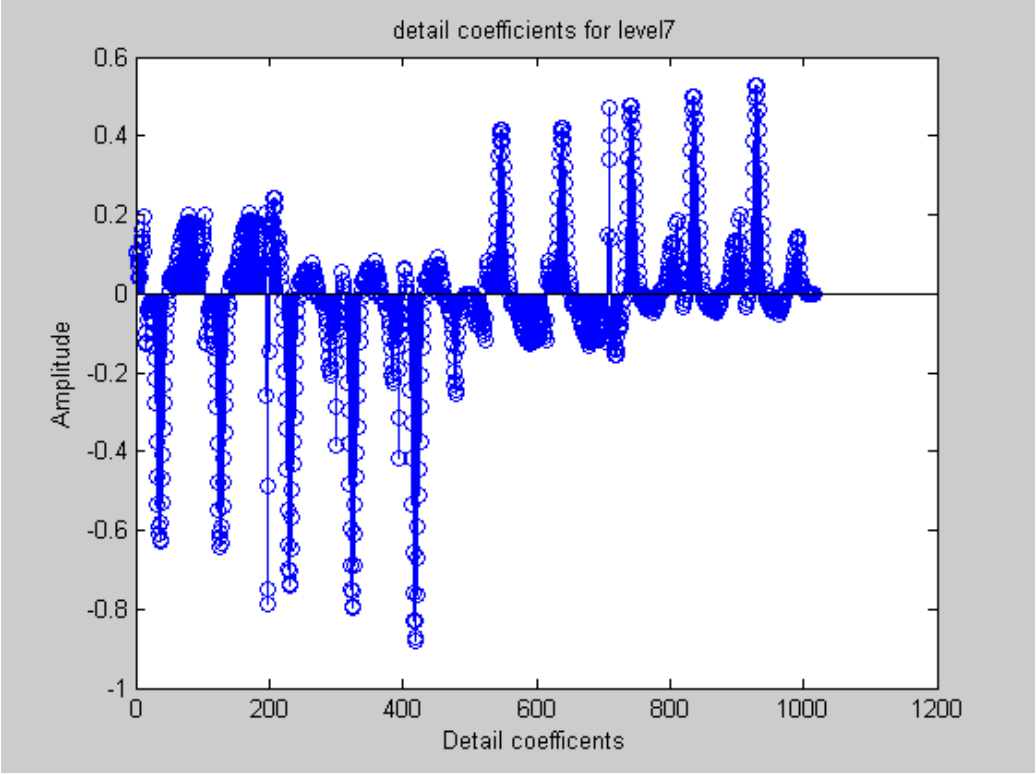

Fig 6.17: Detail coefficients after 7 levels of Daub4 decomposition.

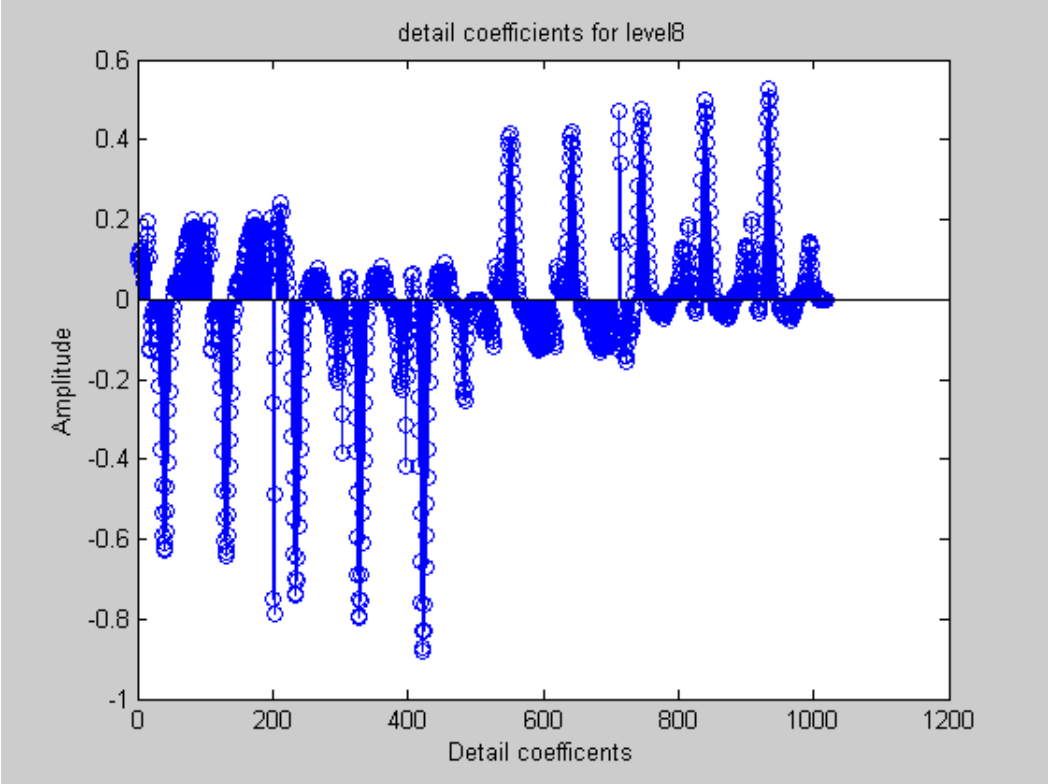

Fig 6.18: Detail coefficients after 8 levels of Daub4 decomposition.

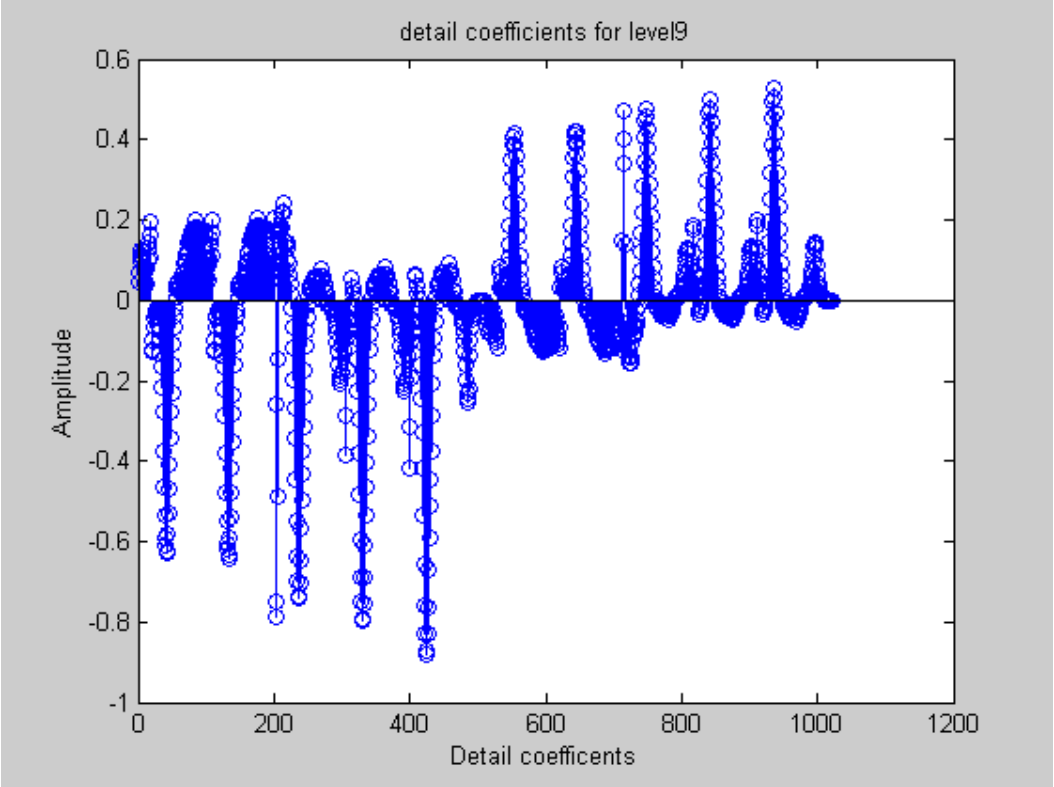

Fig 6.19: Detail coefficients after 9 levels of Daub4 decomposition.

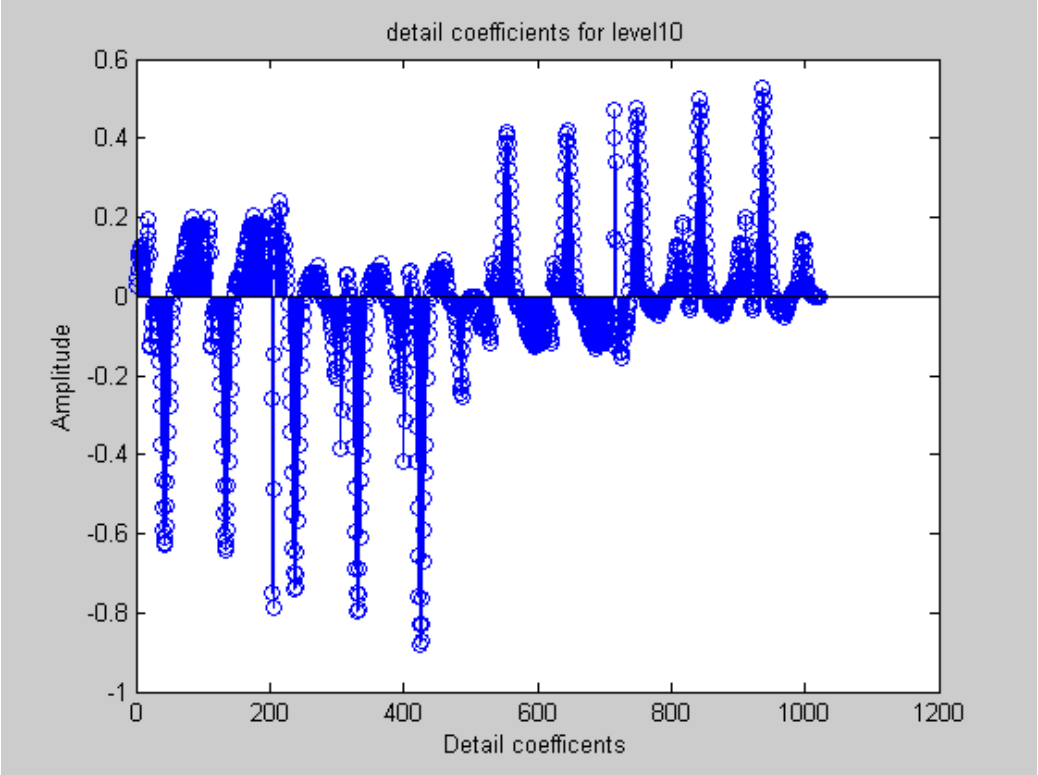

Fig 6.20: Detail coefficients after 10 levels of Daub4 decomposition.

6.3 SIGNAL TO NOISE RATIO ANALYSIS

The signal to noise ratio is determined to know the measure of cleanliness of the signal.

The **table (6.1)** shows that the wavelet analysis removes the noise well with an adequate thresholding function. It can be seen that the SNR is almost the same except the change in the fourth decimal and this is because of the kind of thresholding function chosen for a particular type of signal. **[13, 20, 33]**

$$SNR = -20log_{10}\big(0.01 \times log_{10}(PRD)\big) \qquad dB$$

where,

PRD-Percentage Root Mean Square Error

(The original signal to noise ratio used for the analysis is 0.324.)

TABLE 6.1: SNR ANALYSIS

LEVELS	**SNR (dB)**
1	31.2546
2	31.2546
3	31.2546
4	31.2546
5	31.2546
6	31.2545
7	31.2541
8	31.2551
9	31.2562
10	31.2556

6.4 ENERGY COMPRESSION PROFILE

Energy compression profile tells about the energy of the wavelet transformed signal for each level of decomposition. The **fig (6.21)** and its data in **table (6.2)** show that the energy is compressed for each level of decomposition. The reason behind the compression is that the detail coefficients of a level are not present for the decomposition at the next level. Hence, the trend signal is alone passed for further wavelet analysis and its energy is calculated.

R

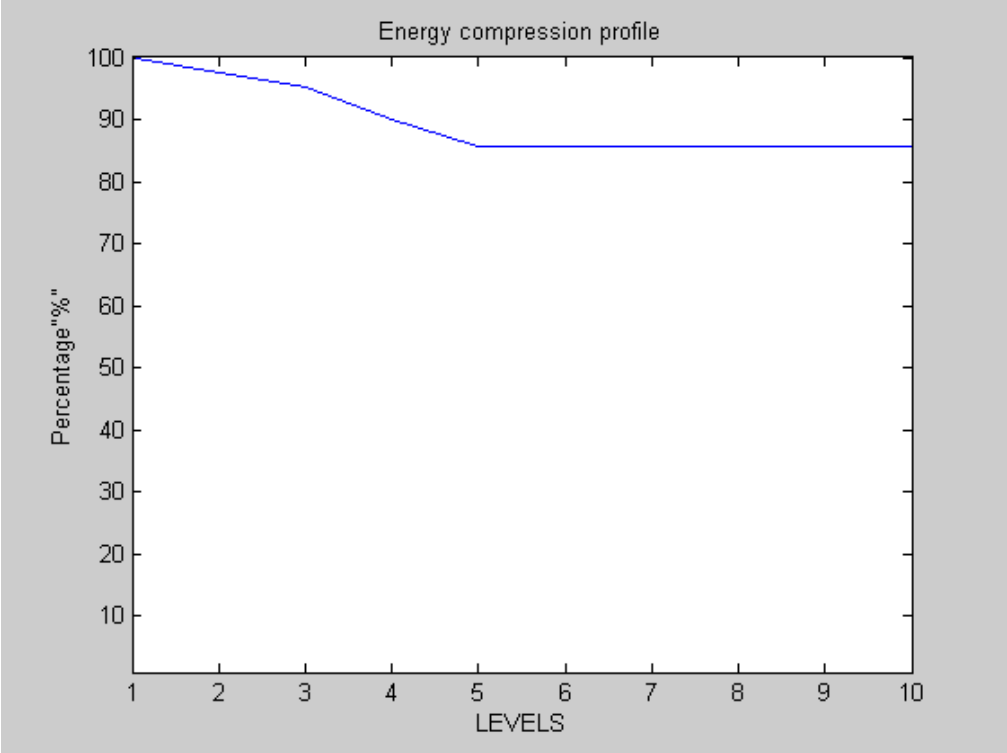

Fig 6.21: ENERGY COMPRESSION PROFILE

TABLE 6.2: ENERGY COMPRESSION PROFILE

LEVELS	**ENERGY OF THE SIGNAL (%)**
1	100.0000
2	97.5410
3	95.1784
4	89.9283
5	85.7895
6	85.7529
7	85.7526
8	85.7514
9	85.7493
10	85.5545

6.5 ERROR ANALYSIS

The optimal threshold for the noise removal is found by determining the minimum PRD in a predetermined number of iterations.

TABLE 6.3: PERCENTAGE ROOT MEAN SQUARE ERROR

LEVELS	**PRD (%)**
1	545.7153
2	545.7149
3	545.7140
4	545.7113
5	545.7309
6	545.7642
7	545.9325
8	545.5063
9	545.0676
10	545.3249

The **table (6.4)** shows the thresholds calculated for each level after determining the minimum PRD. The threshold level starts decreasing with increase in the level of decomposition. The reason behind this is that the noise coefficients reduce by the threshold amount at each level and finer tuning takes place with increase in the level. **[10]**

$$PRD = \sqrt{\left(\frac{\sum_1^n (signal_{original} - signal_{reconstructed})^2}{\sum_1^n signal_{original}}\right)} \times 100 \quad \%$$

where,

n is the length of the signal

TABLE 6.4: THRESHOLD LEVELS FOR EACH LEVEL OF DECOMPOSITION

LEVELS	**THRESHOLD**
1	0.6146
2	0.6126
3	0.6016
4	0.5868
5	0.5594
6	0.3095
7	0.1841
8	0.0935
9	0.0613
10	0.0877

6.6 HAAR ANALYSIS

6.6.1 APPROXIMATION COEFFICIENTS FOR EACH LEVEL OF DECOMPOSITION

The approximation coefficients are similar to the decomposition done for Daub4 transformation except there are slight changes in the amplitudes of the approximation coefficients at the higher levels of decomposition.

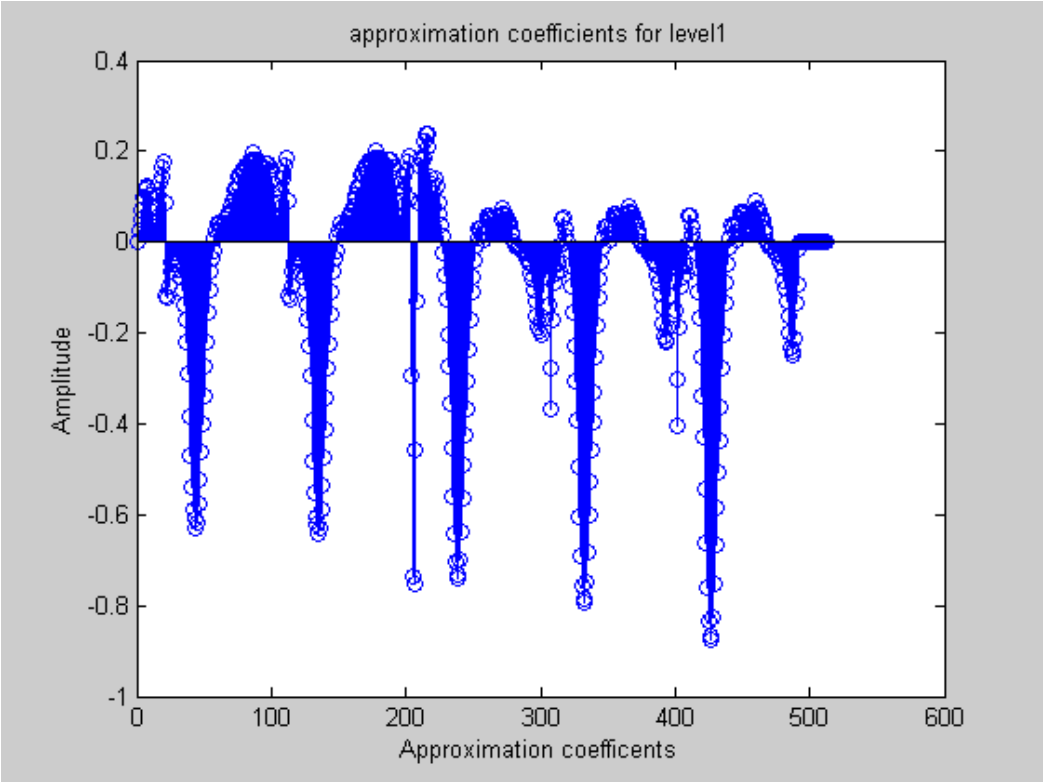

Fig 6.22: Approximation coefficients after 1 level of Haar decomposition

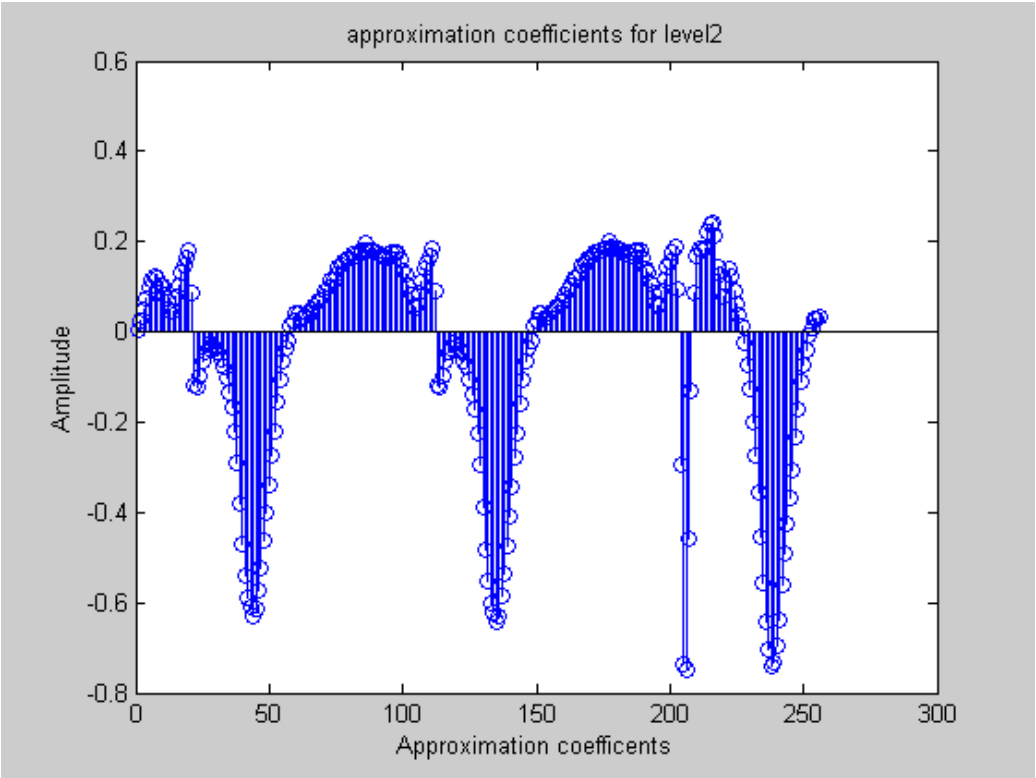

Fig 6.23: Approximation coefficients after 2 levels of Haar decomposition

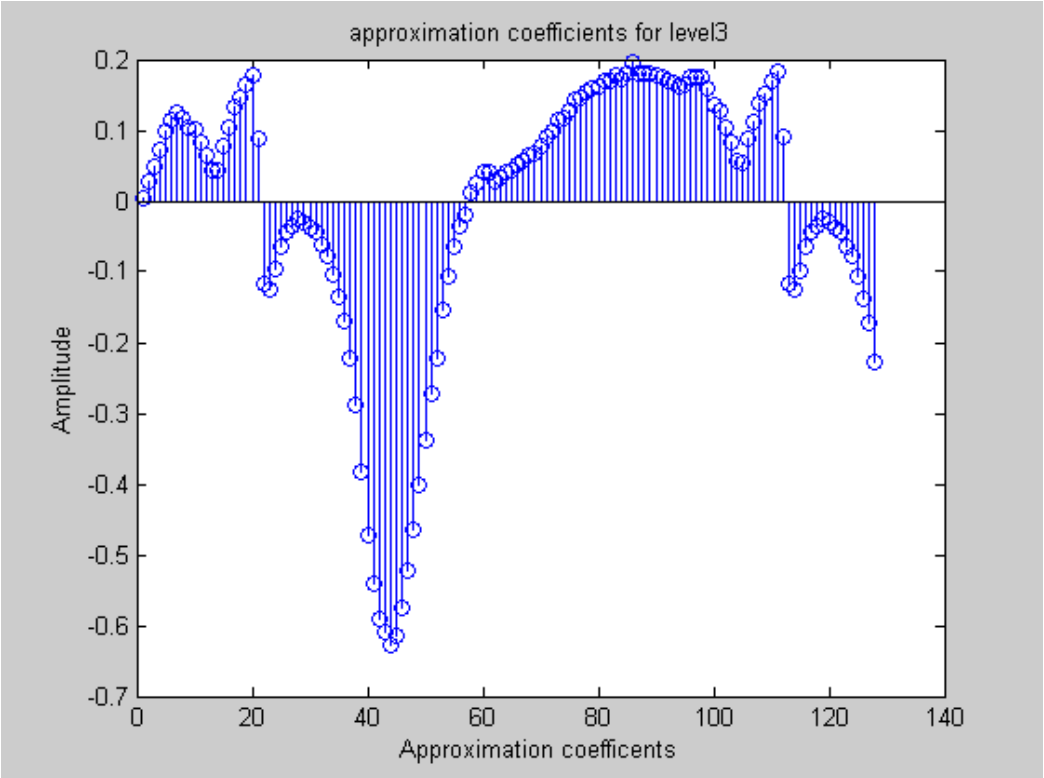

Fig 6.24: Approximation coefficients after 3 levels of Haar decomposition

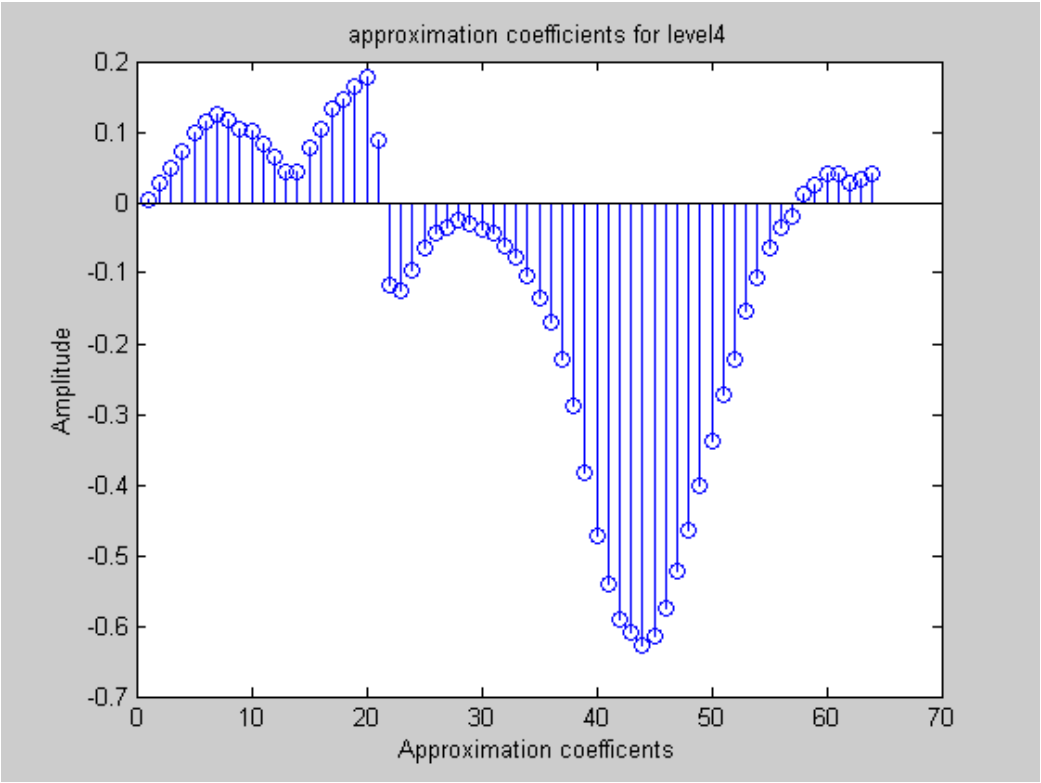

Fig 6.25: Approximation coefficients after 5 levels of Haar decomposition

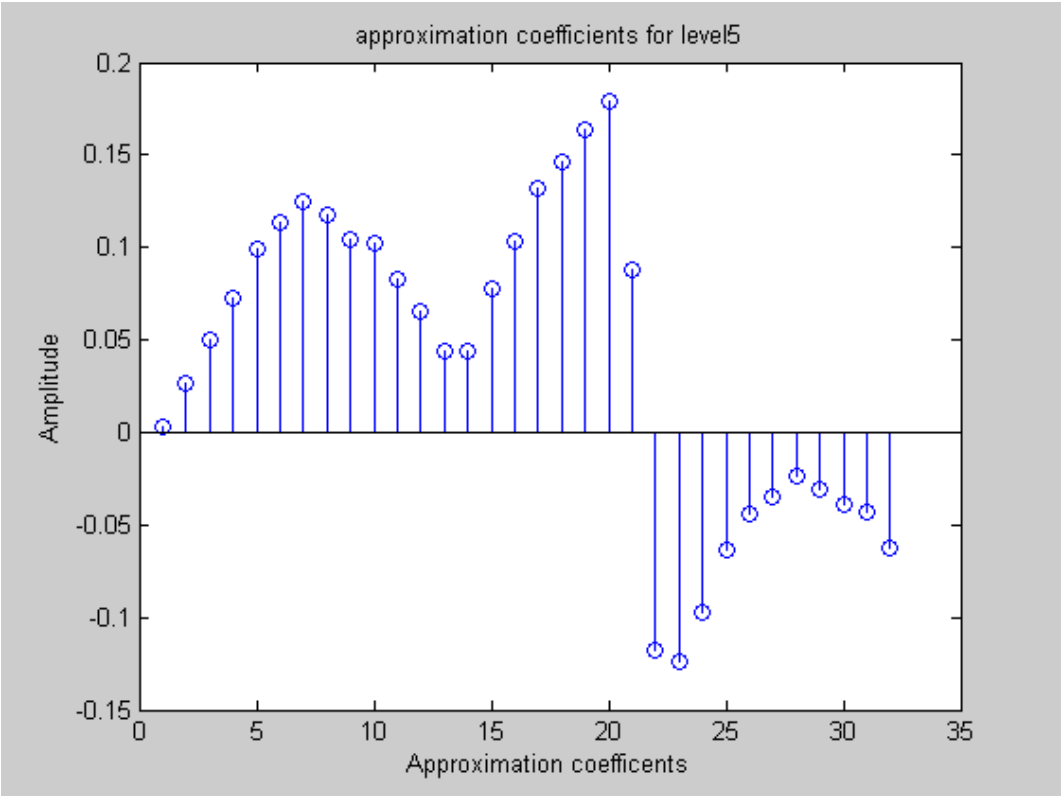

Fig 6.26: Approximation coefficients after 5 levels of Haar decomposition

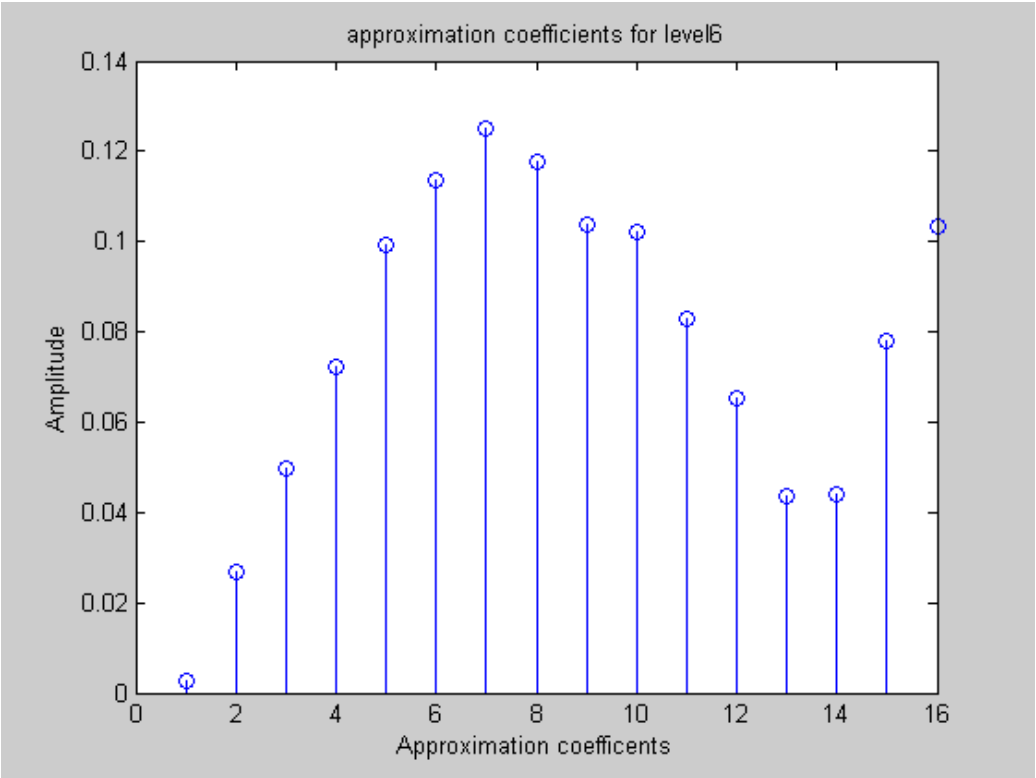

Fig 6.27: Approximation coefficients after 6 levels of Haar decomposition

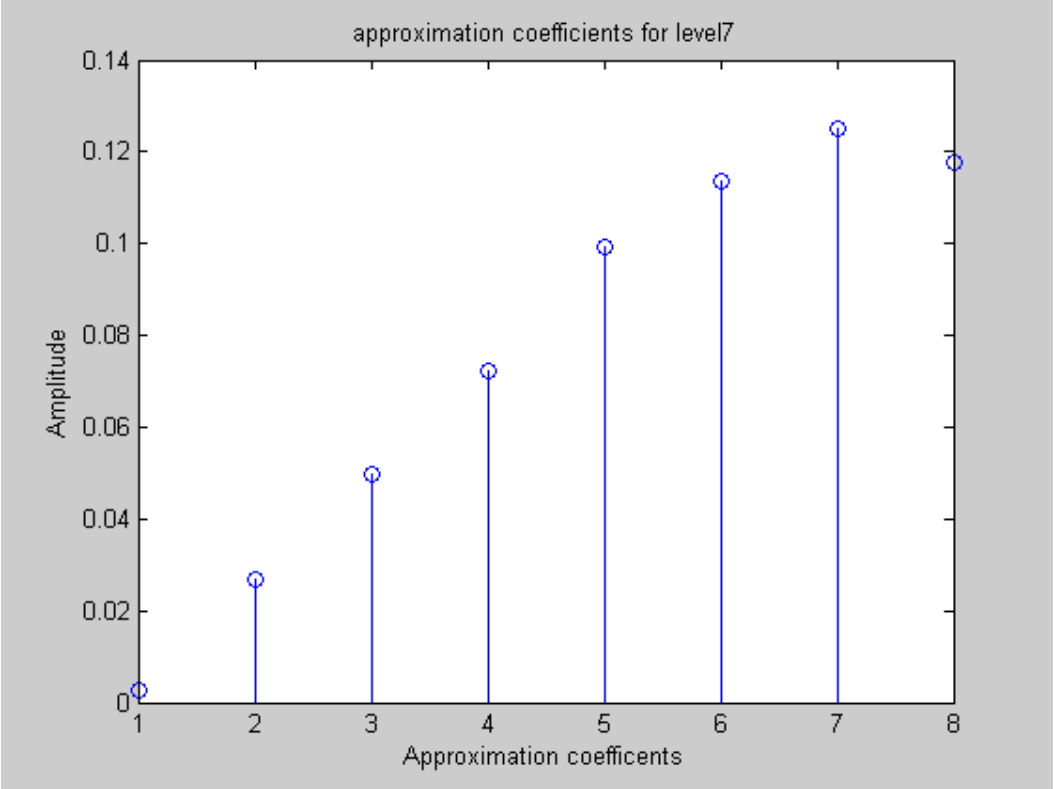

Fig 6.28: Approximation coefficients after 7 levels of Haar decomposition

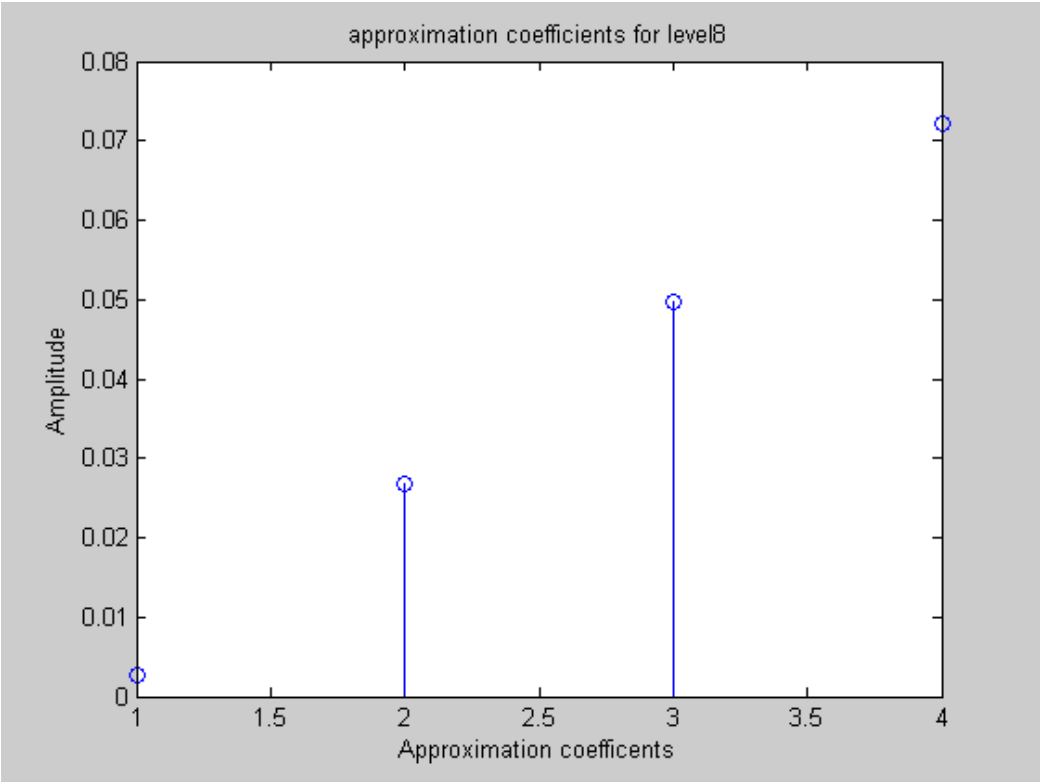

Fig 6.29: Approximation coefficients after 8 levels of Haar decomposition

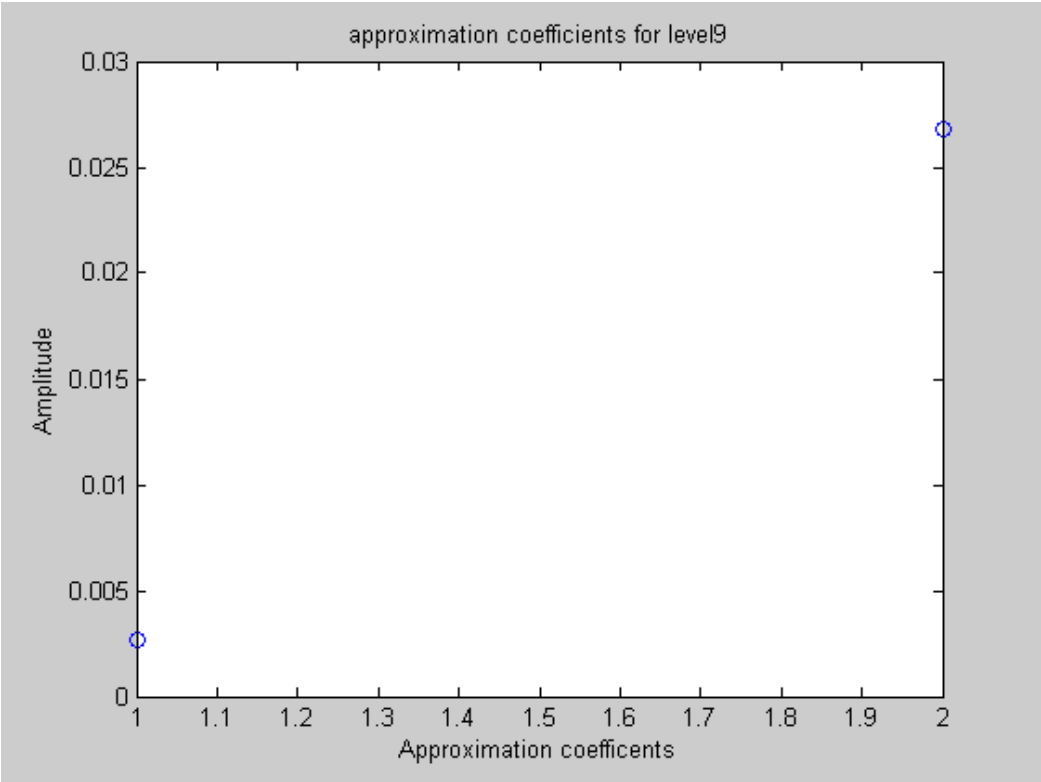

Fig 6.30: Approximation coefficients after 9 levels of Haar decomposition

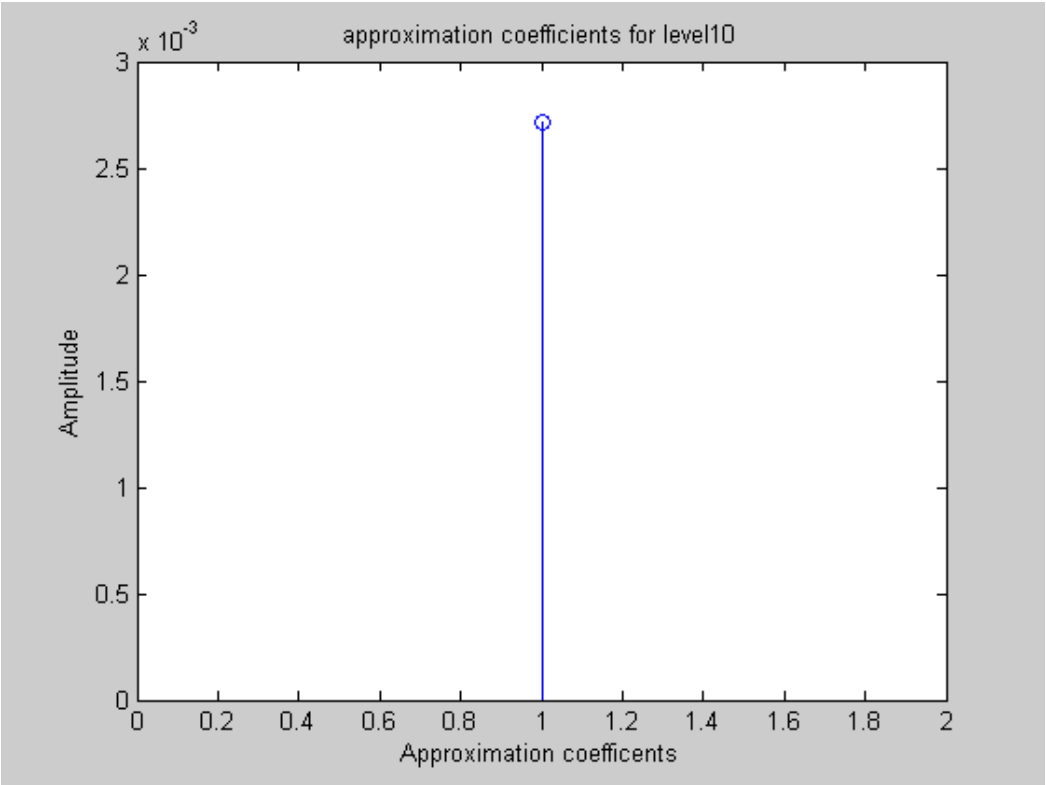

Fig 6.31: Approximation coefficients after 10 levels of Haar decomposition

6.6.2 DETAIL COEFFICIENTS FOR EACH LEVEL OF DECOMPOSITION

There are slight changes in these detail coefficients in the magnitude compared to the Daub4 transformed detail signals. These changes are observed more in the higher levels of decomposition.

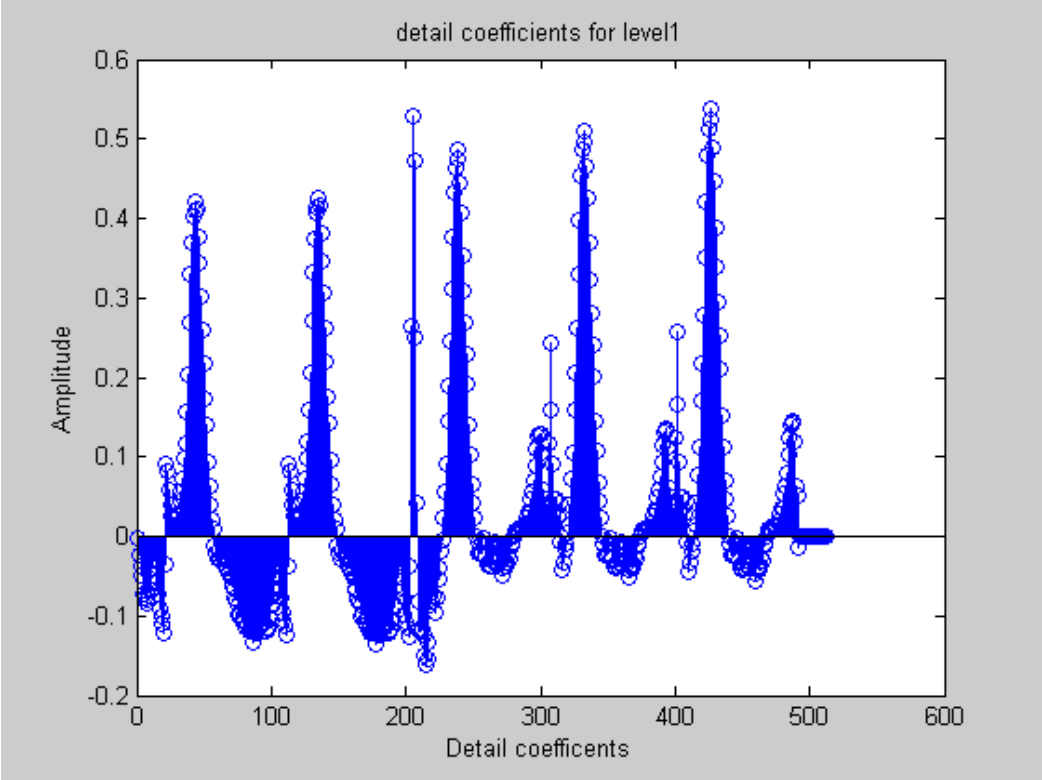

Fig 6.32: Detail coefficients after 1 level of Haar decomposition

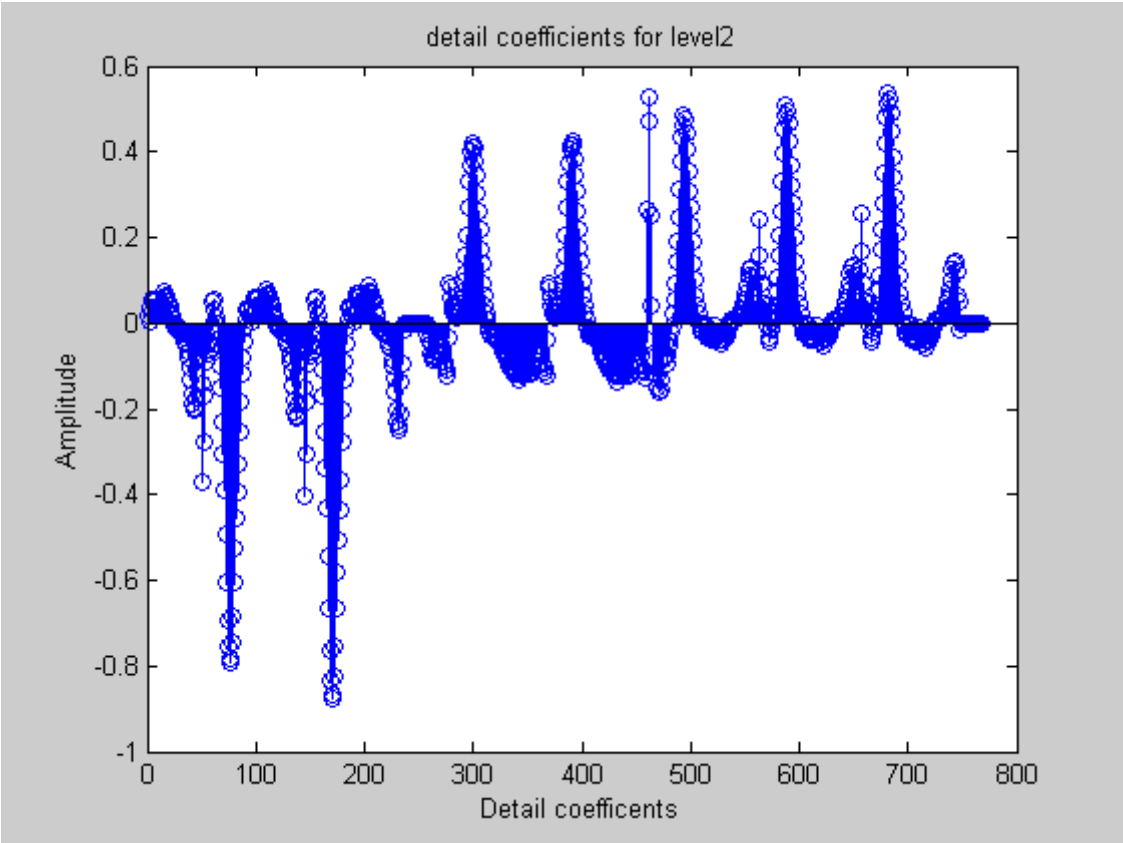

Fig 6.33: Detail coefficients after 2 levels of Haar decomposition

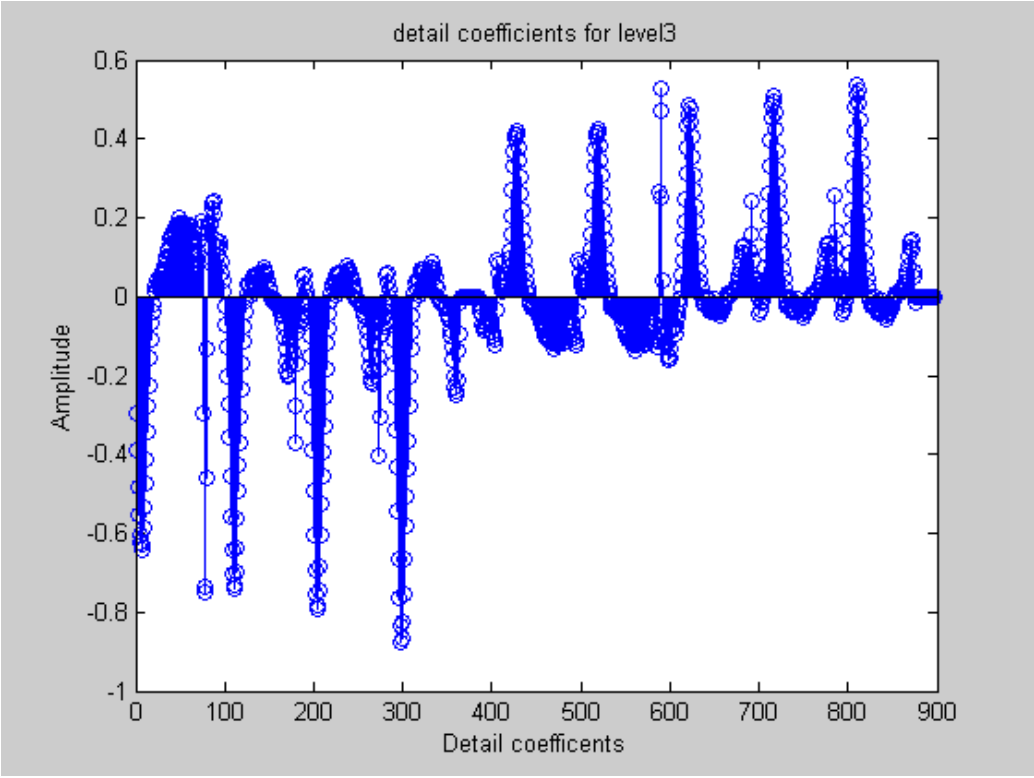

Fig 6.34: Detail coefficients after 3 levels of Haar decomposition

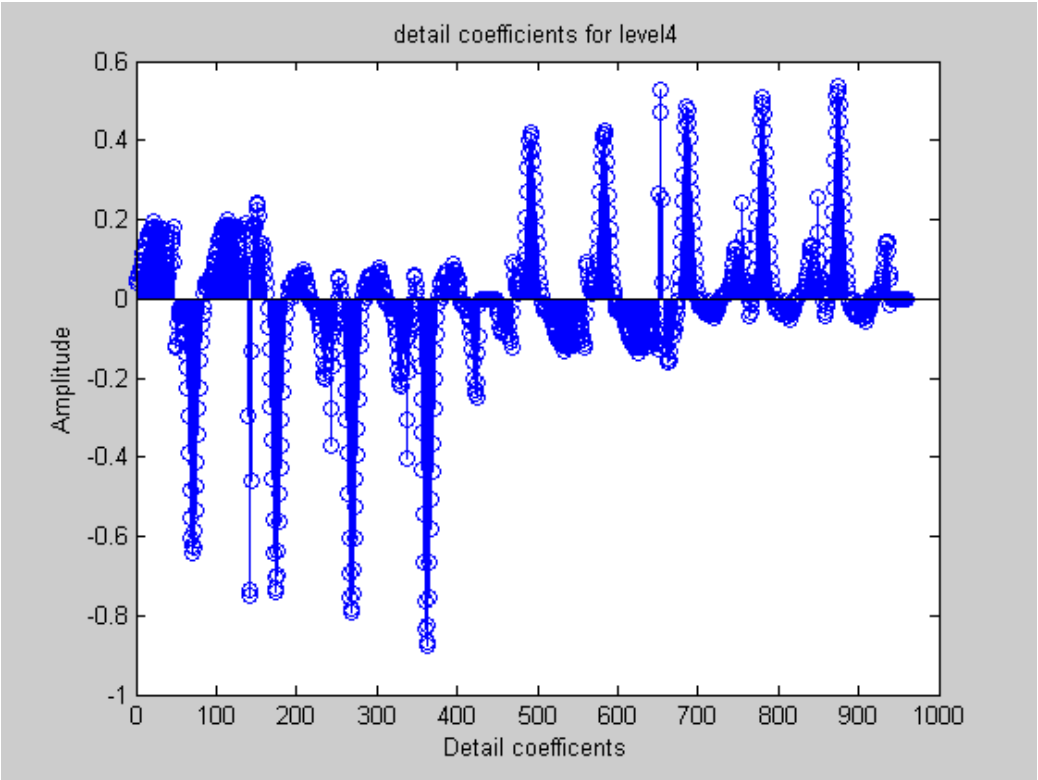

Fig 6.35: Detail coefficients after 4 levels of Haar decomposition

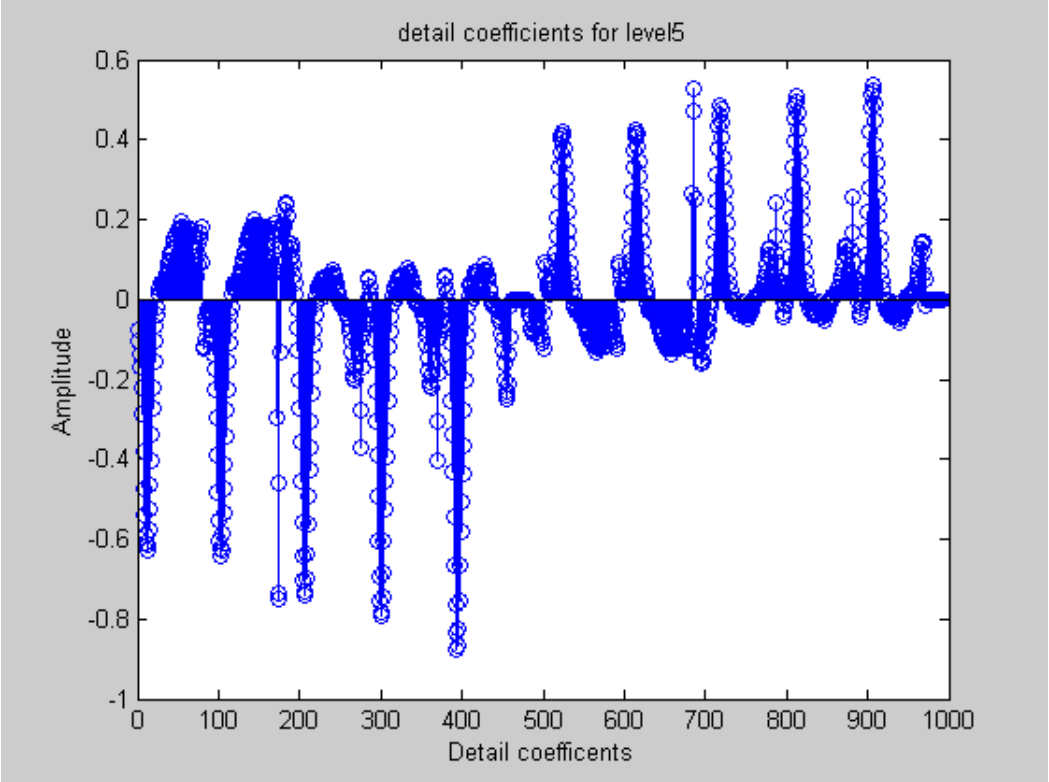

Fig 6.36: Detail coefficients after 5 levels of Haar decomposition

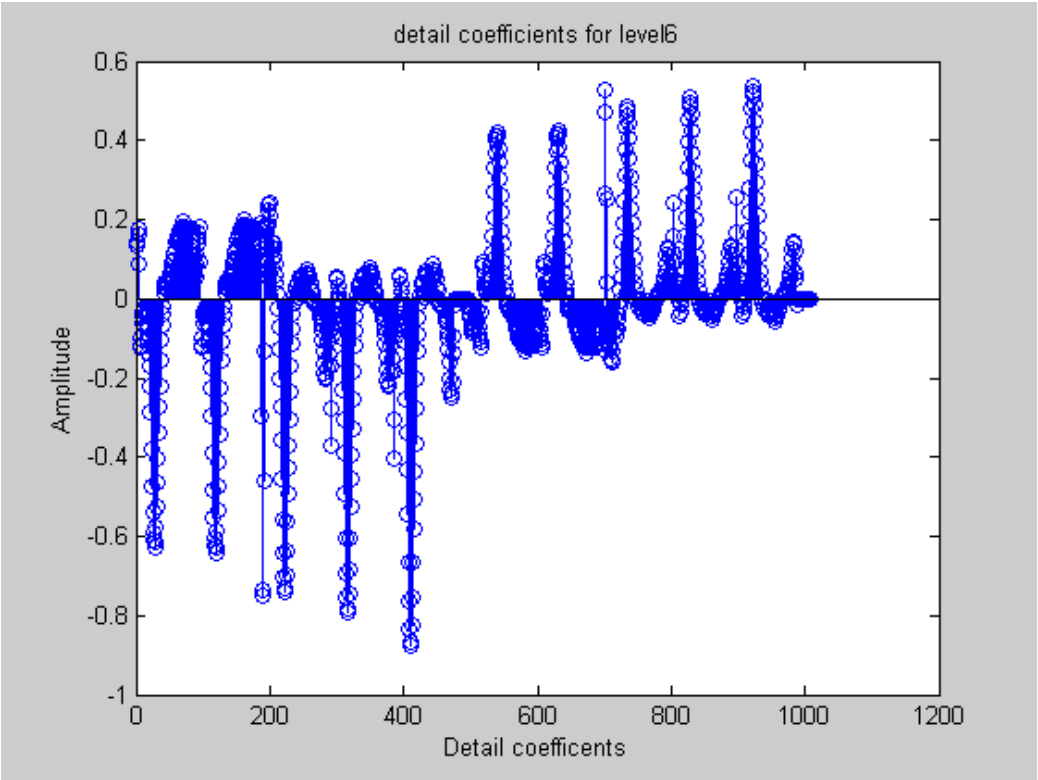

Fig 6.37: Detail coefficients after 6 levels of Haar decomposition

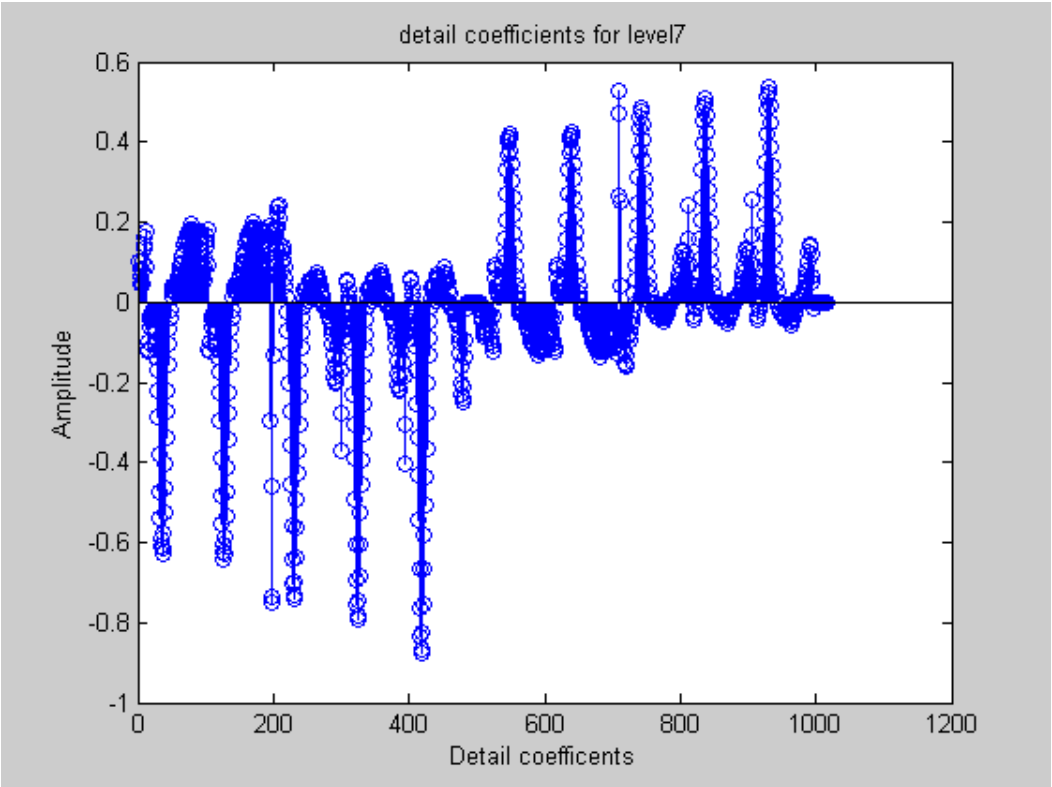

Fig 6.38: Detail coefficients after 7 levels of Haar decomposition

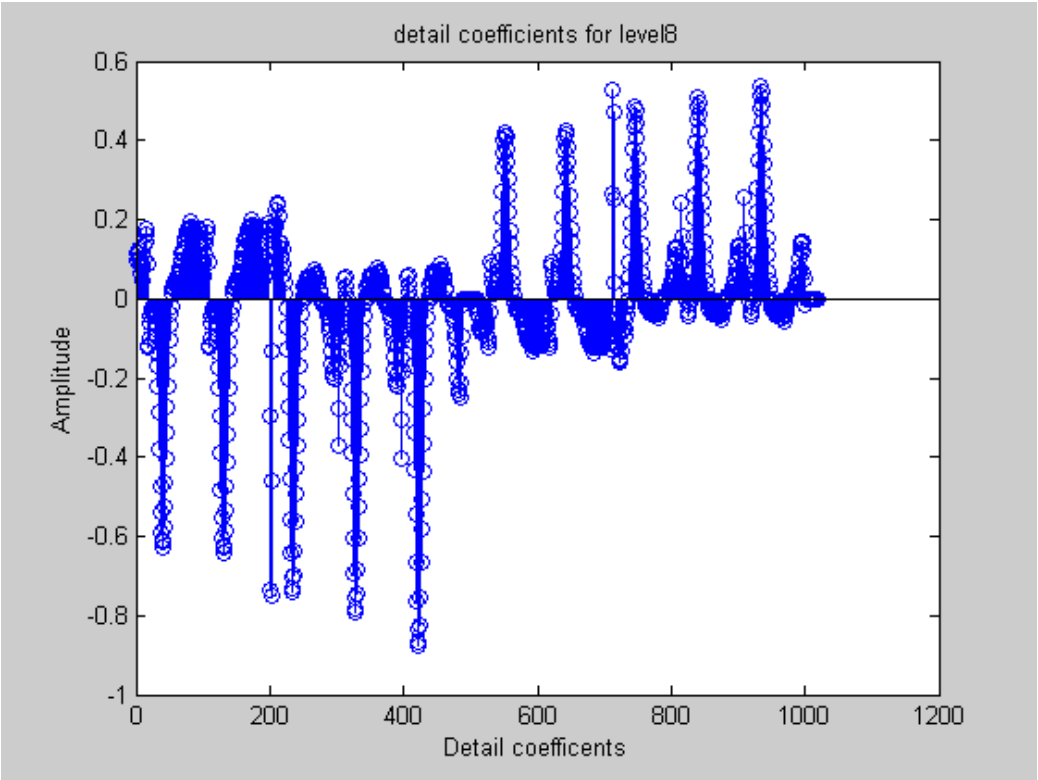

Fig 6.39: Detail coefficients after 8 levels of Haar decomposition

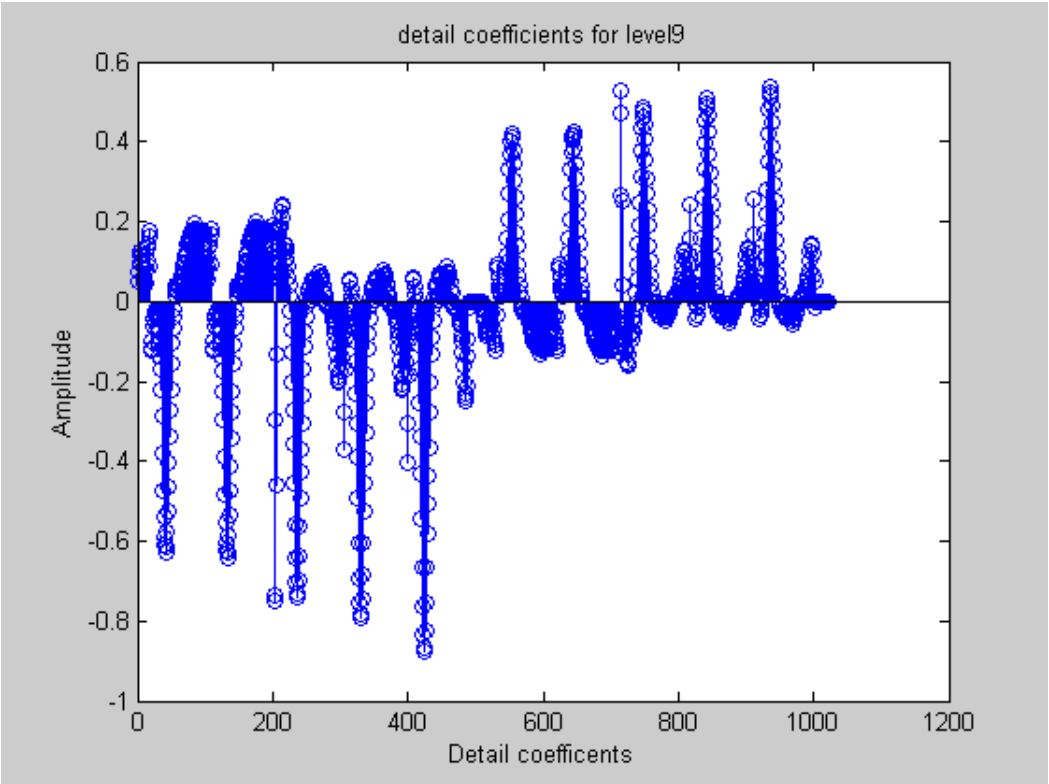

Fig 6.40: Detail coefficients after 9 levels of Haar decomposition

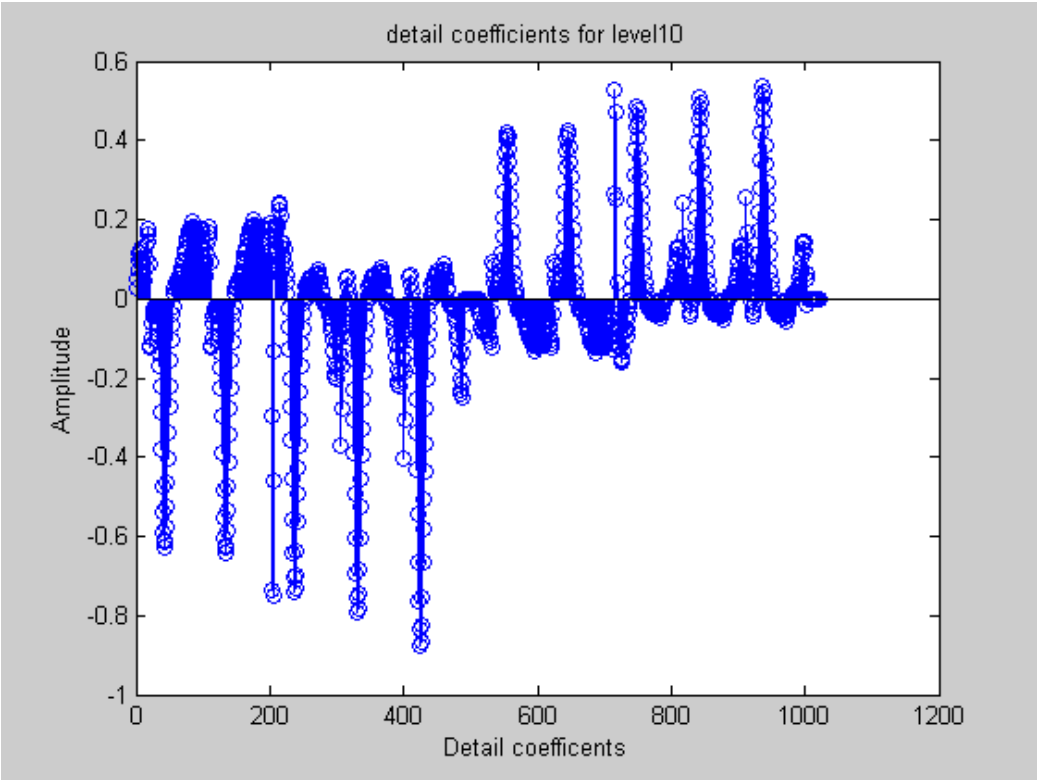

Fig 6.41: Detail coefficients after 10 levels of Haar decomposition

6.6.3 SIGNAL TO NOISE RATIO ANALYSIS

Comparing, **table (6.5) and table (6.1)**, it shows clearly that the Haar analysis is a poor analyzer compared to the Daub4 analysis. The SNR for the same level of decomposition is more after Haar analysis compared to the Daub4 analysis.

The SNR, however, is more or less same for each level of decomposition, as it requires only fine tuning at each level of analysis. **[10, 20, 33]**

$$SNR = -20log_{10}\big(0.01 \times log_{10}(PRD)\big) \qquad dB$$

where,

PRD-Percentage Root Mean Square Error

TABLE 6.5: SNR ANALYSIS

LEVELS	SNR (dB)
1	31.2547
2	31.2547
3	31.2568
4	31.2594
5	31.2611
6	31.2618
7	31.2619
8	31.2620
9	31.2620
10	31.2620

6.6.4 ENERGY COMPRESSION PROFILE

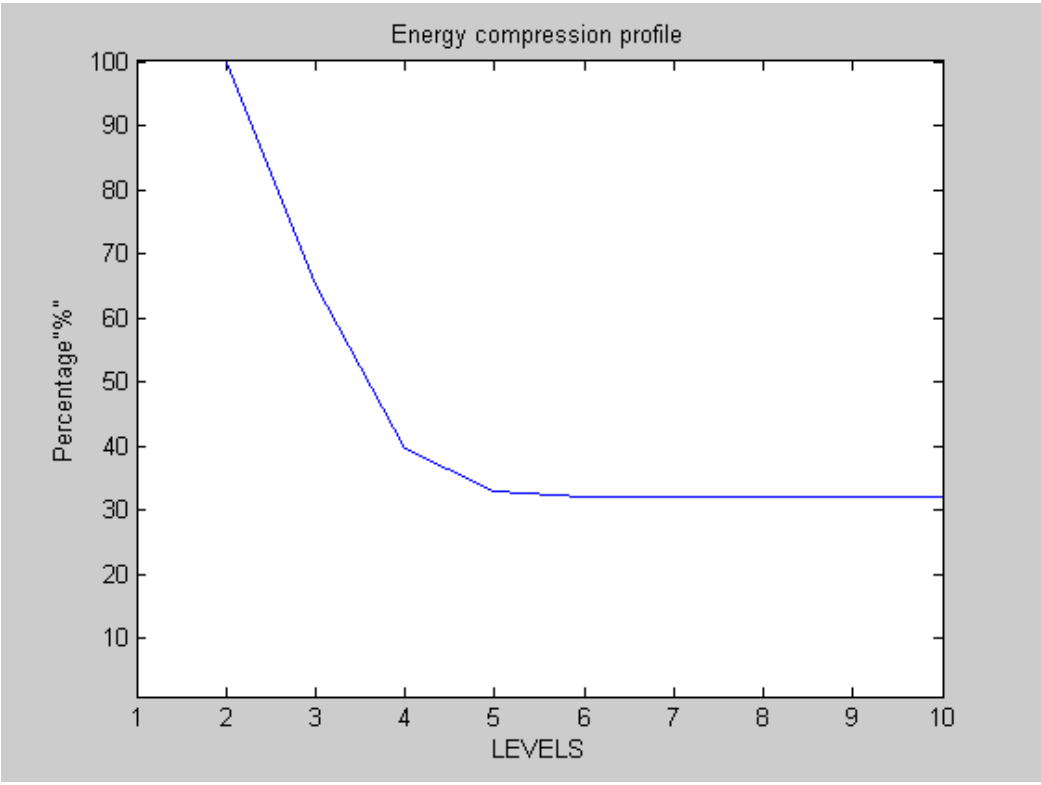

Fig 6.42: ENERGY COMPRESSION PROFILE

TABLE 6.6: ENERGY COMPRESSION PROFILE

LEVELS	ENERGY OF THE SIGNAL (%)
1	100.0000
2	100.0000
3	65.0558
4	39.6918
5	32.9532
6	32.2335
7	32.2015
8	32.2010
9	32.2010
10	32.2010

As, the **fig (6.42)** and the **table (6.6)** tells, the energy after Haar analysis for 10 levels is compressed to 32% compared to 85% after Daub4 transformation. The reason is the very high approximation of the signal by using Haar transformation, as it doesn't represent the signal very well because of the insufficient two coefficients.

6.6.5 ERROR ANALYSIS

The PRD analysis is done and the minimum PRD is chosen in a determined number of iterations for each level. This index of the minimum PRD is then used to determine the threshold for the Haar modified analysis.The threshold levels differ for each level of modified decomposition compared to the Daub4 transform as shown in **table (6.8)**. **[10]**

$$PRD = \sqrt{\left(\frac{\sum_1^n (signal_{original} - signal_{reconstructed})^2}{\sum_1^n signal_{original}}\right)} \times 100 \quad \%$$

where, *n* is the length of the signal

TABLE 6.7: PRD ANALYSIS

LEVELS	**PRD (%)**
1	545.6950
2	545.6950
3	544.8484
4	543.8265
5	543.1659
6	542.8949
7	542.8205
8	542.8066
9	542.8047
10	542.8046

TABLE 6.8: THRESHOLD ANALYSIS

LEVELS	**THRESHOLD**
1	0.6120
2	0.6082
3	0.5072
4	0.2558
5	0.0691
6	0.0146
7	0.0024
8	0.0002
9	0.0000
10	0.0000

CHAPTER 7

7. CONCLUSION AND FUTURE WORK

7.1 CONCLUSION

The type of the system which generates a desired output that is not distorted and noisy, is identified by Fourier combined wavelet transformation.

The system is assumed to be a noisy and a convoluted signal with the system function. The Fourier transformation used, deconvolutes the system characteristics from the signal. The ratio of the distortion of the signal to the noise is made application dependent with the usage of a regularization parameter in the Fourier deconvolution. Thus, the deconvoluted signal is observed to be out of phase by 180^0 and is noisy but with the reduction in the amount of distortion. The noise and the distortion are further reduced by using the wavelet denoising algorithm.

The denoising algorithm compares two wavelets, Haar and Daubechies4. The results conclude that the Daubechies4 perform well than the Haar wavelet. Hence, it was analyzed that as the number of coefficients to represent a wavelet increases, more complex signal can be deciphered.

Compression of the signal was observed in the wavelet denoising stage and this increase with the increase in the level of wavelet decomposition. Compression has a side-effect of distorting the signal. Hence, the optimal compression ratio with an allowable distortion is always chosen.

7.2 FUTURE SCOPE OF THE PROJECT

The project can be further extended as follows:

1) The algorithm can be used for real time 1-D signals by transferring the signal into the embedded microcontroller with a microphone and an ADC setup. The signal analyzers can be used to analyze the electrical signal amplified by the microphone. Spectrum analysis should then be done with the output of the microcontroller and the compared with the original signal.
2) The concept can be extended to 2-D signals like images using real-time analysis.
3) Compression of the 1-D signal and 2-D signals can further be experimented using various user defined wavelets for achieving the optimal compression ratio with the minimal distortion.

BIBLIOGRAPHY

[1] S. Mallat, "A theory of multiresolution signal decomposition: the wavelet representation", *IEEE Trans. Pattern Recognition and Machine Intelligence, vol.11, pp. 674-693,* 1989.

[2] Leontios J. Hadjileontiadis , "Lung Sounds: An Advanced Signal Processing Perspective", *Morgan & Claypool Publishers series- Synthesis Lectures On Biomedical Engineering # 9,* 2009.

[3] Gilbert Strang and Truong Nguyen,"Wavelets and Filter Banks" *Wellesley-Cambridge Press, Wellesley MA, First edition,* 1996.

[4] Olivier Rioul, " Regular wavelets: a discrete-time approach", *IEEE Trans. on Signal*

Processing, 41(12):pp.3572 - 3579, Dec. 1993.

[5] Chiu, C. K., "An Introduction to Wavelets" *Academic Press, Harcourt Brace Jovanovich, pp.266,* 1992.

[6] Donoho, D. L., "Denoising by soft thresholding", *IEEE Trans. Info Theory, 41, 3, pp.613-627,* 1995.

[7] V. Cherkassky and X. Shao, "Model selection for wavelet-based signal estimation", *in Proc. IJCNN-98, Anchoradge, Alaska,* 1998

[8] D. Donoho, I. Johnstone, G. Kerkyacharian, and D. Picard, "Wavelet shrinkage:

Asymptopia?" *J. Roy. Stat. Soc., vol. 57, pp. 301-369,* 1995.

[9] James S.Walker, "A primer on wavelets and their scientific applications", Second edition, *Chapman & Hall,* 2008.

[10] Mikhled Alfaouri and Khaled Daqrouq, ”ECG Signal Denoising By Wavelet Transform Thresholding”, *American Journal of Applied Sciences 5 (3):pp. 276-281*, 2008

[11] A.Djohan, T.Q.Nguyen, and W.J.Tompkin,”ECG compression using discrete symmetric wavelet transform”, *17th Int Conf. IEEE in medicine and Biology,* 1995.

[12] John G.Proakis,”Advance Digital Signal Processing”, Macmillan 1992.

[13] D. Puthankattil Subha, Paul K. Joseph, Rajendra Acharya U & Choo Min Lim, “EEG Signal Analysis: A Survey”, *J Med Syst*, DOI 10.1007/s10916-008-9231-z.

[14] Bidyut Parruck and Sedki M. Riad, “An Optimization Criterion for Iterative Deconvolution”, *IEEE TRANSACTIONS ON INSTRUMENTATION AND MEASUREMENT, VOL. IM-32, NO. 1,* MARCH 1983.

[15] Y. Dorfan A. Feuer and B. Porat, “Modeling and Identification of LPTV Systems by Wavelets”, *Department of EE, Technion,* Haifa 32000, Israel. 29 December 2003.

[16] Jani Even and Kenji Sugimoto, “Estimation of MIMO System with Nonlinear Distortion at the input: An Adaptive Approach”, *SICE-ICASE International Joint Conference,* Oct. 18-21, 2006 in Bexco, Busan, Korea.

[17] Chen Shiguo, Zhang Ruanyu, Wang Peng and Li Taihua, “Enhance Accuracy in Pole Identification of System by Wavelet Transform De-Noising”, *IEEE TRANSACTIONS ON NUCLEAR SCIENCE, VOL. 51, NO. 1,* FEBRUARY 2004.

[18] Issabelle Payan, Murat Kunt, Werner FREI, "Subsurface Radar Signal Deconvolution", *Signal Processing 4, North-Holland Publishing company, pp.249-262,* 1982.

[19] J.A.d'Arcy, D.J.Collins, I.J.Rowland,A.R.Padhani and M.O.Leach, "Applications of sliding window reconstruction with Cartesian sampling for dynamic contrast enhanced MRI", *NMR biomed;15; pp.174-183,* 2002.

[20] Yuanjin Zheng, David B.H.Tay, Lemin Li, "Signal extraction and power spectrum estimation using wavelet transform scale space filtering and Bayes shrinkage", *Signal Processing 80, pp.1535-1549,* 2000.

[21] Yating Lin, Jianli Cai, "A New Threshold Function for Signal Denoising Based on Wavelet Transform", *IEEE International Conference on Measuring Technology and Mechatronics Automation,* DOI 10.1109/ICMTMA.2010.347, 2010.

[22] M. C. E. Rosas-Orea, M. Hernandez-Diaz, V. Alarcon-Aquino, and L. G. Guerrero-Ojeda, "A Comparative Simulation Study of Wavelet Based Denoising Algorithms", *Proceedings of the 15th International Conference on Electronics, Communications and Computers (CONIELECOMP 2005).*

[23] http://users.rowan.edu/~polikar/wavelets/wtpart1.html.

[24] http://users.rowan.edu/~polikar/wavelets/wtpart2.html.

[25] http://users.rowan.edu/~polikar/wavelets/wtpart3.html.

[26] http://users.rowan.edu/~polikar/wavelets/wtpart4.html.

[27] http://cas.ensmp.fr/~chaplais/wavetour_presentation/Wavetour_presentation_US.html.

[28] http://www.me.cmu.edu/ctms/modeling/tutorial/systemidentification/mainframes.htm.

[29] http://terpconnect.umd.edu/~toh/spectrum/TOC.html

[30] http://www.complextoreal.com/fft1.htm

[31] http://www.complextoreal.com/fft2.htm

[32] http://www.complextoreal.com/fft3.htm

[33] H.G.Rodney Tan, A.C.Tan, P.Y.Khong, V.H.Mok, " Best Wavelet Function Identification System for ECG Signal Denoise Applications", *IEEE International Conference on Intelligent and Advanced Systems*, 2007

[34] Ramesh Neelamani, Hyeokho Choi and Richard Baraniuk, "Wavelet-Based Deconvolution For Ill-Conditioned Systems", *0-7803-5041 -3/99, pp.241-3244, IEEE*, 1999.

[35] www.mathworks.com

[36] Tam´as Dab´oczi," Nonparametric Identification Assuming Two Noise Sources: A Deconvolution Approach", *IEEE TRANSACTIONS ON INSTRUMENTATION AND MEASUREMENT, VOL. 47, NO. 4*, AUGUST 1998

[37] http://www.scribd.com/doc/16545830/fourier

APPENDIX

The different types of wavelets which are used for various applications are given below:

- Haar
- Daubechies
- Symlets
- Coiflets
- BiorSplines
- ReverseBior
- Meyer
- Meyer
- Gaussian
- Mexican hat
- Morlet
- Complex Gaussian
- Shannon
- Frequency B-Spline
- Complex Morlet

HAAR WAVELET

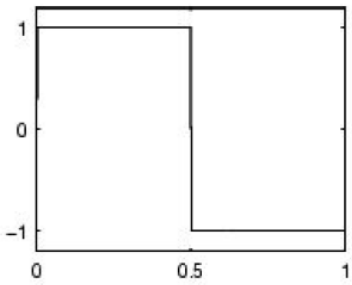

Fig a: Haar wavelet; *source: [35]*

DAUBECHIES WAVELET

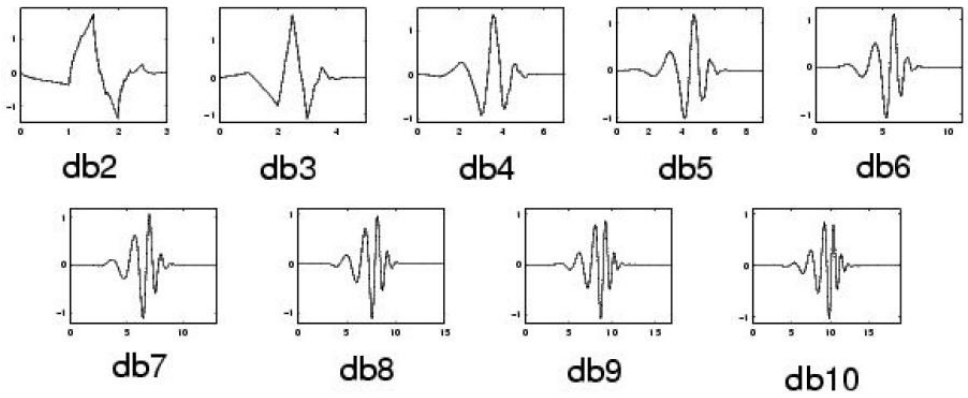

Fig b: Daubechies wavelet; *source: [35]*

MEXICAN HAT WAVELET

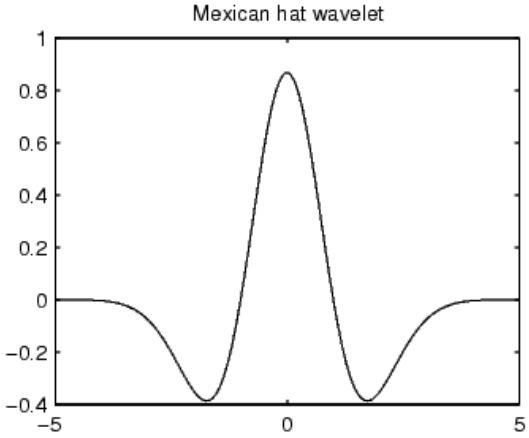

Fig c: Mexican hat wavelet; *source: [35]*

MEYER WAVELET

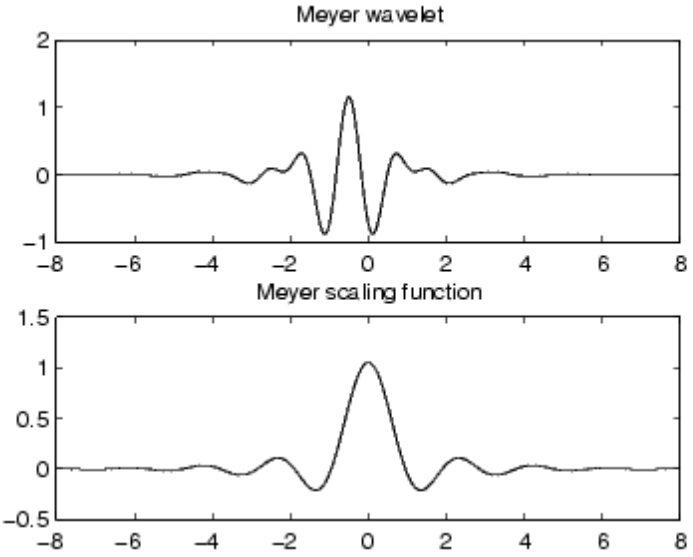

Fig d: Meyer wavelet; *source:[35]*

MORLET WAVELET

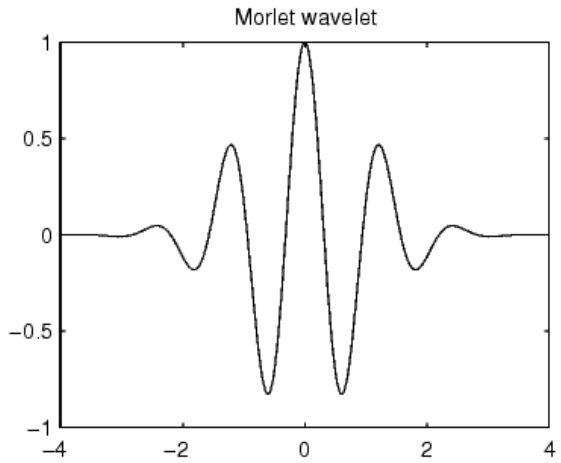

Fig e: Morlet wavelet; *source:[35]*

COMPLEX SHANNON WAVELET

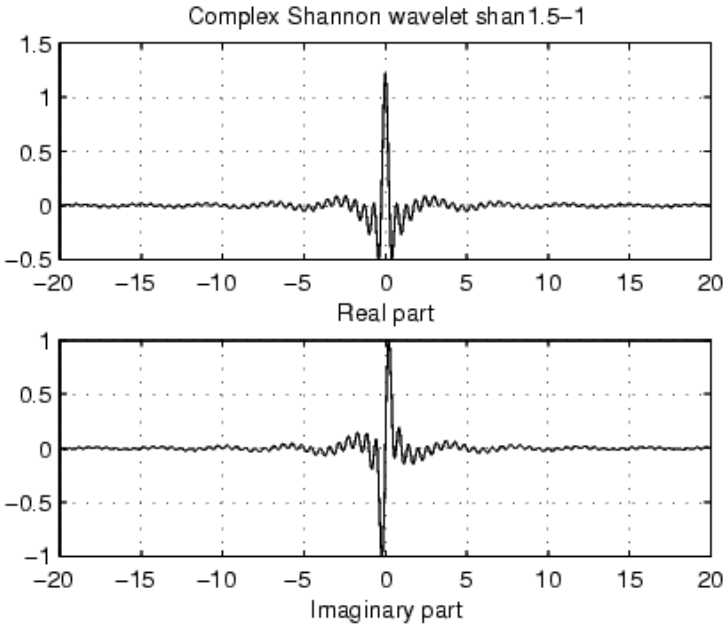

Fig f: Complex Shannon wavelet; *source:[35]*

COMPLEX FREQUENCY B-SPLINE WAVELET

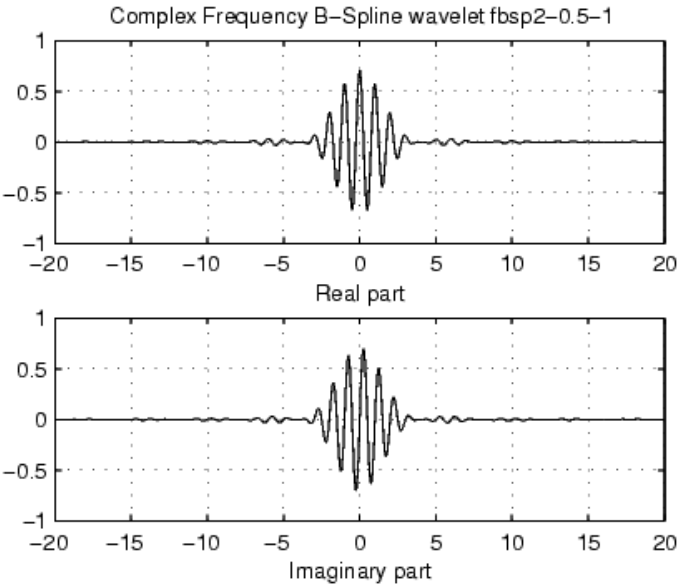

Fig g: Complex frequency B-spline wavelet; *source:[35]*

COIFLETS

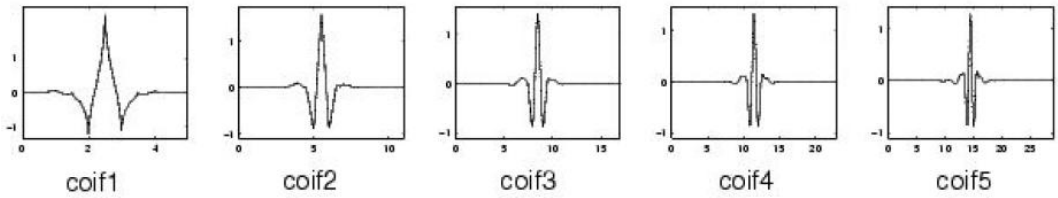

Fig h: Coiflets; *source:[35]*

SYMLETS

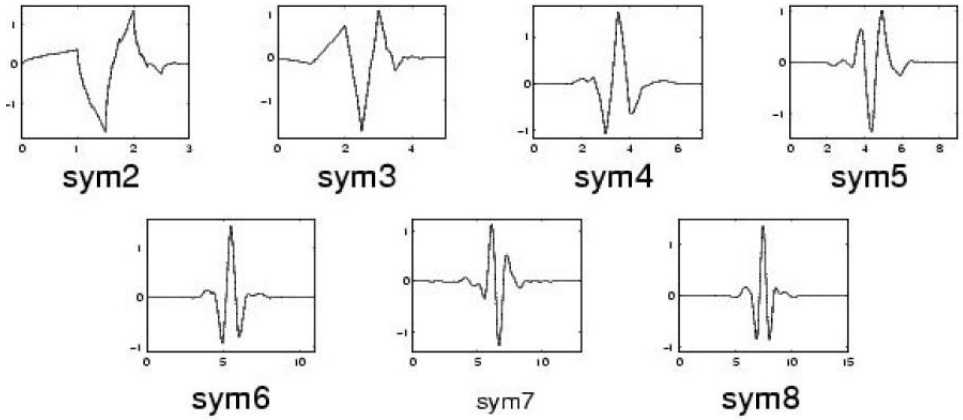

Fig i: Symlets; *source:[35]*

BIORTHOGONAL WAVELETS

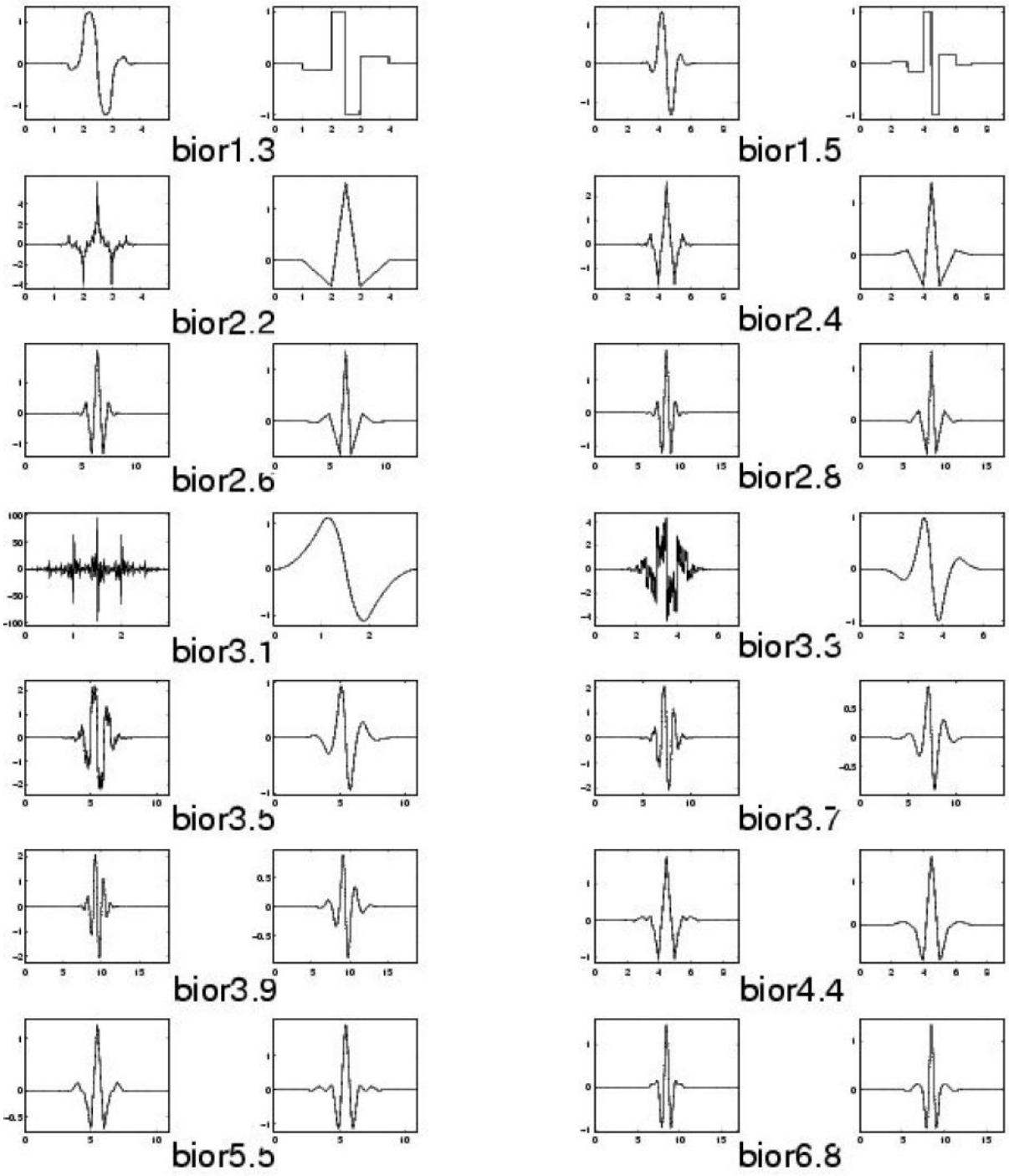

Fig j: Biorthogonal wavelet; *source:[35]*